ISSN 1173-5996

Radiant Ignition of New Zealand Upholstered Furniture Composites

by
Flora F Chen

Supervised by

Dr Charley Fleischmann

Fire Engineering Research Report 01/2

March 2001

This report was presented as a project report as part of the
M.E. (Fire) degree at the University of Canterbury

School of Engineering
University of Canterbury
Private Bag 4800
Christchurch, New Zealand

Phone 643 364-2250
Fax 643 364-2758
www.civil.canterbury.ac.nz

ABSTRACT

This experimental research evaluates the radiant ignitability of New Zealand upholstered furniture composites using the ISO Ignitability Test (ISO5657). It is a part of a larger research project on the combustion of domestic upholstered furniture at the University of Canterbury.

The project aims to predict the ignition time of New Zealand upholstered furniture composites. Fourteen fabrics, one of which was fire retardant cotton, were chosen for testing according to their compositions and content. They represented the most common used fabrics in the manufacture of upholstered furniture in New Zealand. One foam was chosen as it is the most commonly used foam for domestic and commercial furniture. In total, the study tested fourteen types of fabric-foam combination composites, of which there were 750 specimens in this project.

The time-to-ignition data are presented in a statistical way with mean, maximum, minimum, standard deviation and included the ratio of standard deviation to mean. The Flux Time Product concept and linearized thermal ignition model were applied to predict the time-to-ignition, the critical heat flux for ignition and the ignition temperature for the fabric foam composites. Predicting the ignition of upholstery composites by applying the thermally thin theory obtains a reasonably good comparison to the measured ignition data. Therefore, it is applicable to apply the thermally thin theory in engineering calculations and design. The prediction by the thermally thick theory is not as accurate as that by the thermally thin theory.

In this research, it was found that Flux Time Product index is smaller than 1.0 for melting fabrics and greater than 1.0 for charring fabrics, when the best-fit linear correlation is achieved. There needs to be further research to justify these values for the FTP index for the fabric-foam composites.

The ignition data obtained by the ISO Ignitability Apparatus in this study was compared with that obtained from previous research in the Cone Calorimeter. The comparison shows that the two test methods have a good agreement.

ACKNOWLEDGEMENTS

I would like to sincerely show appreciation to the following persons who have helped me during this project.

Firstly, I am extremely grateful to my supervisor Dr. Charles Fleischmann for his continued support and direction. His friendly encouragement and technical guidance at all stages have been a driving force of the progress throughout this research. His direction challenged my mind in analysis that it is demanding and educational and it will benefit me in my future career.

Thanks to Dr. Andrew Buchanan for his time management and reporting advice.

Sincere gratitude to my lecturer Mr. Michael Spearpoint for his time and advice all the way through both technique in fire engineering and computer skills.

Thanks to Grant Dunlop, Colin Bliss, Frank Greenslade and Ian Sheppard, for their assistance, while conducting the ignitability tests.

Appreciation to the New Zealand Fire Service commission for their financial contribution.

Appreciation to the staff of the Engineering Library, in particular Christine Mckee, for their friendly assistance in information searching.

Thanks to Mr. Barry Rea for his grammar and proof reading correction to my report writing.

Lastly, I would like to thank my husband and my two lovely children for their understanding, which make all this possible.

TABLE OF CONTENTS

LIST OF FIGURES

APPENDICES:

LIST OF TABLES

APPENDICES:

NOMENCLATURE

a	Slope of the straight line of the linear correlation
b	Intercept of the straight line of the linear correlation
n	The flux time product index
$\dot{q}''$	Heat flux (kW/m^2)
t	Time (seconds)
T	Temperature (K or ^oC)
T_o	Ambient temperature (K)
T_{ig}	Ignition temperature (K)
c	Specific heat, (kJ/kg K)
k	Thermal conductivity of the solid (kW/m K)
L_o	The thickness of the fuel (m)
h_c	Convective heat transfer coefficient (kW/m^2 K)

Greek symbols

α	Thermal diffusivity ($k/\rho c$) (m^2/s)
ρ	Density (kg/m^3)
ε	Emissivity
σ	Stefan-Boltzmann Constant ($5.67x10^{-11}$ kW/m^2 K^4)

Subscripts

ig	Ignition
cr	Critical
e	External

Superscripts

·	Signifies rate of change as in $\dot{q}$
'	Single prime (Signifies 'per unit width')
''	Double prime (Signifies 'per unit area')

List of abbreviations

ISO	International Organisation for Standardisation
FTP	The Flux Time Product
NI	No ignition
SD	Standard deviation

Chapter One

INTRODUCTION

1.1 Impetus for this research

The fire behaviour of modern upholstered furniture and bed-assemblies has received considerable attention over the past 10-15 years. It is because a significant proportion of modern upholstered furniture and bed-assemblies are considered to be relatively easy to ignite with small sources and then to burn rapidly. It produces large quantities of heat, smoke and toxic gases, which form the main real-life fire hazards. Fires may pass through several stages: ignition, growth to flashover, spreading to adjacent rooms and buildings. It is the first stage which are of major importance when considering upholstered furniture fire, because without ignition there can be no fire. The ignitability of an upholstery composite determines the likelihood of its igniting in a given environment. In other words, ignitability affects the probability of a fire occurring, though it does not necessarily affect the severity or the life hazard of the resultant fire (Paul, 1986). Due to the above consideration, ignitability tests of upholstered furniture are required to determine the fire performance of upholstered composites.

In some overseas countries such as the United Kingdom, and in the State of California in the United States, there are some flammability regulations that upholstered furniture must adhere to (Babraukas and Krasny, 1991). In New Zealand the manufactures of upholstery fabrics, foams and the furniture makers are free to use any composition and combination of materials when making furniture for consumers. It is an effective approach to reduce fire hazards, if furniture manufacturers are recommended to improve the fire performance of their products, by giving top priority to ignition resistance to small sources.

1.2 The objectives of this project

This Research Project is a part of a larger research project on the combustion of domestic upholstered furniture. It evaluates the ignitability of New Zealand furniture. The emphasis in this project is focusing on predicting time to ignition of New Zealand upholstered furniture by applying the ISO Ignitability Test according to the description of BS467: Part 13: 1987. This part of BS 467 had been prepared under the direction of the Fire Standards Committee. It is identical with ISO 5657 – 1986 'Fire tests – Reaction to fire – Ignitability of building products', published by the International Organisation for Standardisation.

Attempts were made to make sure that chosen materials are commonly used in real life situation in New Zealand upholstered furniture. To examine the most common fabrics that the furniture manufacturers use, a wide survey was conducted in a major upholstered furniture retailer in Christchurch. About 350 fabric samples of various designs from a range of suppliers were found, excluding colour difference. Fourteen fabrics were selected for testing for their representative compositions and content. The selection of polyurethane foams that were analysed was chosen as a continuation of Denize's research (Denize, 2000). Due to the time limitation, only one type of foam was tested, which was the most commonly used for domestic and commercial furniture. In total, fourteen types of upholstered furniture composite combinations (fourteen fabrics, one foam), were subjected to 750 tests and completed in this research.

This project applied mathematical models – the Flux Time Product method and Mikkola & Wichman's linearized thermal ignition model, to predict the critical/minimum heat flux and ignition temperature for New Zealand upholstered furniture composites.

1.3 Outline of this report

This project report consists of six parts as from Chapter Two to Chapter Seven.

Chapter Two, investigates the background and development of ignitability measurement. The ignitability tests with the ISO Ignitability Apparatus and the Cone Calorimeter are compared in their physical mechanisms of the apparatuses, and the test protocols. Some measurement results from previous research are presented. This part also introduces the fundamental theory applied to ignitability prediction and the correlating methods for ignition data in previous research.

Chapter Three, describes the ISO Ignitability Apparatus used in this research, the criteria of foam and fabric selection, and these products details. The construction of test specimens and its preparation detail are also demonstrated in this chapter. This is followed by a detailed description of the experimental set up and the test procedure. It also explores the items tested and details of the experimental runs.

Chapter Four, presents phenomenon observed during the experiments and explores the findings obtained from the experiments. It includes the correlation of the ignition data, predicting the time-to-ignition, the critical ignition heat flux and the effective ignition temperature for the fabric and foam composites.

Chapter Five, discusses the findings from the experiments with the ISO Ignitability Apparatus, and examines the applicability of the thermally simple theory in the prediction, factors effecting the ignitability of the upholstery composites and uncertainties of the tests. This part also compares the test results with those from previous research with the Cone Calorimeter.

Chapter Six, which outlines conclusions drawn from the discussion and is followed by Chapter Seven, Recommendation, which suggests further research.

Chapter Two

LITERATURE SURVEY

2.1 Background of ignitability measurement

Early ignitability testing was generally based on a furnace exposure to a small specimen, which was assumed to be of nearly uniform temperature. It was widely used in the late 1940s. The test procedure consisted of determining the furnace temperature at which ignition was first observed. Such a test could not be used to study composite materials, nor to compare specimens of varying thickness (Babraukas and Parker, 1987).

It was found to be more useful in assessing the performance of materials and products if substantially larger specimens were used and the correlation between the time to ignition and the given heating flux could be determined. Consequently, ignitability apparatuses were designed where the heating source was primarily radiant heat, convective heat and heating from direct flame impingement, respectively. As the heating from direct flame impingement was non-uniform, its analysis became mathematically difficult. The convective heating was less important in room fires and had practical difficulties. Thus, radiant heating was considered to be the preferred form for an ignitability test (Babraukas and Parker, 1987).

- **The radiant heater**

The radiant heater is the most important feature of the ignitability test. The heater should be able to achieve adequately high irradiances, have a relatively small convective heating component, and present a highly uniform irradiance over the entire exposed face of the specimen. It should not change its irradiance when the main voltage varies, when heater element ageing occurs, or when the apparatus retains some residual heat from the exposure given to a prior specimen.

In larger fires, where the fires reach a hazardous condition, the radiant from the soot tends to dominate. It results in an approximation to a grey body radiation. Electrical heaters tend to have a near-grey body characteristic and a high emissivity (Babraukas and Parker, 1987).

The geometry of the conical heater in the ISO Apparatus and in the Cone Calorimeter appears to be ideal for the use.

- **Means of ignition**

The ignition source should not impose any additional localised heating flux on the specimen. The igniter should reliably ignite a combustible gas mixture in its vicinity. This means that pilot flames should be optically thin and their emissivity is low. The igniter should be designed so as not to be extinguished by fire retardant compounds coming from the specimen nor by airflow within the test apparatus. Initial experience at NBS with electrical spark ignition was successful (Babraukas and Parker, 1987).

The location of the igniter should be at the place where the lower flammable limit is expected to first be reached when the specimen begins its pyrolysis. It should, however, not be close to the specimen surface that minor swelling of the specimen would interfere with the ignition source. In the Cone Calorimeter, the igniter locations were chosen so that the spark plug gap is located 13mm above the centre of the specimen when testing in the horizontal orientation (Babraukas and Parker, 1987).

- **Specimen size and thickness**

The area effect on ignition is smaller when irradiances are high than when they are low (Simms, 1960). For specimens of area 0.01 m^2 or larger, the increase in ignition time is typically only 10% or so over what would be seen with a specimen of infinite area.

The ignition times of larger specimens 200 mm by 200 mm were compared against 100 mm by 100 mm ones in the Cone Calorimeter. It shows that quadrupling the specimen area decreases the ignition time by about 20% (Babraukas and Parker, 1987).

For a thermally thick specimen, further increases in thickness are not expected to change ignitability results. For a thermally thin specimen, there can be expected to be a thickness effect, and the backing or substrate material's thermophysical properties are of importance (Babraukas and Parker, 1987). The specimen thickness should be the thickness of the finished product, as much as possible.

2.2 The ISO Ignitability Test versus the Cone Calorimeter

2.2.1 Test apparatus

The ISO Ignitability Apparatus represented the first widely used apparatus specifically designed for testing radiant ignitability. Its thermal radiation source was designed to be in the form of a truncated cone. It eliminates that the specimen centre is heated more than the edges. The heat flux, provided up to 50 kW/m^2 by the cone, is constant and highly uniform. A general view of the ISO Ignitability Apparatus is shown as Figure 2-1.

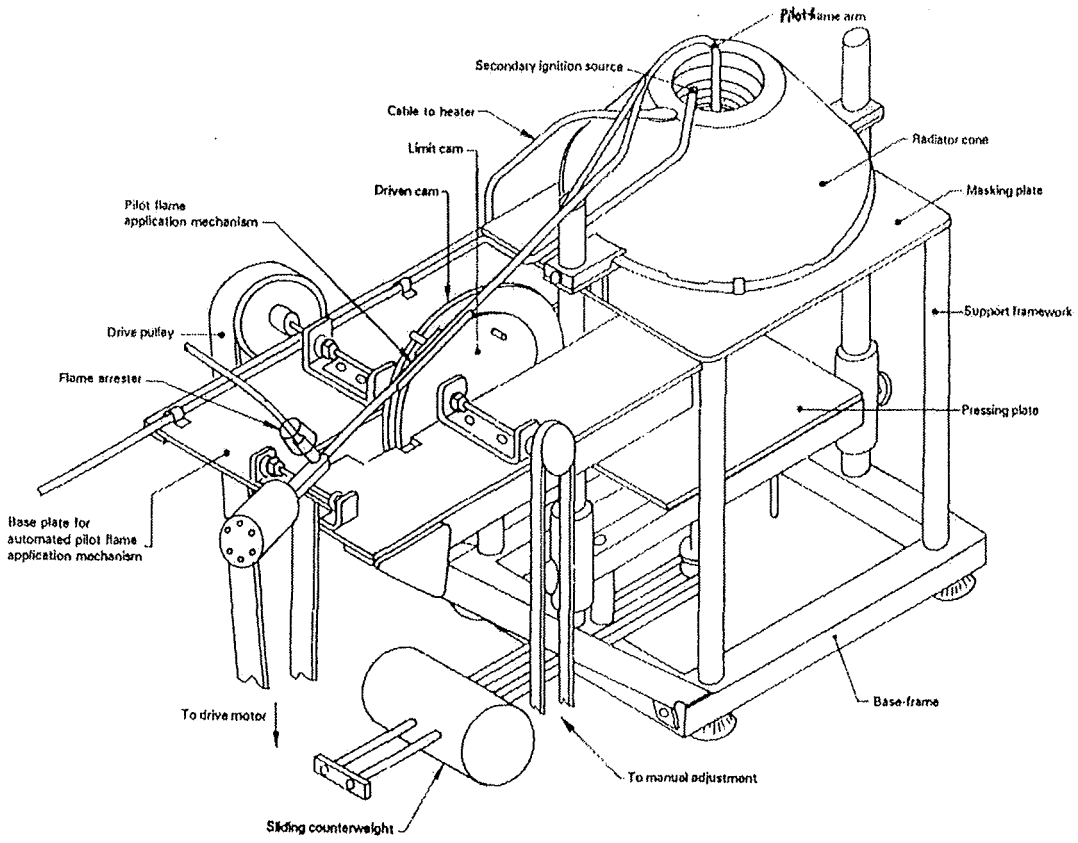

Figure 2-1 General view of the ISO apparatus (BS 476 Part 13: 1987)

Based on the design of the ISO Ignitability Apparatus, the Cone Calorimeter was developed to be able to make ignitability, heat release, mass loss and smoke measurement. The constant heat flux provided by the conical electrical heater is up to 100 kW/m^2 with uniformity.

The Cone Calorimeter was designed to test specimen in both horizontal and vertical orientation. Figure 2-2 shows the general view of the Cone Calorimeter (horizontal).

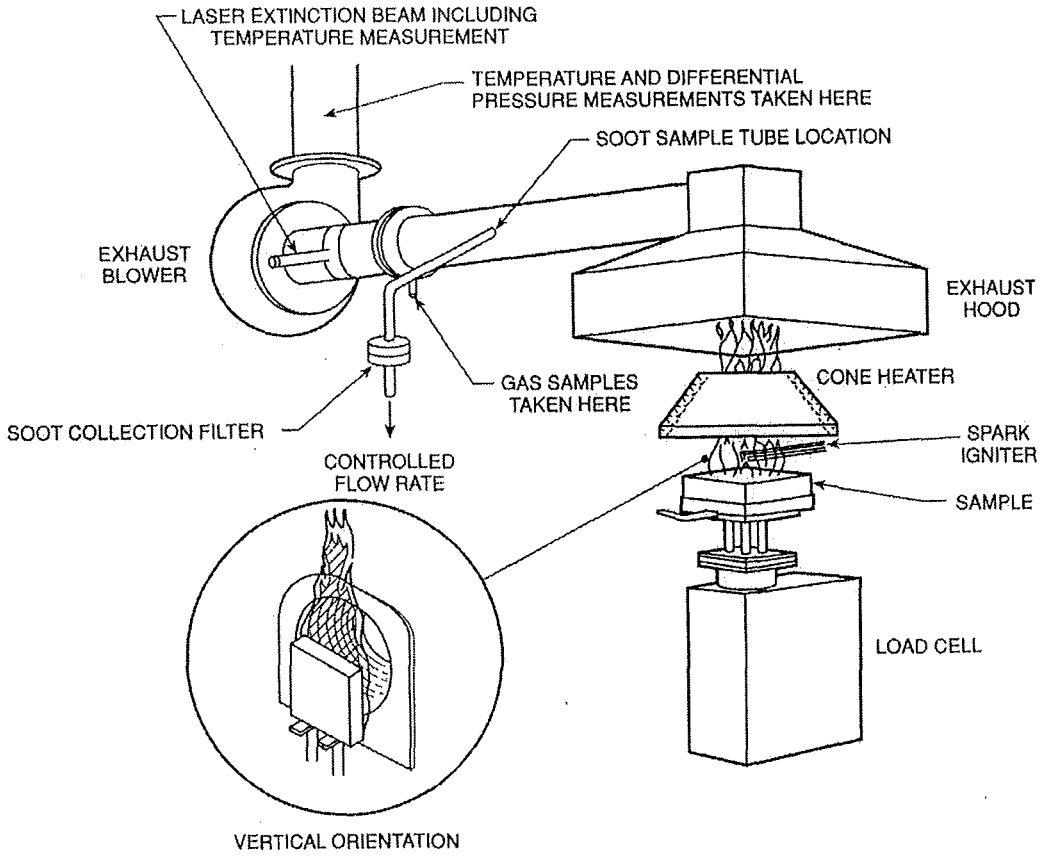

Figure 2-2 General view of the Cone Calorimeter (horizontal) (SFPE Handbook, 1995)

Figure 2-3 and Figure 2-4 shows the radiator cone of the ISO Ignitability Apparatus and the Cone Calorimeter, respectively.

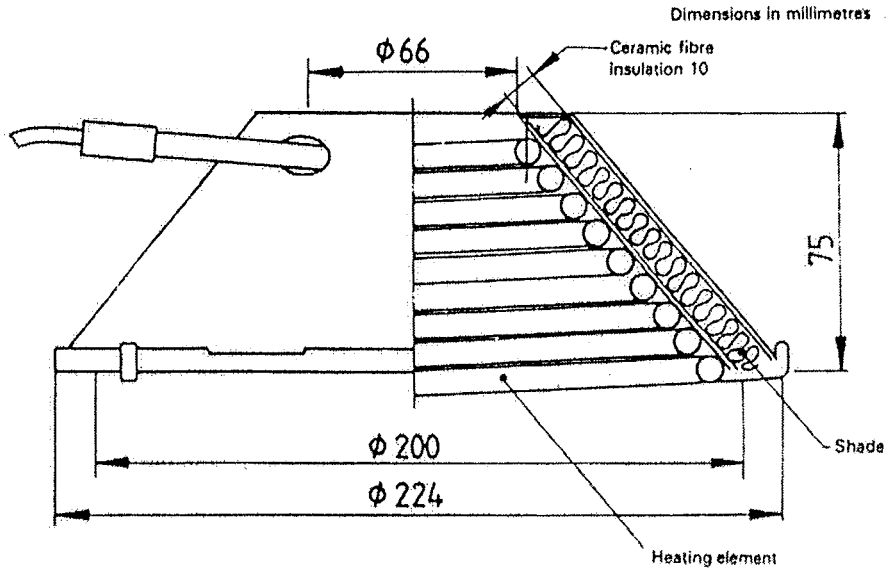

Figure 2-3 Radiator cone of ISO apparatus (BS 476 Part 13: 1987)

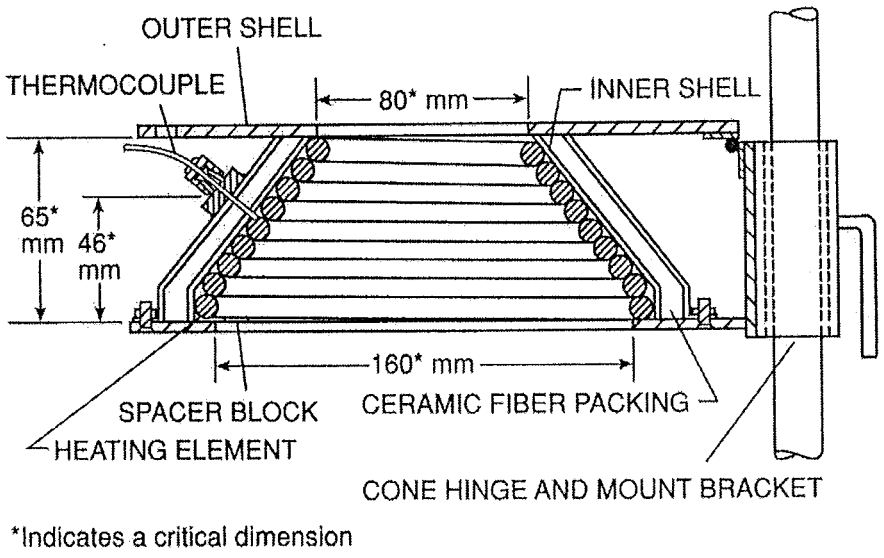

Figure 2-4 Radiator cone of the Cone Calorimeter (SFPE Handbook, 1995)

2.2.2 Test method

The main differences in measuring ignitability between the Cone Calorimeter Test and the ISO Ignitability Test are in the size and wrapping of the specimen, the backing material, the type of ignition source, and ventilation near the specimen (Mikkola, 1991).

The specimen size of the ISO ignitability test is 165 mm x 165 mm. Specially prepared aluminium foil (nominal thickness 0.02mm), having a 140 mm diameter circular hole cut from its centre, is wrapped around both sample and backing board. This arrangement exposes a constant area of the sample to heat flux. An automatic mechanism brings a pilot flame above the centre of the specimen once every forth second to ignite the volatiles. The pilot flame remains near the specimen surface for one second. Sustained ignition is defined as inception of flame on the surface of the specimen, which is still present at the next application of the pilot flame. The test arrangements and the operation were according to ISO 5657.

The specimen size of the Cone Calorimeter test is 100 mm x 100 mm, which is exposed to heat flux when no retainer frame is used. An electrical spark is used to ignite the pyrolyzates. The sustained ignition is defined as the existence of flames for periods of over 10 seconds. The operation and test arrangements were according to ISO DIS 5660.

2.2.3 Comparison of measurement results

Shields, Mikkola and Babrauskas compared the ignitability difference for wood based materials between the ISO ignitability test and the Cone Calorimeter, and influence of ignition mode. They are demonstrated respectively as follow.

- **Shields, Silcock and Murray**

The study (Shields *et al,* 1993) investigated the times to ignition obtained using the Cone Calorimeter and the ISO Apparatus for pilot flame, spark igniter and spontaneous ignition modes. It compares the test results for chipboard (15mm), plywood (12mm) and softwood (20mm) with the incident heat flux from 20 kW/m^2 to 70 kW/m^2, as listed in Table 2-1.

It can be seen from Table 2-1 that:

- The times to ignition in the Cone Calorimeter are typically shorter. Allowing for error associated with the periodic delay time of the ISO Ignitability Apparatus, the time to ignition obtained by the Cone Calorimeter and the ISO

Apparatus for gas flame pilot mode of ignition is similar over the range of imposed incident fluxes (40 to 70 kW/m^2).

- By the Cone Calorimeter the ignition time for a spark mode is longer than that for gas flame pilot mode.
- When incident flux levels are greater than 50 kW/m^2, the mode of ignition does not significantly influence the time to ignition.

Table 2-1 Comparison of mean times-to-ignition for materials in normal orientation (horizontal) (C= Cone, I=ISO) (Shields *et al.*, 1993)

Material	Ignition mode	Incident flux (kW/m^2)											
		20		30		40		50		60		70	
		C (s)	I (s)	C (s)	I (s)	C (s)	I (s)	C (s)	I (s)	C (s)	I (s)	C (s)	I (s)
Chipboard (15mm)	Gas flame	163	132	51	57	27	28	17	20	13	16	10	11
	Spark	169		54		32		20		14		10	
	Spontaneous	NI	312	123	70	61	38	27	25	19	19	14	15
Plywood (12mm)	Gas flame	120	228	48	71	32	40	19	25	15	22	9	15
	Spark	135		53		32		22		15		11	
	Spontaneous	NI	NI	585	607	211	72	80	29	42	20	29	15
Softwood (20mm)	Gas flame	323	316	47	85	25	40	11	22	8	11	5	7
	Spark	374		53		25		17		8		7	
	Spontaneous	NI	730	NI	154	74	82	25	28	17	12	9	10

- **Babrauskas and Parker**

The study (Babraukas and Parker, 1987) indicated that ignition times, as measured in the Cone Calorimeter, are in most cases shorter than that measured in the ISO Apparatus. This is coincident to the results of presented previously (Shields *et al.*, 1993).

- **Mikkola**

Table 2-2 compares the test ignition times for 12 mm plywood with the Cone Calorimeter and the ISO Ignition Apparatus.

Table 2-2 Results for 12 mm thick birch plywood (Mikkola, 1991)

Heat flux	Number of test	Time to ignition	Standard deviation		Time to ignition	Standard deviation	
(kW/m^2)		(s)	(s)	(%)	(s)	(s)	(%)
12mm thick		**ISO 5657**			**Cone Calorimeter**		
20	10	251	22	9	379	117	31
25	3	110	13	12	146	5	3
30	5	61	2	3	80	7	9
40	5	32	1.7	5	38	2.5	7
50	15	21.9	1.6	7	23.5	2.0	8
	5	20.8[1]	1.3	6	26.1[2]	2.3	9

[1] Spark ignition
[2] Retainer frames used

Mikkola provided a simple approximate relation between the results of time to ignition in the Cone Calorimeter and in the ISO Apparatus as Equation 2-1:

$$\left(t_{i,CC}/t_{i,ISO}\right)^{-n} = 0.86 \qquad \textbf{Equation 2-1}$$

Where n is 1, 2/3, or 1/2 for thermally thin, intermediate or thick cases, respectively. Variation in the factor 0.86 is the order of 6%. These show that ignition times in the Cone Calorimeter test are slightly higher than in the ISO ignitability test (Mikkola, 1991).

This conclusion indicates a reverse trend presented by Shields (Shields *et al,* 1993), where ignition time is slightly higher in the ISO Test.

Comparing the test result for 12 mm plywood in Table 2-1 and Table 2-2, it was noticed that with the ISO Ignition Apparatus, time-to-ignition is higher in Table 2-1, while with the Cone Calorimeter, the ignition time is higher in Table 2-2. This may cause from the uncertainty of the test between labs and the different properties of the tested plywood.

2.3 Simple thermal theory

2.3.1 Assumption of the theory

Ignition is assumed to occur when the surface reaches a material dependent temperature. This is defined as the ignition temperature. The material is assumed to be homogenous, opaque and chemically inert. These assumptions simplify the problem to the radiant heating of a one-dimensional solid. The chemistry and mass transfer are ignored. In addition, an exact solution is available when the exposing radiation and thermal properties are assumed constant and the boundary conditions are linearized (SFPE, 2001).

2.3.2 Thermal thickness

The heat wave penetration must be less than the physical depth so that increasing in the physical thickness of the specimen will not influence the time-to-ignition for a give set of conditions. Such specimen is considered to be a thermally thick sample. For thinner specimens a thickness effect can be expected and the specimen's backing or substrate can become an important factor (Shields, *et al,* 1994).

Drysdale (Drysdale, 1999) recommended that the characteristic thermal conduction length ($\sqrt{\alpha t}$) could be used as an indicator of the depth of the heated layer of a thick material, where α is the thermal diffusivity of the material and t is exposure time. Heat losses from the rear face of a material would be negligible if $L_o > 4x\sqrt{\alpha t}$, which indicates "semi-infinite behaviour" – thermally thick. L_o is the physical thickness of the specimen. A thermally thin material could be defined as one with $L_o < \sqrt{\alpha t}$. "Thermally thickness" increases with $\sqrt{t}$, and for a sufficiently long exposure time, a physically thick material will no longer behave as a semi-infinite solid, and begin to show behaviour that is neither "thick" nor "thin".

2.3.3 The critical irradiance ($\dot{q}''_{cr}$) and the ignition temperature (T_{ig})

The critical irradiance $\dot{q}''_{cr}$ is a theoretical lower limit on the flux necessary for ignition. It is equal to the heat loss from the surface at ignition because below this irradiance level the surface temperature can never reach the ignition temperature, T_{ig}, which has been defined in Section 2.3.1. The relationship between the critical irradiance and the ignition temperature can be expressed by the equation of energy balance (Equation 2-2). It is assumed that there is no conduction into the solid, and all of the heat striking the surface must be lost from the surface either by radiation or convection.

$$\varepsilon \dot{q}''_{cr} = h_c(T_{ig} - T_0) + \varepsilon\sigma\,(T_{ig}^4 - T_0^4) \qquad \textbf{Equation 2-2}$$

Where,

h_c	Convective heat transfer coefficient (kW/m^2 K)
ε	Emissivity
σ	Stefan-Boltzmann Constant (5.67x10^{-11} kW/m^2 k^4)
T_o	Ambient temperature (K)

2.3.4 Correlating ignition data using the Flux Time Product (FTP)

A considerable amount of data has been gathered on "the time to ignition" as a function of the incident heat flux in the Cone Calorimeter, in the ISO Ignitability Test and in other experimental apparatus (Drysdale, 1999).

Smith and Green originally developed the Flux Time Product (FTP) method within a thermally closed system, i.e., OSU apparatus (Toal *et al*, 1989). Toal, Silcock, and Shields recommended this method be extended for use on data from the Cone Calorimeter and the ISO Ignitability Test (Toal *et al*, 1989).

The relationship between the time-to-ignition, t_{ig}, for a sample under the impact of an effective flux ($\dot{q}'' - \dot{q}''_{cr}$) is expressed as follow (Equation 2-3) (Shields *et al*, 1994):

$$FTP = t_{ig}(\dot{q}''_e - \dot{q}''_{cr})^n$$ **Equation 2-3**

Where,

FTP	The Flux Time Product
n	The Flux Time Product index, an empirical constant, which for an open systems such as a the Cone Calorimeter and the ISO Ignitability Apparatus, typically $1 \leq n \leq 2$.
t_{ig}	The time-to-ignition (s)
$\dot{q}''_e$	The external heat flux (kW/m^2)
$\dot{q}''_{cr}$	The critical irradiance (kW/m^2)

By rearranging Equation 2-3, a linear relationship can be obtained for the incident flux and the reciprocal of n^{th} power of the time-to-ignition (Equation 2-4):

$$\dot{q}''_e = \left(FTP\right)^{1/n} \Big/ t_{ig}^{1/n} + \dot{q}''_{cr}$$ **Equation 2-4**

A material can thus be characterised in terms of its time-to-ignition by $FTP^{1/n}$, $\dot{q}''_{cr}$, and n (an empirical constant).

2.3.5 Correlating ignition data by Mikkola and Wichman method

Mikkola and Wichman solved the differential form of the heat transfer equation and provided a functional relationship between the ignition time and the incident heat flux, which can be systematically used to correlate experimental data with a theoretical foundation. Two ignition models were examined as described below:

- General integral model
- Linearized thermal ignition model

2.3.5.1 General integral model

This model (Mikkola and Wichman, 1989) provides the approximate solutions of the integral equations for the general non-linear problem for the thermally thick, thin and intermediate cases.

When the material is thermally thin, the equation is given as Equation 2-5:

$$t_{ig} \approx \rho \; c \; L_0 \frac{\left(T_{ig} - T_0\right)}{\left(\dot{q}''_{in} - \dot{q}''_{out}\right)} \qquad \textbf{Equation 2-5}$$

Where,

t_{ig}	The time to ignition (s)
ρ	Density of the material (kg/m^3)
c	Specific heat of the material (kJ/kg K)
L_o	The thickness of the solid (m)
T_o	Ambient temperature (K)
T_{ig}	Ignition temperature (K)
$\dot{q}''_{in} - \dot{q}''_{out}$	Net heat flux (kW/m^2)

When the material is thermally thick, it yields as Equation 2-6:

$$t_{ig} \approx \rho \; ck \left(\frac{T_{ig} - T}{\dot{q}''_{in} - \dot{q}''_{out}} \right)^2 \qquad \textbf{Equation 2-6}$$

where,

k	Thermal conductivity of the solid (kW/m K)

For the thermally intermediate case, the equation appears to be (Equation 2-7):

$$t_{ig} \propto \rho\, c\sqrt{(kL_0)}\left(\frac{T_{ig}-T_0}{\dot{q}''_{in}-\dot{q}''_{out}}\right)^{3/2} \qquad \textbf{Equation 2-7}$$

This model is not sensitive and produces only the proper functional relationships, since multiplicative constant factors cannot be deduced.

2.3.5.2 Linearized thermal ignition model

This model (Mikkola and Wichman, 1989) provides the exact solution of a linearized heat-transfer problem for the surface temperature for both the thermally thick and thin cases.

Thermally thin

For the thermally thin case the characteristic thermal conduction length is much greater than the sample thickness. The method for thermally thin fuel is derived from the solution of the one-dimension inert heat transfer equation called the lumped heat capacity equation. It assumes a uniform temperature across the sample thickness. The time to ignition, t_{ig}, can be approximated using the following equation (Equation 2-8):

$$t_{ig} = \rho\, cL_0 \frac{\left(T_{ig}-T_0\right)}{\left(\dot{q}''_e-\dot{q}''_{cr}\right)} \qquad \textbf{Equation 2-8}$$

Where,

$\dot{q}''_e-\dot{q}''_{cr}$ An overall heat flux including surface heat losses and identical to $\dot{q}''_{in}-\dot{q}''_{out}$ in Equation 2-5.

This relationship (Equation 2-8) applies to thin materials only. Although precise limits are not defined, Mikkola and Wichman (Mikkola and Wichman, 1989) felt that

the thermally thin usually means a sample thickness less than 1-2 mm. It is (SFPE 2001) suggested that a sample could be considered to be thermally thin if

$$L_0 / \sqrt{\alpha\, t_{ig}} \leq 0.4 \qquad \textbf{Equation 2-9}$$

This (Equation 2-9) is a more conservative suggestion when compared with Drysdale's recommendation (Drysdale, 1999), which was described in the previous section.

Thermally thick

For thermally thick materials, the sample thickness is much greater than the characteristic thermal conduction length. An approximate solution for the time to ignition is derived using the first term of the series expansion and submitting in the ignition temperature for the surface temperature. The equation for the time to ignition is:

$$t_{ig} = \frac{\pi}{4} k\rho\, c \frac{\left(T_{ig} - T_0\right)^2}{\left(\dot{q}''_e - \dot{q}''_{cr}\right)^2} \qquad \textbf{Equation 2-10}$$

The above relationship (Equation 2-10) applies to thick fuels. Usually, thermally thick means more than 15-20 mm. Again, although a precise limit is not defined, a sample is suggested to be thermally thick (SFPE, 2001) if

$$L_0 / \sqrt{\alpha\, t_{ig}} \geq 4 \qquad \textbf{Equation 2-11}$$

This suggestion (Equation 2-11) is coincident to the recommendation by Drysdale, which was presented in the previous section (Drysdale, 1999)

Chapter Three

MATERIALS AND EXPERIMENTS

3.1 The ISO Ignitability Apparatus

A general view of the test apparatus was shown previously (Figure 2-1). It was made according to the description BS467: Part 13: 1987 (This part of BS 467 had been prepared under the direction of the Fire Standards Committee. It was identical with ISO 5657 – 1986 'Fire tests – Reaction to fire – Ignitability of building products', published by the International Organisation for Standardisation).

It consisted of a support framework, which clamped the test specimen horizontally between a pressing plate and a masking plate. The defined area of the upper surface of the specimen was exposed to a constant radiative flux, which was provided by the radiator cone (Figure 3-1). The intensity of the radiation was measured using a radiometer, which was removed prior to the sample being inserted.

- **Radiator cone**

The radiator cone consisted of a heating element, contained within a stainless steel tube, coiled into the shape of a truncated cone and fitted into a shade. The shade consisted of two layers of 1mm thick stainless steel with a 10 mm thickness of ceramic fibre insulation of nominal density 100 kg/m^3 sandwiched between them (Figure 2-3). The radiator cone was capable of providing irradiance in the range 0 to 50 kW/m^2 at the centre of aperture in the masking plate and in a reference plane coinciding with the underside of the masking plate. The temperature of the cone was controlled by reference to the reading of a thermocouple.

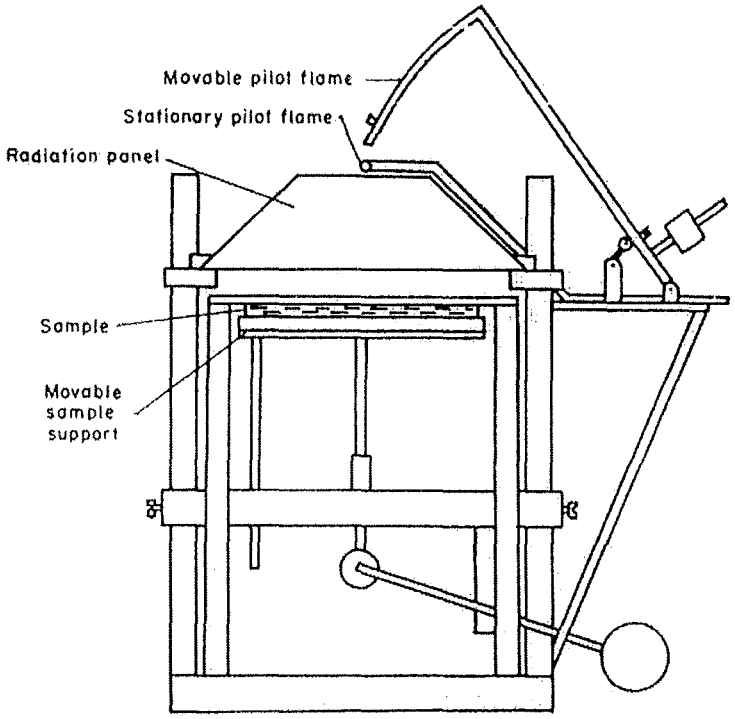

Figure 3-1 The ISO ignitability test (BS 476 Part 13: 1987)

- **Spark ignition application**

There were two igniters fitted in this particular apparatus – a flame igniter and a spark igniter. In this test, the electrical spark was used to ignite the out-coming volatiles. The spark was located 13 mm above the specimen surface.

- **Specimen screening plate**

A specimen plate was applied to slide over the top of the masking plate during the period of insertion of the specimen, thus shielding the specimen from radiation until commencement of the test. The plate was made from 2 mm thick polished stainless steel.

3.2 Materials

3.2.1 Criteria of material selection

Attempts were made to make sure that chosen materials were close to the compositions that are commonly used in New Zealand upholstered furniture. The selection of polyurethane foams and fabrics coverings was important.

Polyurethane foam samples were chosen based on the following criteria:

- Commonly used as seating foam in upholstered furniture.
- Main foam supplier.
- Grade of foam and special application.

This was coincident to Denize's research (Denize, 2000).

Fabric samples were chosen on the following criteria:

- Commonly used as a covering fabric for upholstered furniture
- Composition of the fabrics.
- Availability.

3.2.2 Foams

As this project was a part of a larger research project on the combustion of domestic upholstered furniture at the University of Canterbury, the foams were chosen as a continuation of Denize's research (Denize, 2000), where the above criteria had been considered. The coding, colour, density and manufacturer's designed applications of the foams are listed in Table 3-1.

Table 3-1 Foam coding identification and specification

Code	Colour	Density (kg/m^3)	Application
K	Green	27-29	Domestic and commercial furniture seat backs, seat-cushion and arms.

3.2.3 Fabrics

It was typical for a furniture designer to use a common fabric for its products. To examine the most common fabrics that the furniture manufacturers use, a wide survey was conducted in a major upholstered furniture retailer in Christchurch. About 350 fabric samples of various designs from a range of suppliers were found,

excluding colour difference. According to the criteria described, fourteen fabrics were selected for testing.

To distinguish the fabrics from one another, each fabric was coded with a number from 23 to 36, which were consistent with other research coding in the University of Canterbury. They are listed in Table 3-2, where coding, colour and composition of the fabrics are detailed.

Table 3-2 Fabric coding identification and specification

Fabric		Compsition (%)							
code	color	polypropulene	polyester	acrylic	cotton	olefin	viscose	Nylon pile	total
23	pacific	100							100
24	cement		100						100
25	saffron			100					100
26	azure					100			100
27	gold							100	100
28*	dark red				100				100
29	cadet		42	58					100
30	blue		51		49				100
31	sage		50			50			100
32	navy		51				49		100
33	forest	60	40						100
34	denim		31	21	48				100
35	spring		43	41		16			100
36	taupe		39		40		21		100

* Fabric 28 is a fabric treated with fire retardant additive.

3.3 Specimen construction and preparation

- **Forming blocks**

The blocks were made of median density fibreboard in dimensions of 162 × 162 × 50 mm. All surfaces of the blocks were cut straight, true and smooth. The edges were not rounded, but the corners were slightly rounded.

- **Cutting of foam blocks**

The thickness of the foam block was 50mm, which resulted in a total specimen thickness of approximately 50.9 mm. Each foam block (Figure 3-2) was cut square, with 90° corners and face dimensions of 167±0.5 mm by 167±0.5 mm. This size ensured that the foam would be compressed during composite assembly, leading to tight, well-formed specimens. Foams were cut with a band saw and a foam-cutting blade was used.

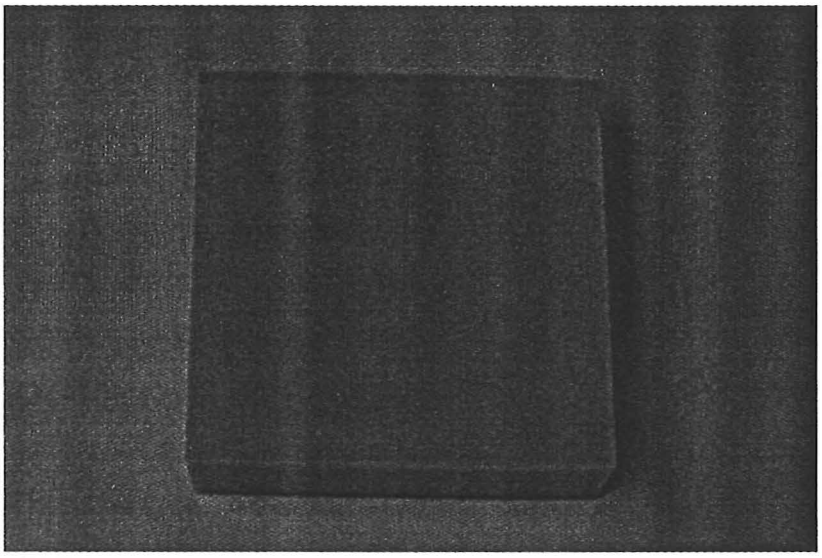

Figure 3-2 Foam block

- **Weighing and accepting foam blocks**

For the purpose that the results were repeatable, foam specimens that had been prepared were checked for mass. No foam was acceptable if it had a mass of more than 105% of the mean of the five, nor any less than 95%. The preparation of composites could not start until five foam blocks had been obtained which conformed to the above 5% deviation limit.

- **Cutting and weighing of fabrics**

A square fabric of 265 mm by 265mm was cut and made sure it was not cut on the bias. When the fabric weave was such that the threads in the two directions did not

lie at 90° to each other, it was not allow to cut the sample along threads in both direction. The fabric piece was checked to be skew free. For the results to be repeatable, fabric for the different replicates was cut in a uniform way. Fabric material closer than 25 cm to the selvage was not used.

When five replicate pieces had been cut, they were weighed to verify the uniformity of specimens. No piece of fabric was acceptable if it had a mass of more than 105% of the mean of the five, nor any less than 95%.

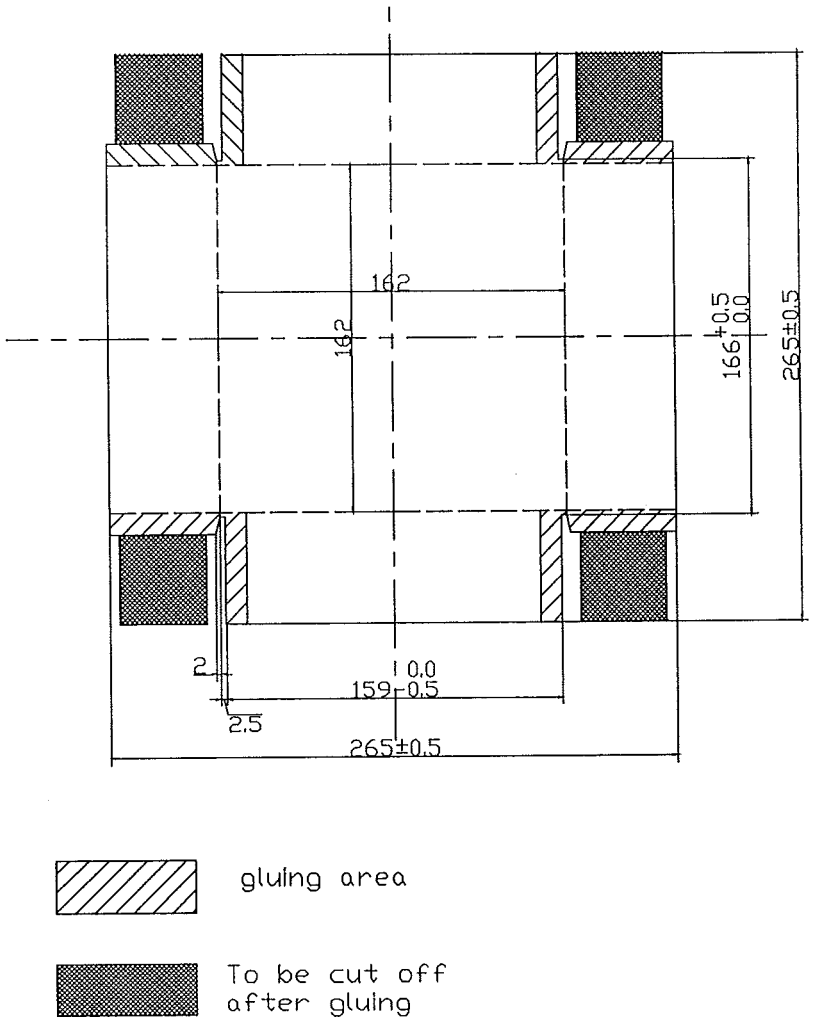

Figure 3-3 Fabric cutting shape

Each specimen was cut to the shape indicated in Figure 3-3. The 159 mm and 166 mm dimensions were checked both before and after cutting. When a fabric having thick thread was cut, the dimension was not allowed to be smaller than 168 mm.

- **Preparing the fabric shell**

The fabric was placed topside down on the table. Then the forming block was placed on the top of the fabric, making sure that it was well centred. The short sides were bent up and taped on to the top of the forming block in the centre of the top edge. Masking tape was applied. Then, the long sides were bent up and also taped to the top of the block. Four corners of the top face were checked to make sure that the fabric did not slip sideways on the block.

A 10 mm gluing area as marked with a stripe in Figure 3-3 on each corner flap, which belonged to the "long" side, was glued down onto its mating short-side surface by flocking glue. The adhesive was applied to both the underneath surface of the flap and to the surface against which it joined and then pressed down immediately. A 7 to 8 mm wide brush was used to ensure that the glued area was approximately 10 mm wide. After the first two corners were glued up, the block was turned so as to rest on the just-glued short side and glued up the two other corners.

A masking tape piece was applied on top to hold the joint in place and wrap the block while it was drying for 24 hours with facing down. The specimens were not allowed to be stacked. After drying, the two flaps were trimmed off down to the indicated offset mark, so that only the 10 mm glued-down portion was left.

- **Assembling the foam and the fabric shell**

After 24 hours, all pieces of masking tape were removed. Any fabric protruding below the bottom edge of the forming block was trimmed off with scissors. Then, the forming block was removed from the fabric shell.

The selected foam block was inserted into the fabric shell by compressing the four corners of the block slightly with the fingers. The specimen was inspected to make sure the foam block was inserted straight and the corners of the block lined up exactly at the corners of the fabric shell. The top face of the specimen was checked to see the foam block was inserted fully into the shell with appropriate gaps. The

bottom of the foam block was check to be neatly lined up with the bottom edge of the fabric.

An assembled specimen is shown as Figure 3-4. It was checked to be square, with sides measuring 165^{0}_{-5} mm. Before the test, each specimen was conditioned for at least 48 hours at a temperature of $23 \pm 2^{o}C$ and a relative humidity of $50 \pm 5\%$.

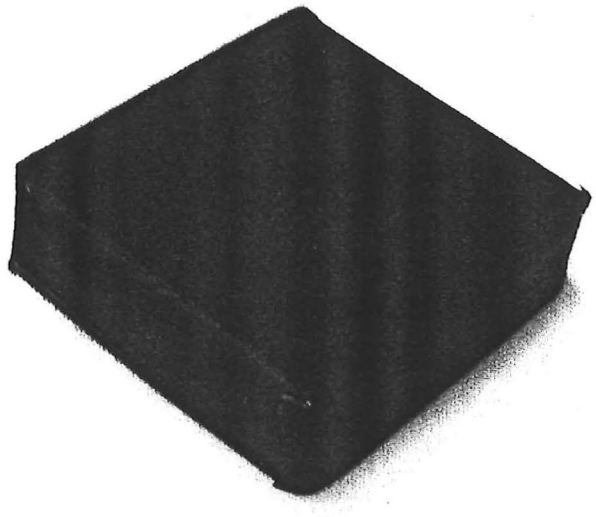

Figure 3-4 A fabric shell/assembled specimen

- **Baseboards**

One baseboard was required for each test specimen. The baseboard was square with sides measuring 165^{0}_{-5} mm. The nominal thickness was 6mm. It was made of Firelite insulation board with density complying to the standard.

Before test, the baseboards were conditioned for at least 24 hours at a temperature of $23 \pm 2^{o}C$ and a relative humidity of $50 \pm 5\%$, with free access of air to both sides. The baseboard was checked as clean and not contaminated.

- **Wrapping of specimen**

A conditioned specimen was placed on a treated baseboard. The combination was wrapped in one piece of aluminium foil, from which a circle 140 mm diameter had

been cut (Figure 3-5). The nominal thickness of the foil was 0.02 mm. The circular cutout zone was centrally positioned over the upper surface of the specimen. The wrapping of specimen and baseboard and a wrapped specimen are shown in Figure 3-6 and Figure 3-7. The specimen-baseboard combination was returned to the conditioning atmosphere until required for test.

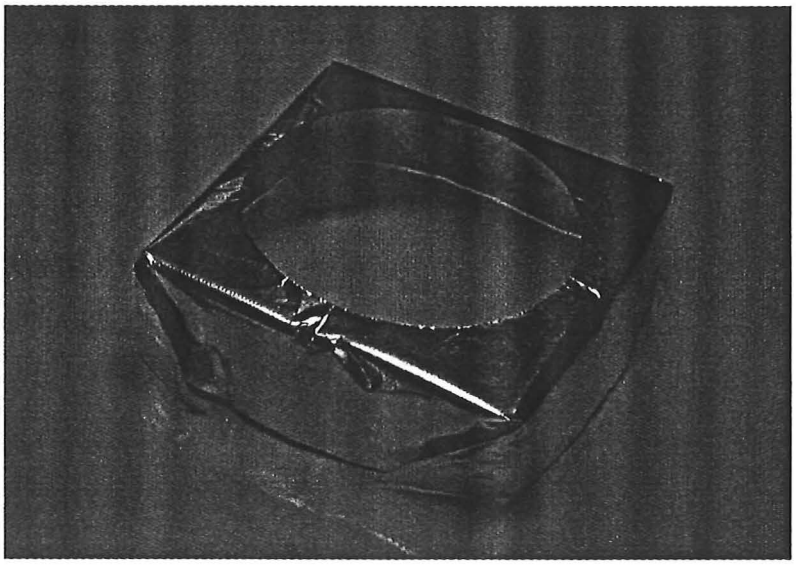

Figure 3-5 A wrapping foil

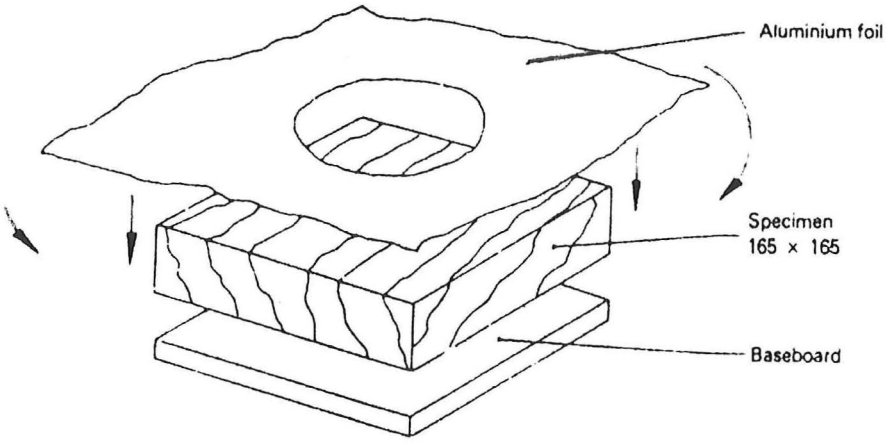

Figure 3-6 Wrapping specimen and baseboard

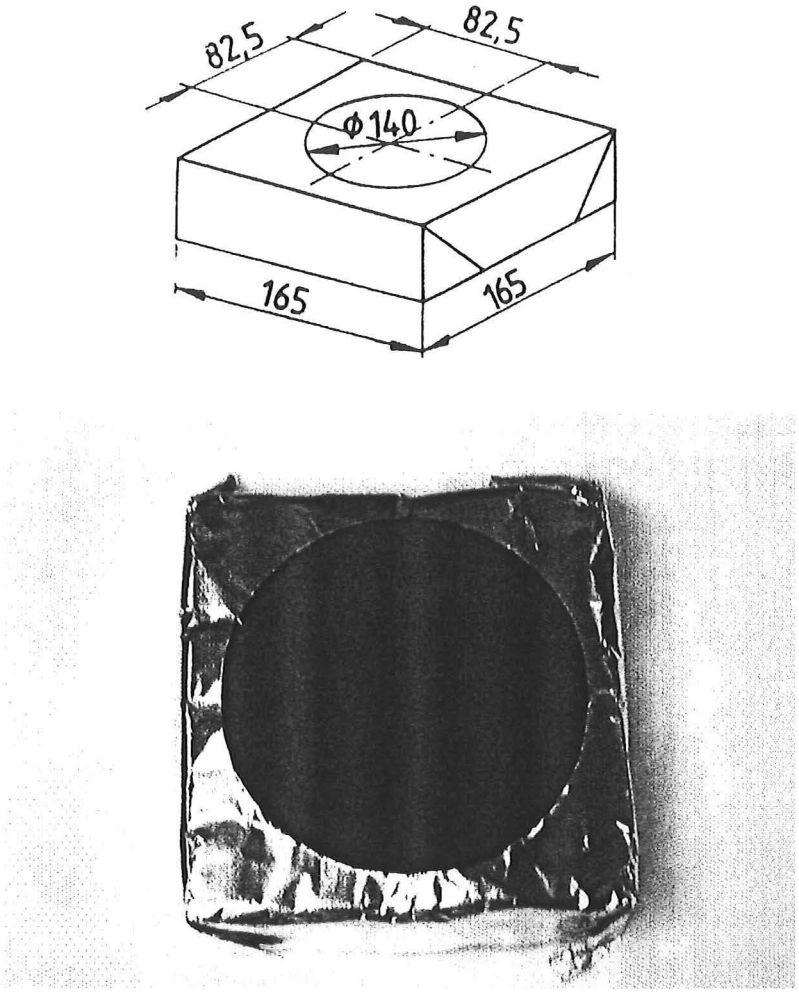

Figure 3-7 A wrapped specimen

3.4 Test procedure

Test set-up and procedures were performed according to the strict specification of the protocol of ISO Ignitability Test, which was described in BS467: Part 13: 1987. It was identical with ISO 5657 – 1986. Test environment is suggested in Clause 8, BS476: Part 13:1987.

> *The test shall be carried out in an environment essentially free of air currents and protected, where necessary, by a screen. The air velocity close to the test apparatus should be not more than 0.2 m/s. The operator should be protected from any products of combustion generated by the specimen. The effluent gases shall be extracted without causing forced ventilation over the apparatus.*

To make sure the test environment reached this requirement, a special mask was made for the apparatus, as shown in Figure 3-8.

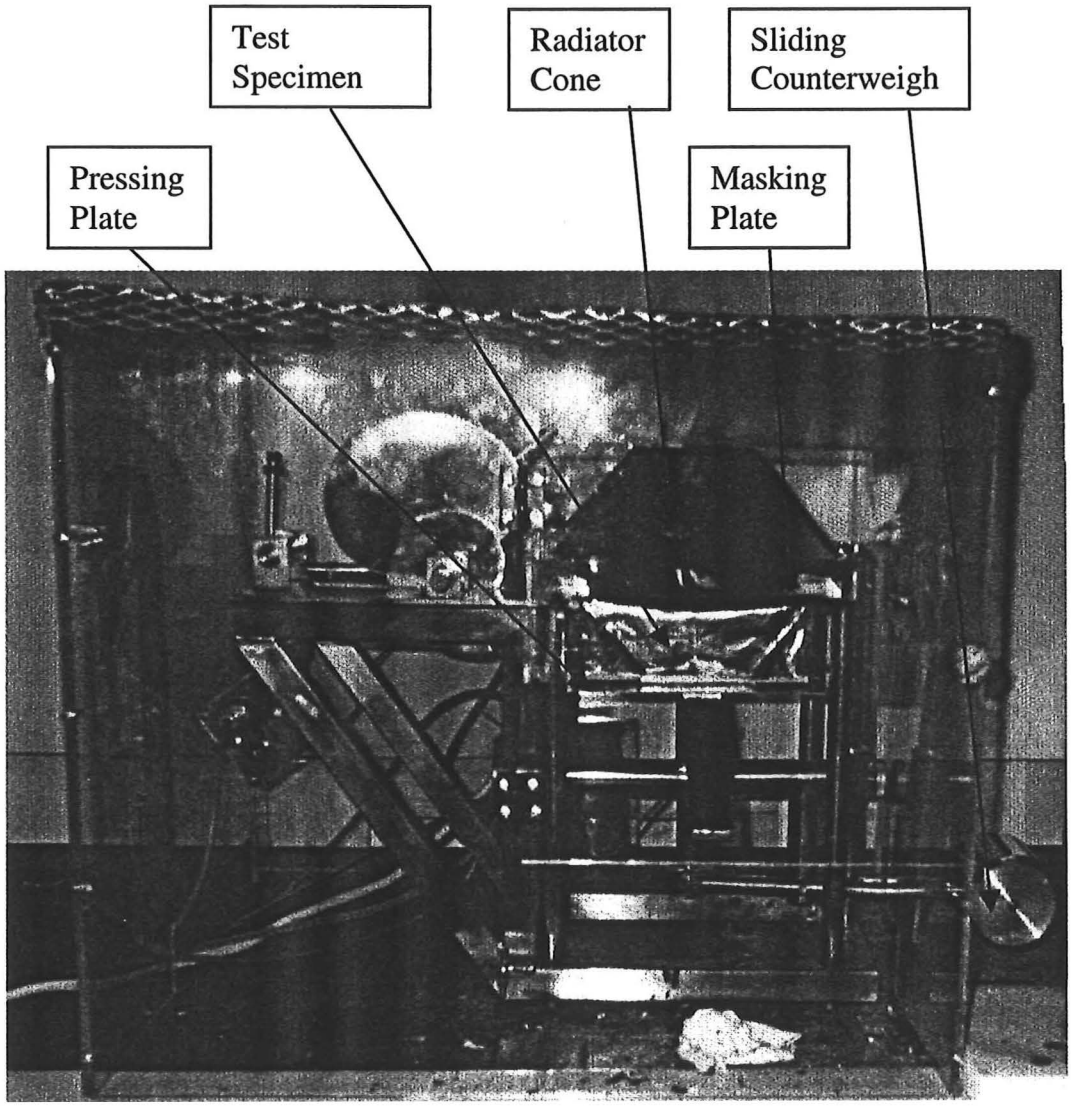

Figure 3-8 Setting up of the ISO ignitability test

Five specimens were tested at each level of irradiance selected and for each different fabric surface as consideration of uncertainty.

For each fabric, a minimum of six heat levels of incident iradiance were applied (40, 35, 30, 25, 20, 15 kW/m^2). Depending on the individual fabric, some further tests were undertaken at lower incident heat fluxes.

In this particular apparatus, heat fluxes corresponding to cone temperature and voltage readings are listed in Table 3-3.

Table 3-3 Cone temperature versus heat flux

Target heat flux (kW/m^2)	Target voltage (mV)	Cone Temperature (^oC)	Target heat flux (kW/m^2)	Target voltage (mV)	Cone Temperature (^oC)
6	1.12	380	17	3.18	573
7	1.31	408	18	3.37	587
8	1.50	431	20	3.74	605
9	1.68	448	25	4.67	650
10	1.87	465	30	5.61	690
11	2.06	482	35	6.54	727
15	2.81	547	40	7.48	757

In this study, a test was terminated in 15 minutes if no sustained surface ignition occurred and deemed that the specimen had not ignited.

Chapter Four

ANALYSIS AND RESULTS

4.1 Characteristic of fabrics

This study investigated the ignition performance of 14 upholstered furniture composites with 1 type foam. About 750 specimens were tested. Characterising the fabrics' heating processes, two categories of fabric were observed. One is the fabric that ignites with charring. Another is the fabric that melts at first and ignites after melting.

The response of igniting (charring) fabrics to heating, proceeds in four partially overlapping stages:

- Inert heating of the fabrics.
- Thermal decomposition, drying, change in shape, splitting, accompanied by the evolution of combustible and non-combustible gases.
- Ignition, which the spark ignites the volatiles.
- Combustion with char formation.

The response of melting fabrics to heating proceeds in four partially overlapping stages as well. They are:

- Inert heating of the fabrics.
- Melting proceeded and accompanied by change in shape, shrinking, splitting, drying and evolution of volatiles.
- Disintegration, shrinking away, falling off, followed by ignition.
- Burning or charring the formation.

Characteristic behaviours of 14 types of composites are listed in Table 4-1. The composite remains of charring fabric- and melting fabric-foam are shown in Figure 4-1 and Figure 4-2, respectively. Fabric 35 presented to be a melting fabric when the

incidence of irradiation was high. When the heat flux was lower (≤10 kW/m^2), part of fabric was staying in place after ignition.

Table 4-1 Characteristics of fabrics

Fabric	Ignition behaviour	Fabric	Ignition behaviour
23	Melting	30	Charring
24	Melting	31	Melting
25	Melting	32	Charring
26	Melting	33	Melting
27	Charring	34	Charring
28	Charring	35	Melting/charring
29	Melting	36	Charring

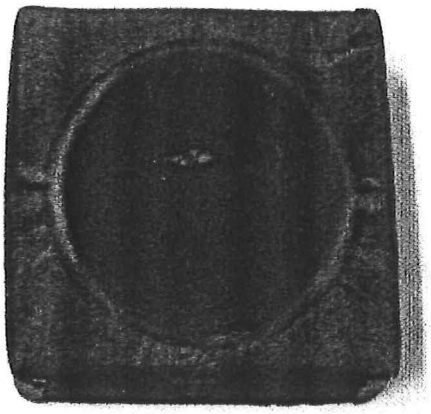

Figure 4-1 The remains of charring fabric and foam composite

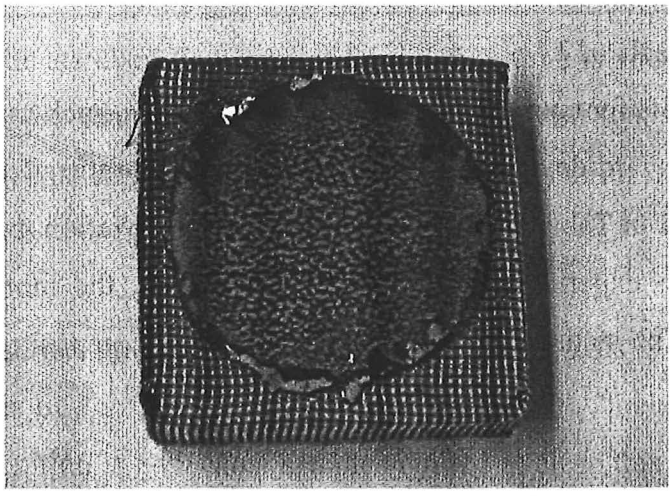

Figure 4-2 The remains of melting fabric and foam composite

4.2 Time to ignition results

The times to ignition for 14 types of fabric-foam composites (14 fabrics and 1 foam) are summarised in Table 4-2.

Table 4-2 Summary of time-to-ignition

Irradiance q_e (kW/m^2)	Time to ignition t_{ig} (s)						
	Fabric 23	**Fabric 24**	**Fabric 25**	**Fabric 26**	**Fabric 27**	**Fabric 28**	**Fabric 29**
40	8	10	10	9	13	15	10
35	9	12	12	10	17	17	11
30	12	15	16	13	21	22	14
25	15	19	20	14	30	28	17
20	20	24	28	17	54	36	22
18	-	-	-	-	70	-	-
17	-	-	-	-	NI	-	-
15	31	38	39	28	NI	56	36
10	88	109	134	81	NI	180	104
8	189	NI	156	122	NI	360	134
7	NI	NI	NI	NI	NI	736	NI
6	NI	NI	NI	NI	NI	NI	NI
Irradiance q_e (kW/m^2)	**Time to ignition t_{ig} (s)**						
	Fabric 30	**Fabric 31**	**Fabric 32**	**Fabric 33**	**Fabric 34**	**Fabric 35**	**Fabric 36**
40	10	8	11	9	9	12	11
35	12	9	12	10	10	12	12
30	16	12	17	13	12	17	16
25	19	14	20	15	18	21	21
20	26	18	29	20	21	28	30
15	42	30	60	31	36	44	49
10	210	89	182	84	159	113	177
8	553	117	512	179	219	695	413
7	NI	NI	NI	NI	NI	NI	NI

The statistics results for composites of Fabric 23 and foam, such as mean, maximum, minimum and standard deviation of ignition time and the ratio of standard deviation to mean, are listed in Table 4-3. The ratio of standard deviation to mean reflects the uncertainty of the experiment. The higher the ratio is, the more uncertainty the experiment has. The statistics results for other types of composites can be found in Appendix B.

Composites with Fabric 27 (nylon pile) and Fabric 28 (cotton with fire retardant addition) had a relatively longer time to ignition than other fabrics did. Fabric 27 had

the highest minimum heat flux among all the fabrics, 17 kW/m^2. Fabric 28 had the lowest minimum heat flux, 6 kW/m^2.

Table 4-3 Statistics results of ignition time for Fabric 23

Irradiance q_e (kW/m^2)	t_{ig}				
	Mean (s)	Max (s)	Min (s)	SD (s)	Ration of SD/mean
40	8	9	7	0.5	0.06
35	9	10	8	0.7	0.07
30	12	13	11	0.9	0.07
25	15	16	14	0.5	0.03
20	20	21	17	1.8	0.09
15	31	35	28	2.3	0.07
10	88	104	72	13.4	0.15
8	189	189	189	-	-
7	NI	-	-	-	-

Notice: NI = No Ignition; SD = Standard deviation

4.2.1 General observations

- The standard deviation of the ignition time data shows that the scatter increases with decreasing incidence of irradiation, but the ratio of the standard deviation to the mean presents another trend. Generally, the smallest ratio of the standard deviation to the mean happens when the incident heat flux is between 20 to 30 kW/m^2. It increases when the incident heat flux is getting lower or higher.

- For a melting fabric, no ignition was observed after 190s (less than 4 minutes), irrespective of incident heat flux. Under a relatively low incident heat flux, $\dot{q}_e'' \leq 10$ kW/m^2, a melting fabric was ignited at close its mean time-to-ignition. In other words, the standard deviation of the ignition time is small. If time elapsed one minute longer than the expected average value and ignition did not occur, then ignition would never happen. But for a charring fabric, ignition at 778s (13 minutes) was observed. This is further described as follows.

Table 4-4 demonstrates an example of such phenomenon. This is a part of test data for the composites of Fabric 33 and foam. With 10 kW/m^2 incident heat flux, the average time to ignition is 84s. Most samples ignited at close this value, except that non-ignition happened in Test 4. It could be inferred from the general observations that under this condition, the ignition would unlikely happen if this type of specimen

is not ignited by 144s (84s+60s=144s). In the same way, with 8 kW/m^2 of incident heat flux, the ignition would unlikely occur after 239s (179s+60s=239s).

Table 4-4 Test results for the composites of Fabric 33/foam

Heat flux (kW/m^2)		10	8
Measured time to ignition (s)	Test 1	83	184
	Test 2	82	174
	Test 3	73	NI
	Test 4	NI	NI
	Test 5	98	NI
	Average	84	179

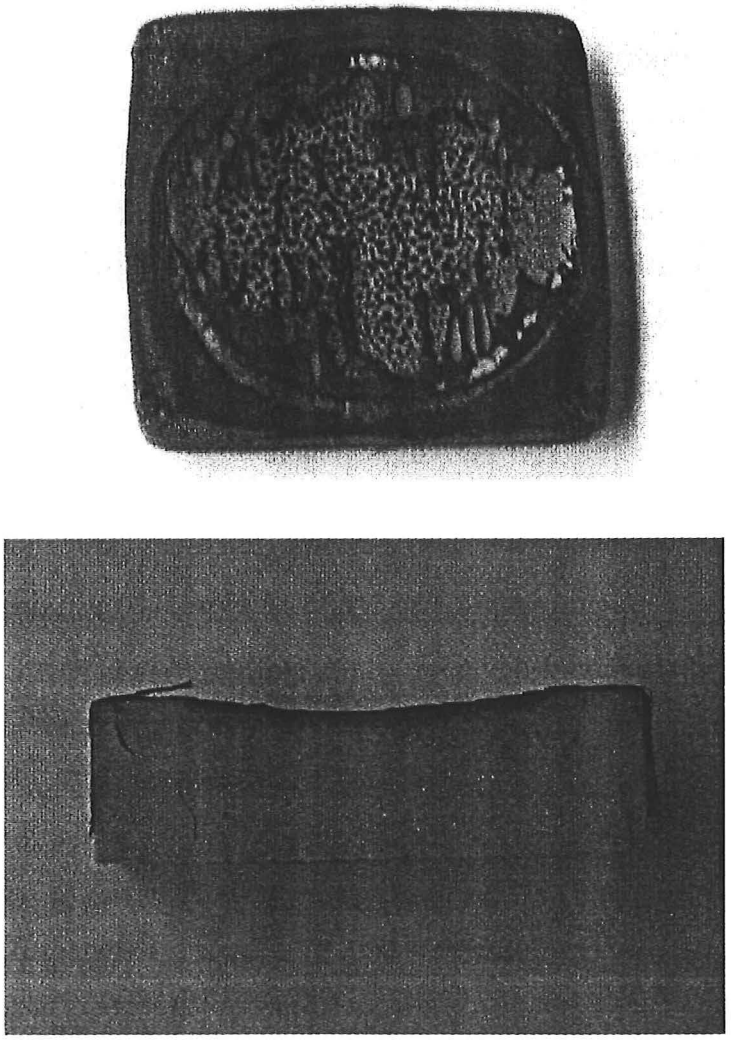

Figure 4-3 The remains of ignited composite (Fabric 31/foam) with the incident heat flux of 8 kW/m^2

- The composite was charring deeply when the ignition did not happen. The remains shown in Figure 4-3 and Figure 4-4 are the identical type of composite (Fabric 31/foam) with the incident heat flux 8 kW/m^2. Figure 4-3 shows the exposure surface and cross-section of the sample that did ignite and its charring formation is relatively thin. Figure 4-4 shows the exposure surface and cross-section of the sample that did not ignite and it was charred deeply.

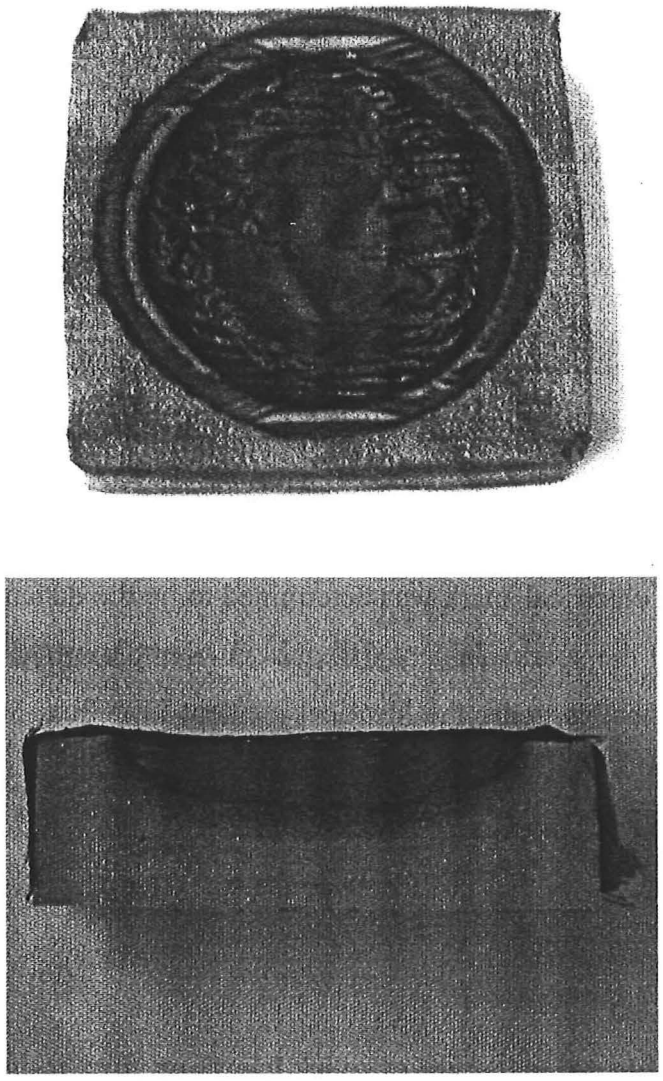

Figure 4-4 The remains of non-ignited composite (Fabric 31 /foam) with the incident heat flux of 8 kW/m^2

- When the incident heat flux was lower, the ignition time was longer, and consequently the char depth was deeper. In other words, the charring depth of foam increases with decreasing incidence of heat flux when ignition occurs.

- Influence of airflow in the test environment was observed to be significant. Table 4-5 shows an example set of test data for Fabric 23/foam composites under 10 kW/m^2 incident heat flux with different air velocities (higher than 0.5 m/s and lower than 0.2 m/s, respectively) in test environment. It is found that under the same conditions, a higher air velocity may delay ignition or result in no ignition.

Table 4-5 Influence of airflow on time-to-ignition

Fabric 23/foam		
V_{air}(m/s)	>0.5	<0.2
Time to ignition (s)		
q_e =10 (kW/m^2)	NI	84
	NI	NI
	NI	72
	NI	104
	127	92

- Influence of the electrical spark length was observed to be significant in the tests. The length of electrical spark was determined to be the distance of the two poles that generated the spark. Table 4-6 shows an example set of test data for Fabric 35/foam composites under the identical incident heat flux, 30 kW/m^2. With the spark length of approximate 7 to 8 mm, the highest ignition time was 21s, while with the spark length of approximate 3 to 4 mm, the ignition time of 48s was observed. This shows that increasing of the spark length will result in decreasing of the time to ignition.

Table 4-6 Influence of spark length on time-to-ignition

Fabric 35/foam		
Spark length (mm)	7~8	3~4
Time to ignition (s)		
q_e =30 (kW/m^2)	16	26
	21	21
	14	24
	18	41
	17	48

4.2.2 Observations for individual type of composite

Under a high incident heat flux, $\dot{q}_e'' \geq 30$ kW/m^2, Fabric 26 was observed to peel from the composite when it was exposed to the heat source. The peeled fabric wrapped the spark igniter. This might exaggerate the uncertainty of the tests and lead to higher ratio of standard deviation to mean.

In the heating process leading up to ignition, the composites of Fabric 27 and foam were observed that flashes occurred prior to the flame becoming sustained.

Before ignition, relatively less pyrolyzate was observed for the composites of Fabric 28 and foam. Ignition started in a small area around the centre of exposure area. After ignition, the flame spread very quickly and black smoke was released.

Fabric 34 was noted to have relative high ratio of standard deviation to mean. In the heating process, the fabric split in certain location, which was fairly dependent on the pattern orientation, and exposed the foam to the heat. When the splitting area was closer to the spark, the composite ignited sooner.

4.3 Correlations of time-to-ignition data

Previous research described in Chapter Two indicated that the time-to-ignition is a function of incident irradiance. Rearranging Equation 2-3 gives Equation 4-1.

$$t_{ig}^{-1/n} = (\dot{q}_e'' - \dot{q}_{cr}'')(FTP)^{-1/n} \qquad \textbf{Equation 4-1}$$

Correlating $t_{ig}^{-1/n}$ versus $\dot{q}_e''$ with a straight line, n is determined when the best-fit line is achieved. In this study, the data is also linearly correlated as t_{ig}^{-1} versus $\dot{q}_e''$ and $t_{ig}^{-1/2}$ versus $\dot{q}_e''$, where the samples are assumed to be thermally thin and/or thermally thick, respectively.

Notice should be taken when correlating the ignition data. According to the ISO Ignitability Test protocol, a specimen is considered to have no ignition if no sustained surface ignition occurs within 15 minutes. When correlating the data for a

non-ignition specimen, t_{ig} is described as infinite and t_{ig}^{-1}, $t_{ig}^{-1/2}$ and $t_{ig}^{-1/n}$ are determined as zero. The mean, maximum and minimum ignition times are plotted on t_{ig}^{-1}, $t_{ig}^{-1/2}$ and $t_{ig}^{-1/n}$ versus $\dot{q}_e''$ graphs in Figure 4-5 for the Fabric 23/foam composites. The correlation for all fabrics can be found in Appendix C.

Table 4-7 Summaries of R^2 and n for linear correlation

Fabric code		23	24	25	26	27
FTP index(n)	best fit value	0.99	0.94	1.03	0.82	0.79
	range	(0.98-1.01)	(0.94-0.95)	(1.02-1.05)	(0.81-0.84)	(0.78-0.80)
R^2	n= best fit	0.9993	0.9954	0.9953	0.9876	0.9926
	n=1	0.9993	0.9946	0.9951	0.9818	0.9811
	n=2	0.9285	0.8894	0.9236	0.8755	0.8159
Fabric characteristic		melting	melting	melting	melting	charring
Fabric code		**28**	**29**	**30**	**31**	**32**
FTP index (n)	best fit value	1	0.88	1.03	0.9	1.16
	range	(0.96-1.01)		(1.02-1.04)	(0.89-0.91)	(1.15-1.18)
R^2	n= best fit	0.9985	0.9982	0.9963	0.9964	0.9954
	n=1	0.9985	0.9957	0.9961	0.9947	0.9918
	n=2	0.9413	0.9024	0.939	0.9057	0.9569
Fabric characteristic		charring	melting	charring	melting	charring
Fabric code		**33**	**34**	**35**		**36**
FTP index (n)	best fit value	0.9	1.02	1.02		1.08
	range	(0.9-0.91)	(1.00-1.03)	(1.02-1.03)		(1.07-1.10)
R^2	n= best fit	0.9983	0.9939	0.9893		0.9973
	n=1	0.9968	0.9939	0.9892		0.9963
	n=2	0.9122	0.9349	0.9235		0.9473
Fabric characteristic		melting	charring	melting/charring		charring

Table 4-7 summarises square of correlation coefficient values, R^2, of the linear correlation and empirical constant n values when the best-fit line is achieved. Generally, the linear correlation with n=1 fits much better than that with n=2. The R^2 value is quite close to the best-fit line when n=1. The composites of the foam-fabric show a quasi-thermally thin property. Further study of the ignition data of the 14 fabrics, indicates that the FTP index, n, of composites with melting fabrics and with charring fabric can be divided into two zones, when their linear correlation is best fit. The linear correlation achieves best fit with a range of $1.16 \geq n \geq 1.0$ for composites with charring fabrics, and with $0.82 \leq n \leq 1.0$ for composites with melting fabrics.

Fabric 23

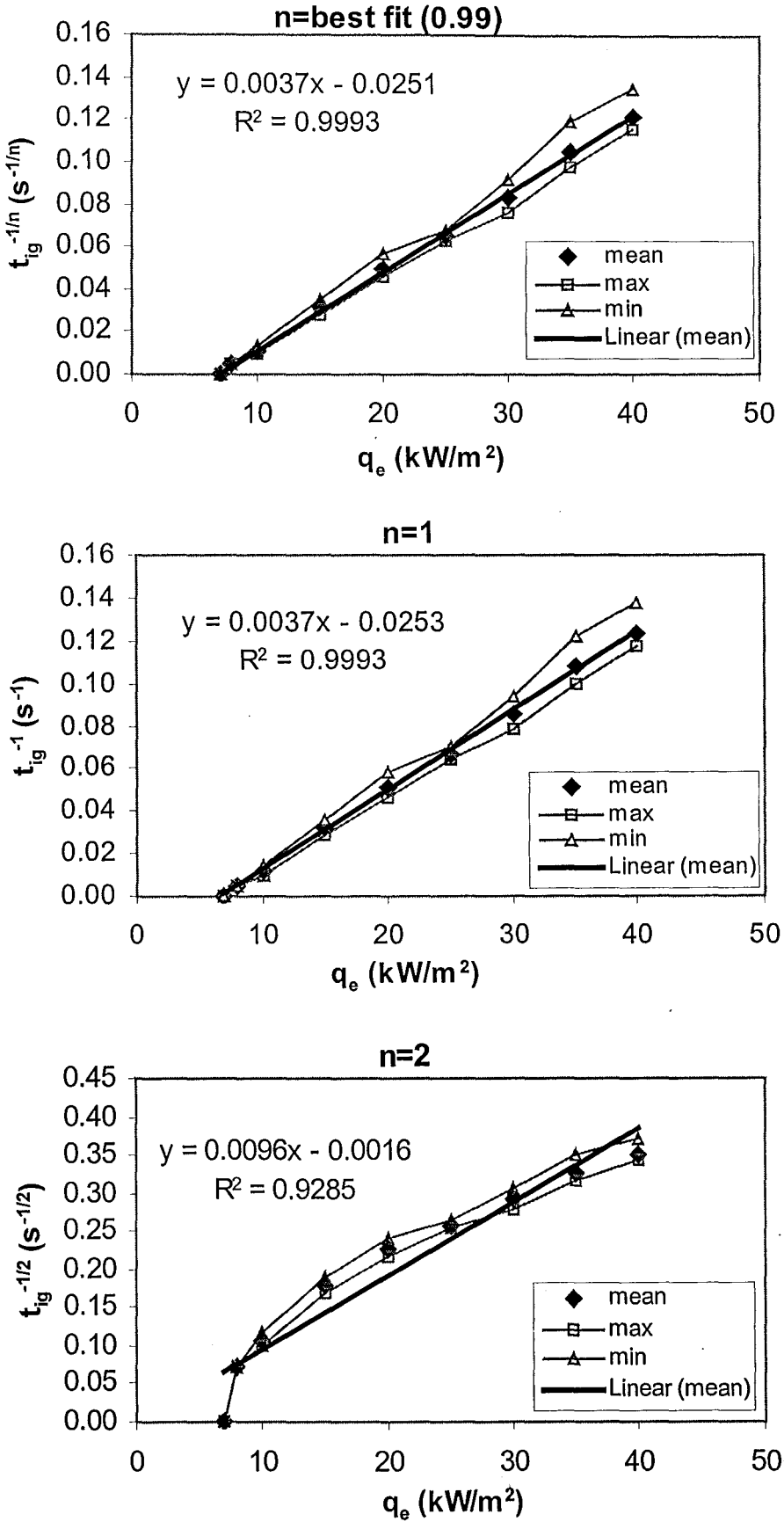

Figure 4-5 Linear correlation for Fabric 23

4.4 Predicting time-to-ignition and the critical heat flux

4.4.1 Analysis time-to-ignition using the Flux Time Product (FTP)

Rearranging Equation 4-1 gives the following form:

$$t_{ig}^{-1/n} = FTP^{-1/n}\dot{q}_e'' - FTP^{-1/n}\dot{q}_{cr}'' = a\dot{q}_e'' + b \qquad \textbf{Equation 4-2}$$

Where,

a the slope of the straight line of the linear correlation in the plot of $t_{ig}^{-1/n}$ versus $\dot{q}_e''$.

b the intercept of the straight line of the linear correlation in the plot of $t_{ig}^{-1/n}$ versus $\dot{q}_e''$.

$$a = FTP^{-1/n} \qquad \textbf{Equation 4-3}$$

$$b = -FTP^{-1/n}\dot{q}_{cr}'' \qquad \textbf{Equation 4-4}$$

From the plot of $t_{ig}^{-1/n}$ versus $\dot{q}_e''$, the slope and the intercept are known. It is easy to obtain:

$$FTP = a^{-n} \qquad \textbf{Equation 4-5}$$

Substituting Equation 4-5 into Equation 4-4, it gives Equation 4-6:

$$\dot{q}_{cr}'' = -\frac{b}{a} \qquad \textbf{Equation 4-6}$$

Equation 4-6 implicates that the critical heat flux is the intercept on the x-axis at $t_{ig} = \infty$, which is the heat flux required to cause ignition after an infinite length of time.

The time to ignition can be predicted by Equation 4-7.

$$t_{ig} = \frac{FTP}{(\dot{q}''_e - \dot{q}''_{cr})^n} \qquad \textbf{Equation 4-7}$$

4.4.2 Analysis time-to-ignition using the linearized thermal ignition model

4.4.2.1 The thermally thin model

This study applied the linearized thermal ignition model for both thermally thin and thermally thick materials to predict the time to ignition. The results were compared with the measurement data.

The linearized thermally thin ignition model described in Section 2.3.5.2, gives a solution for predicting time-to-ignition as below (Equation 2-8):

$$t_{ig} = \rho\, cL_0 \frac{(T_{ig} - T_0)}{(\dot{q}''_e - \dot{q}''_{cr})}$$

The density ρ and the specimen thickness L_o are considered to be independent but it is difficult to measure them separately. In the process of heating up, the material's temperature rises, coupled with evolution of pyrolyzates. This chemical process results in the change of its physical properties. Some materials char while other materials shrink away and melt. Therefore, the density ρ and the specimen thickness L_o are changing with time. The specific heat is a function of the temperature. It is therefore easier that the product of $\rho L_o c$ is calculated from the plot of t_{ig}^{-1} versus $\dot{q}''_e$ by applying the following relationship (Equation 4-8) (SFPE, 2001):

$$\rho L_0 c = \frac{1}{slope(T_{ig} - T_0)} \qquad \textbf{Equation 4-8}$$

Table 4-8 lists the product of $\rho L_0 c$ of composites and masses per unit area of the 14 fabrics.

Table 4-8 The product of $\rho L_0 c$ and mass per unit area of fabrics

Fabric No.	mass per unit area of fabric $(\rho L_0)_{fabric}$ (kg/m^2)	$\rho L_0 c$ (kW/m^2 K)
23	0.23	1.09
24	0.32	1.20
25	0.32	1.29
26	0.20	1.23
27	0.26	0.89
28	0.36	2.17
29	0.27	1.28
30	0.25	1.30
31	0.21	1.21
32	0.33	1.29
33	0.27	1.24
34	0.23	1.13
35	0.36	1.49
36	0.33	1.38
mean	0.28	1.30
standard deviation (SD)	0.06	0.29
SD/mean (%)	19.79	22.03

Notice should be taken that mass per unit area of fabric is a measurement value (equal to the ratio of mass/area of the fabric) for fabric only. The product of $\rho L_0 c$ is a calculated value obtained from the model and is an effective property of the composite.

The values of $\rho L_0 c$ for most fabrics is a range from 1.10-1.50 kW/m^2 K. Fabric 27 (nylon pile)/foam composite obtains the lowest value of $\rho L_0 c$, 2.17 kW/m^2 K. Fabric 28 (fire retardant cotton)/foam composite obtains the highest value of $\rho L_0 c$, 0.89 kW/m^2 K.

The product of $\rho L_0 c$ value for the fabric foam composites can be expressed as:

$$\rho L_0 c = 1.30 \pm 0.29 \quad (\text{kW/m}^2\,\text{K}) \qquad \textbf{Equation 4-9}$$

The critical heat flux $\dot{q}''_{cr}$ can be calculated by the following relationship (Equation 4-10), which is exactly the same as Equation 4-6:

$$\dot{q}''_{cr} = -\frac{\text{intercept}}{\text{slope}} = -\frac{b}{a} \qquad \textbf{Equation 4-10}$$

By submitting Equation 4-8 and Equation 4-10 into Equation 2-8, the time to ignition can be predicted.

4.4.2.2 The thermally thick model

The linearized thermally thick ignition model described in Section 2.3.5.2 gives another solution for predicting time-to-ignition as Equation 2-10:

$$t_{ig} = \frac{\pi}{4} k\rho\, c \frac{(T_{ig} - T_0)^2}{(\dot{q}''_e - \dot{q}''_{cr})^2}$$

Similarly, the product of $k\rho c$ can be calculated by the following relationship:

$$k\rho c = \frac{4}{\pi}\left(\frac{1}{slope(T_{ig} - T_0)}\right)^2 \qquad \textbf{Equation 4-11}$$

The critical heat flux $\dot{q}''_{cr}$ can be calculated by Equation 4-10. By submitting Equation 4-10 and Equation 4-11 into Equation 2-10, the time to ignition can be predicted.

Fire Engineering Guide (SFPE, 2001) summarised the methods for predicting time to ignition and pointed out that when n=1, Equation 4-7 is the same form as thermally thin result in Equation 2-8, where,

$$FTP = \rho\, L_0 c(T_{ig} - T_0) \qquad \textbf{Equation 4-12}$$

When n=2, Equation 4-7 is equivalent to the thermally thick solution given in Equation 2-10, where,

$$FTP = \frac{\pi}{4} k\rho\, c\left(T_{ig} - T_0\right)^2 \qquad \textbf{Equation 4-13}$$

4.4.3 Prediction results for time-to-ignition

In this study, the predicted times to ignition were calculated by n = best fit, 1, 2. Predicting time-to-ignition by FTP is coincident with the linearized thermal ignition model when n is equal to 1 and 2. Figure 4-6 shows the comparative plots of the measured time to ignition versus the predicted time to ignition for Fabric 23/foam composites. Predicted time-to-ignition results for each type of fabrics/foam composites can be found in Appendix D. There are two plots for each type of fabric composites, to present the case with relatively high heat flux levels and over a wider range.

Figure 4-7a is a plot of the predicted time-to-ignition versus measured time-to-ignition for the 14 types of composites. It can be seen that, with n =best fit and 1, the calculated results predict the time to ignition well, while they fit the measured results poorly with n=2.

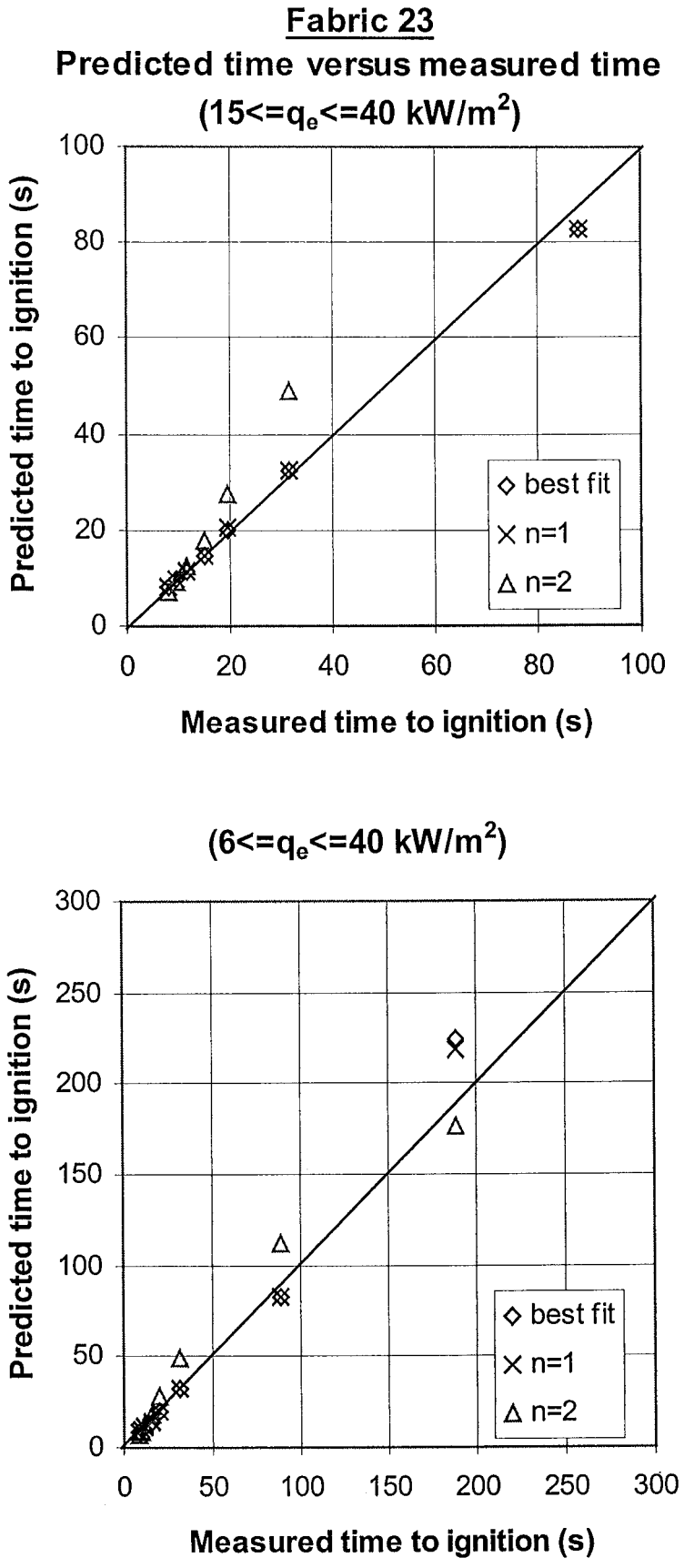

Figure 4-6 Comparative plot of the measured time to ignition versus the predicted for Fabric 23/foam composites

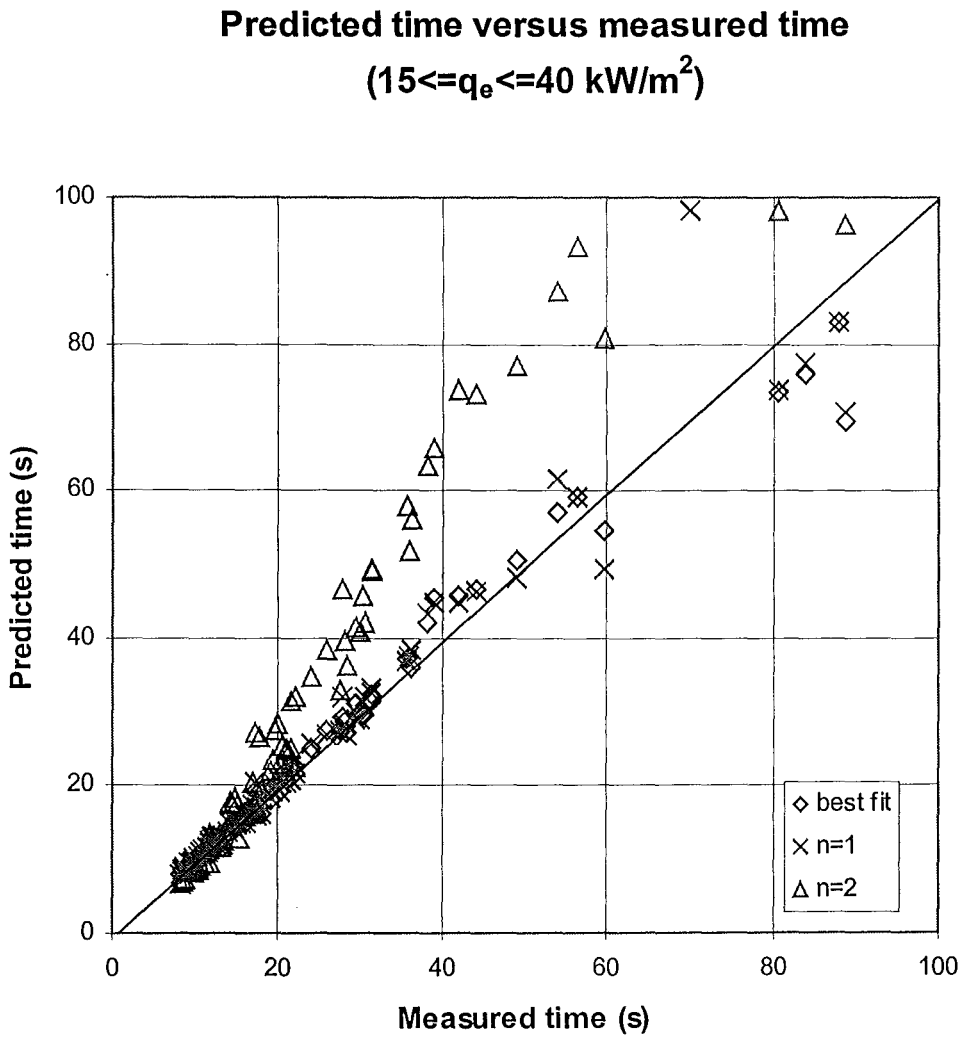

Figure 4-7a Predicted time-to-ignition versus measured time-to-ignition (1)

Table 4-9 lists the percentage of variation between the predicted and measured time-to-ignition when the FTP index is equal to 1, 2 or the value when the best fit correlation achieved, respectively. These values were obtained when external heat flux is $15 \le \dot{q}_e'' \le 40$ kW/m^2, except for the Fabric 27/foam composites, where the values were obtained with $20 \le \dot{q}_e'' \le 40$ kW/m^2. The percentage variation is calculated by Equation 4-14.

$$\Delta\% = \frac{t_{ig,predicted} - t_{ig,measured}}{t_{ig,measured}} X100\% \qquad \textbf{Equation 4-14}$$

It shows in Table 4-9 that the percentage of variation is smaller than 20% when the FTP index, n, is the value with best fit or 1. With n=2, the variation is greater than 20%, and a variation of 60% is observed.

Table 4-9 Variation between predicted and measured time-to-ignition

Fabric Code	Δ%		
	n =best fit	n=1	n=2
23	-2.4~2.9	-2.2~3.5	-19.9~42.0
24	-5.5~9.8	-4.1~12.9	-19.5~60.9
25	-4.3~16.1	-5.3~14.2	-16.0~56.4
26	-11.6~10.9	-10.2~19.4	-40.3~27.8
27*	-2.8~5.9	-3.1~14.5	-24.2~51.7
28	-1.6~4.6	-1.6~4.6	-29.6~40.3
29	-3.8~3.1	-2.8~8.4	-21.5~44.8
30	-6.8~8.9	-7.1~6.8	-25.3~48.8
31	-4.9~7.7	-4.1-12.2	-24.5~43.8
32	-8.5~5.6	-17.3~6.3	-21.3~36.5
33	-4.4~2.0	-3.6~6.1	-29.3~45.5
34	-9.4~6.8	-9.9~5.1	-30.9~33.3
35	-5.8~10.1	-6.1~10.2	-25.9~46.1
36	-2.8~5.4	-3.9~5.9	-23.0~40.1

* The value of Δ% was obtained when $20 \leq \dot{q}''_e \leq 40$ kW/m^2

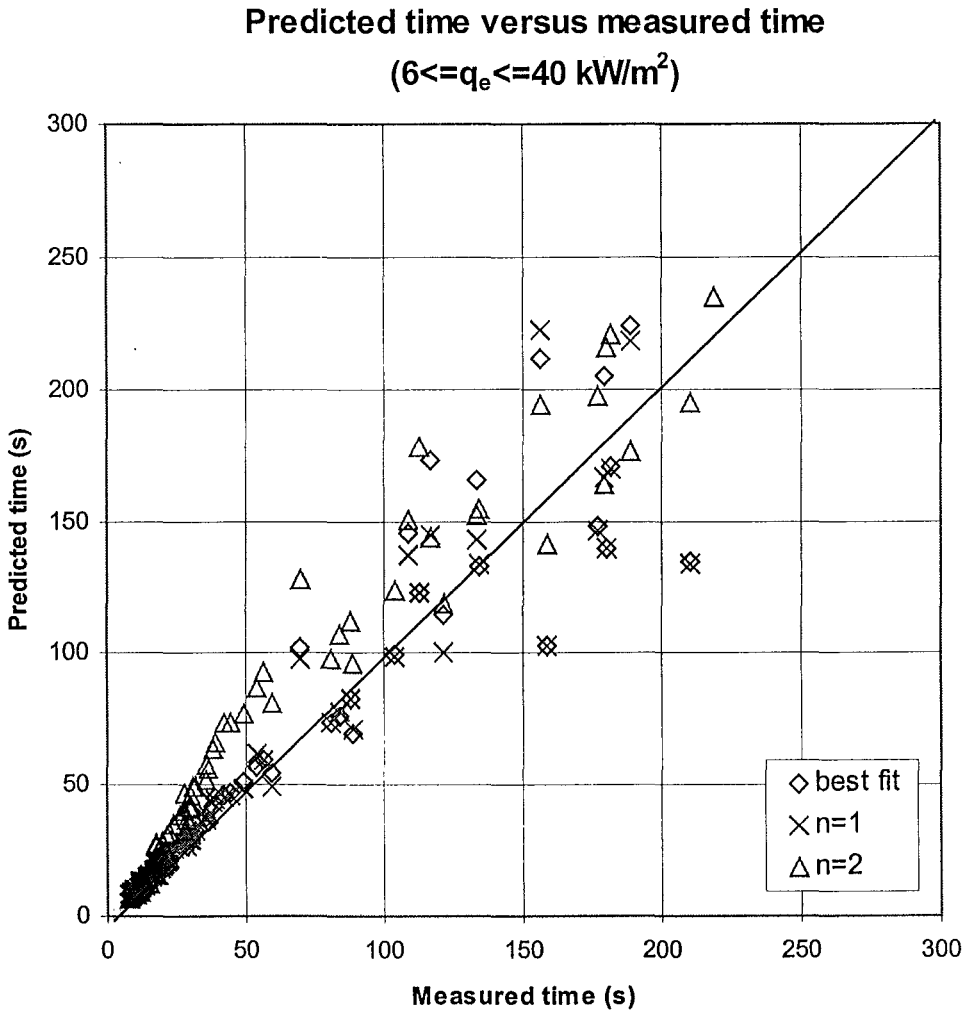

Figure 4–7b Predicted time-to-ignition versus measured time-to-ignition (2)

Figure 4-7b is the same plot as Figure 4-7a, but it presents the case over a wider range. It can be seen that, it generally has a good comparison at high heat fluxes, but poor comparison when approaching the minimum heat flux.

4.4.4 Prediction results for the critical heat flux

In the bench scale test, the heat flux below which ignition cannot occur is defined as the minimum heat flux for ignition, $\dot{q}''_{min}$. Typically the minimum heat flux values are determined by exposing the horizontal sample to various external heat flux values until a value is found at which there is no ignition for about 15 minutes (Tewarson, 1995). Table 4-10 compares the calculated theoretical critical heat flux and the minimum heat flux determined from bench scale tests based on the above definition. The minimum incident irradiances ranged from 6 to 17 kW/m^2. Actually, the minimum heat flux can be some value between the maximum non-ignition heat flux and the minimum ignition heat flux. Table 4-10 also lists bracket values of the minimum heat flux, which were inferred from the test results.

Table 4-10 The critical heat flux and the minimum heat flux

Fabric code.	$\dot{q}''_{cr}$ (kW/m^2) (calculated)			$\dot{q}''_{min}$ (kW/m^2)	
	n=best fit	n=1	n=2	measured	Inferred (bracket value)
23	6.8	6.8	0.2	7	$7<q_{cr}<8$ (7.5)
24	8.2	7.7	0.7	9	$9<q_{cr}<10$ (9.5)
25	7.3	7.5	0.6	8	$8<q_{cr}<9$ (8.5)
26	7.6	6.2	-1.1	8	$8<q_{cr}<9$ (8.5)
27	16.1	14.6	8.6	17	$17<q_{cr}<18$ (17.5)
28	6.3	6.3	0.4	6	$6<q_{cr}<7$ (6.5)
29	7.7	6.8	-0.3	8	$8<q_{cr}<9$ (8.5)
30	7.3	7.5	2.0	7	$7<q_{cr}<8$ (7.5)
31	6.9	6.1	-1.0	7	$7<q_{cr}<8$ (7.5)
32	7.0	7.9	2.3	7	$7<q_{cr}<8$ (7.5)
33	7.0	6.3	-0.6	7	$7<q_{cr}<8$ (7.5)
34	7.1	7.2	1.1	7	$7<q_{cr}<8$ (7.5)
35	6.8	7.0	1.0	7	$7<q_{cr}<8$ (7.5)
36	7.0	7.5	1.7	7	$7<q_{cr}<8$ (7.5)

Again, with n =best fit and 1, the calculated critical heat flux is reasonably close to the measured minimum heat flux. With n=2, the calculated values are further away from the measured values. Some values are smaller than zero, which is physically impossible within the limits of the assumption for the thermal model.

Figure 4-8 plots the distribution of the minimum heat fluxes for 14 fabrics. It shows that 65% fabrics/foam composites' minimum heat fluxes happen at around 7 kW/m^2. Fabric 27 has the highest minimum heat flux among all the fabrics, 17 kW/m^2. Fabric 28, which had been treated with fire retardant additive, has the lower minimum heat flux than any other fabrics do, 6 kW/m^2.

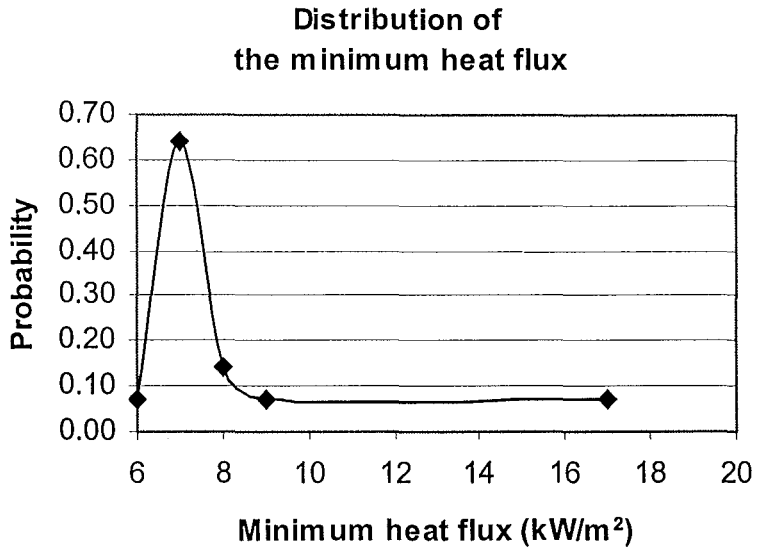

Figure 4-8 Distribution of the minimum heat flux

Figure 4-9 shows the cumulative distribution of the minimum heat flux for 14 type of composites. It was found that the minimum heat flux of 95% fabric/foam composites ranges from 6 to 10 kW/m^2.

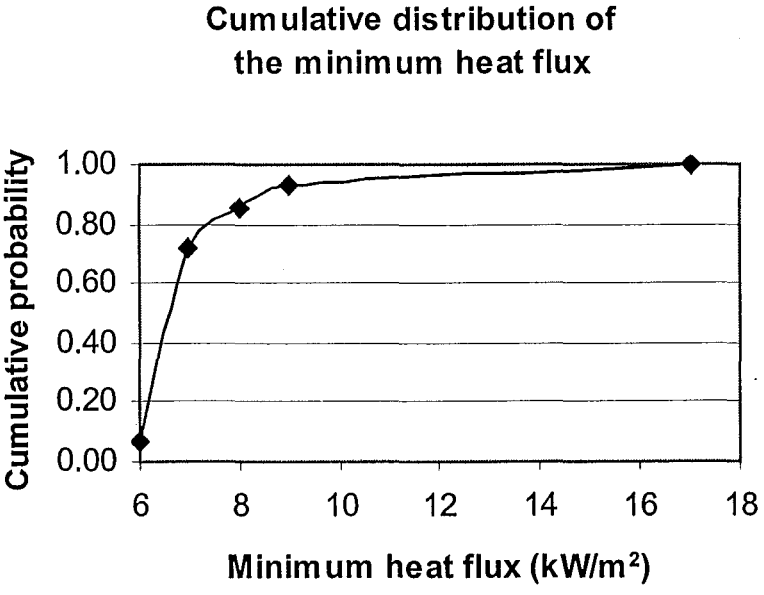

Figure 4-9 Cumulative distribution of the minimum heat flux

Table 4-11 presents the mean and standard deviation of the calculated critical heat flux to ignition, for the composites made up of the 14 types of fabrics and the most commonly used foam in New Zealand, when the FTP index n =best fit and 1. The two sets of results are so close and the critical heat flux can be estimated from the average of $\dot{q}''_{cr} = 7.8$ kW/m^2 with a range of values from 6.1 to 16.1 kW/m^2, as shown in Table 4-10. It can be expressed as form of Equation 4-15:

$$\dot{q}''_{cr} = 7.8 \quad \text{kW/m}^2 \qquad (6.1 \le \dot{q}''_{cr} \le 16.1 \text{ kW/m}^2)$$

Equation 4-15

Table 4-11 Mean and standard deviation of the critical heat flux

	$\dot{q}''_{cr}$ (kW/m^2)		$\dot{q}''_{\min}$ (kW/m^2)
	n= best fit	**n=1**	
mean (kW/m^2)	7.8	7.5	8.0 (8.5*)
SD (kW/m^2)	2.4	2.1	2.7

* The mean of bracket value

As expected, the critical heat flux is smaller than the minimum heat flux. With n =best fit, the minimum heat flux to ignition is 3% ~ 8% ((8.0-7.8)/8.0=3%, (8.5-7.8)/8.5=8%) higher than the calculated critical heat flux to ignition. With n=1, the minimum heat flux to ignition is 6% ~ 12% ((8.0-7.5)/8.0=6%, (8.5-7.5)/8.5=12%) higher than the calculated critical value. Generally, the relationship between the critical heat flux and the minimum heat flux can be simplified as Equation 4-16.

$$\dot{q}''_{\min} = 1.1 * \dot{q}''_{cr}$$

Equation 4-16

4.5 Predicting the effective ignition temperature T_{ig}

The ignition temperature was estimated by assuming a steady state energy balance at the surface. The relationship between the critical irradiance and the ignition temperature was presented in Equation 2-2 as:

$$\varepsilon \dot{q}''_{cr} = h_c(T_{ig} - T_0) + \varepsilon\sigma\,(T_{ig}^4 - T_0^4)$$

The fourth power of temperature makes this equation non-linear and requires iterative solution to solve for T_{ig}. However, it is easy to obtain the results by numerical means.

As the value of the ignition temperature, T_{ig}, is not a measured value by tests, it is a calculated result from the thermal model. Therefore, it is actually an effective value.

h_c, convective heat transfer coefficient (kW/m^2 K)

Surface temperature is a function of external radiant flux as shown in Figure 4-10 for several materials (Quintiere and Harkleroad, 1985). The idealised material represents the conductive heat loss into the solid due to its finite thickness is zero and ε=1. The theoretical curve is based on ε=1 and h_c=15 W/m^2 K, characteristic of the natural convection condition in the test apparatus. It is assumed to be applicable to the test apparatus, and can be used to infer the surface temperature for a material under extended time heating conditions. From Equation 4-15, which was determined from the analysis of the ignition data, the mean critical heat flux for the 14 types of fabric-foam composite is 7.8 kW/m^2. Corresponding to this value in Figure 4-10, the ignition temperature would be 260 °C. The data in this figure suggests that the true surface temperature can be as much as 50 °C below the inferred idealised temperature. This implicates that the true surface temperature of sample may be down to 210 °C. Based on above suggestion, the surface temperature of sample could be somewhere between 210 °C - 260 °C.

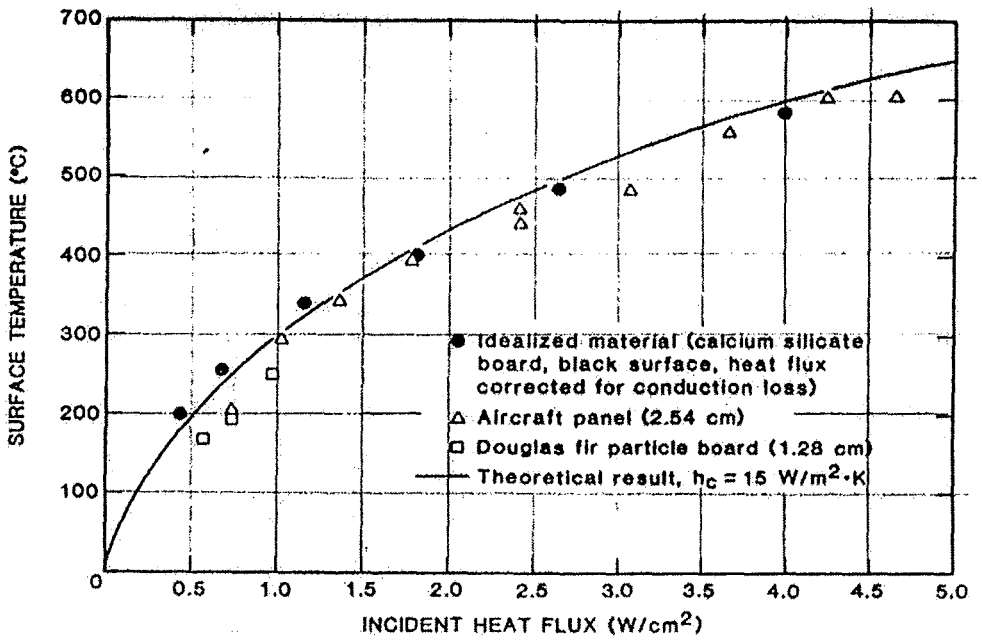

Figure 4-10 Equilibrium surface temperatures as a function of external radiant heating in the test apparatus (Quintiere and Harkleroad, 1985)

The free convective heat transfer coefficient is calculated as the case of horizontal plates (with hot surface up), where formulas derived from first principle are used. The following formulas are used in the calculation (SFPE Handbook, 1995).

$$Nu_L = 0.16 Ra_L^{1/3}, \quad (Ra_L \leq 2\times 10^8)$$
(with constant heat flux)

Equation 4-17

$$Ra_L = \frac{g\beta(T_s - T_o)L^3}{\upsilon\,\alpha}$$

Equation 4-18

Where,

Nu_L Nusselt number

Ra_L Rayleigh number

L Characteristic length (m)

$$L = \frac{A}{P}$$

A Area of exposure area (m^2)

P	Perimeter of exposure area (m)
T_s	Surface temperature (K)
T_o	Ambient temperature (K)
g	Accelerate due to gravity, 9.8 m/s^2
β	The coefficient of volumetric thermal expansion
υ	Viscosity of air (m^2/s)
α	Thermal diffusivity of air (m^2/s)

The convective heat transfer coefficient is 8.8 W/m^2 and 9.3 W/m^2 for the surface temperature of 210 °C and 260 °C, respectively. It is reasonable to use h_c=10 W/m^2 in this study.

Emissivity, ε

Typically, the emissivity of the surface of the material is assumed to be ε=1. Literature reports that the radiant heat source temperature has a significant effect on the material heating over the range of source temperature utilised (700K-1050K) (Thomson and Drysdale, 1988). In this study, the temperatures used by the cone heater were in this range (653K-1030K) as listed in Table 3-3. On the other hand, the surface emissivity is usually greater than 0.8 for common combustibles under infrared conditions (Quintiere and Harkleroad, 1985). So, the effective ignition temperature were also calculated with ε=0.9 and 0.8. The results are shown in Table 4-12. It was found the effective ignition temperature decreases with the decreasing emissivity of the material. Its variation is less than 14 °C when the emissivity decreased by 20%. The ignition temperatures predicted by the thermal thick model (n=2) were found to be lower than 150 °C, which is not applicable in a practical sense.

Most fabric-foam composites were found to ignite between 250 °C to 300 °C. Fabric 27 (nylon pile)/foam composite obtains the highest ignition temperature, around 400 °C. Fabric 28/foam composite (100% cotton with fire retardant addition) is ignited at a lower temperature than any other fabrics, which is under 250 °C.

Table 4-12 Predicted the effective ignition temperatures

T_{ig}							
ε	n= best fit	n=1	n=2	ε	n= best fit	n=1	n=2
Fabric 23				**Fabric 24**			
1	266	265	31	1	294	269	63
0.9	261	259	30	0.9	288	278	60
0.8	253	252	29	0.8	281	271	58
Fabric 25				**Fabric 26**			
1	276	280	55	1	283	251	-894
0.9	270	274	53	0.9	277	245	-916
0.8	262	280	51	0.8	269	237	-942
Fabric 27				**Fabric 28**			
1	414	395	302	1	255	255	44
0.9	409	389	297	0.9	249	249	42
0.8	402	383	289	0.8	242	242	41
Fabric 29				**Fabric 30**			
1	285	265	2	1	276	280	121
0.9	279	259	3	0.9	270	274	117
0.8	272	252	4	0.8	263	267	112
Fabric 31				**Fabric 32**			
1	267	249	-53	1	270	289	136
0.9	261	243	-47	0.9	264	283	131
0.8	254	236	-41	0.8	257	276	125
Fabric 33				**Fabric 34**			
1	270	253	-18	1	271	274	82
0.9	264	247	-15	0.9	265	268	79
0.8	257	240	-12	0.8	258	261	75
Fabric 35				**Fabric 36**			
1	266	269	78	1	271	281	109
0.9	261	263	75	0.9	265	275	105
0.8	253	256	72	0.8	258	268	100

Table 4-13 shows the mean and standard deviation of the effective ignition temperature versus the variation of emissivity (ε=1.0 to 0.8) with n= best-fit value and 1.0, respectively.

Table 4-13 Mean and standard deviation of ignition temperature

	ε	n= best fit	n=1
mean (°C)	1.0	283	277
	0.9	277	272
	0.8	270	266
Standard deviation (°C)	1.0	39	36
	0.9	39	36
	0.8	39	37

Overall the above result shows that the ignition temperature of fabric/foam composites can be determined as Equation 4-19.

$$T_{ig}=280\pm40\ ^{\circ}C \qquad \textbf{Equation 4-19}$$

The convective heat transfer coefficient was checked again as 9.7 W/m^2 when the surface temperature is 320 °C. In this study, that 10 W/m^2 is applied in the calculation is reasonable.

Chapter Five

DISCUSSION

5.1 Characteristics of fabrics

Characterising the heating processes of fabrics, two categories of fabric were observed. One is the fabric that ignites with charring. Another is the fabric that melts at first and ignites after melting. The characteristics of fabrics are mainly dependent on their compositions and content. Polyester is the most common composition existing in fabrics used in upholstered furniture in New Zealand. A cellulosic material, which contains cotton and/or viscose in fabrics, behaves as charring and then ignites when exposed to a heating source. A thermoplastic material, which contains nylon, polyester, polyolefin, polypropylene and/or acrylic, behaves as melting and then igniting when heated up.

Though described by the manufacturer as consists of 100% nylon, Fabric 27 is actually a sort of nylon pile with cotton backing. In this configuration, nylon melts and sticks on the backing. It does not shrink away from the heat source. The melted nylon evolves volatities and becomes charring before ignition. Firstly, nylon is a melting fabric. It explains why its correlated FTP index, n=0.79 (best-fit value), is smaller than 1.0, and it behaves like other melting fabrics. Its ignition behaviour is actually a combination of melting and charring process.

5.2 Ignition modes

A traditional ISO Ignitability Apparatus applied an automatic mechanism which brings a pilot flame above the centre of the specimen once every forth seconds to ignite the pyrolyzates. In this study, two igniters were fitted in this particular test apparatus. One of them is an identical pilot flame igniter to that in the traditional apparatus. Another is an electric spark, which is the same as that in the Cone

Calorimeter. The electric spark igniter was employed for the tests. It was located 13 mm above the surface of the specimen. This may take the advantage of the ISO Apparatus in that test results have slightly smaller standard deviation value as an average (Mikkola, 1991), and the advantages of spark igniter, which provides a reliable ignition source and less uncertainty to the measurement of ignition time. The ignition data obtained in this study would be compatible and comparable to the results with the Cone Calorimeter.

5.3 Time to ignition

5.3.1 Time to ignition versus incident irradiance

The standard deviation of the ignition time data shows that the scatter increases with the decreasing of incident irradiance. This is to be expected since the rate of temperature rise as the surface temperature reaches the ignition temperature is reduced by decreasing the incident heat flux. Any random influences, which affect the heating of the material, will have an exaggerated effect on ignition times at the low heat flux. Therefore, the ratio of standard deviation to mean, which reflects the uncertainty of experiments, is increasing when the incident heat flux is decreasing. On the other hand, when the heat flux increases, the time to ignition decreases. The fabric/foam composite ignites in a few seconds. Because the time to ignition is so short, it is sensitive to measuring errors and any random influences that affect the heating process of the material. Though their standard deviation is relatively small compared to the standard deviation under a lower heat flux, the ratio could be higher because the mean value is so small. This explains why the ratio of the standard deviation to mean is lowest with a certain mid level of incident intensity.

A specimen is supposed to be ignited as long as the incident heat flux is higher than the minimum heat flux in a bench scale test. However, it was observed that if time elapsed longer than 4 minutes for a melting fabric foam composite and ignition did not occur, then ignition would never happen. This time limit for a charring fabric/foam composite can be as long as 13 minutes. This can be explained as follows.

The time to ignition depends upon three factors: (1) the degradative thermal response of the solid to yield the combustible gases – pyrolyzate, which is dependent upon the local instantaneous density and temperature. This is a chemical process, (2) the mixing of the gases with the air; (3) the induction of the temperature-dependent and composition-dependent rate of the combustion reaction to a sufficiently high level to be self-supporting (SFPE Handbook, 1995). This means that an external heat flux should be high enough to cause sufficiently high temperature and sufficient level of the evolution of flammable pyrolysis gases. The mixture of the pyrolyzates with air reaches the lowest flammability limit and is ignited by an electrical spark.

When the ignition does not occur on the fabric/foam composites for some reason, the ignitable condition becomes worse. Firstly, under a certain incident irradiance, the composite evolves pyrolyzates at certain rate and it consumes the fabric and/or foam. The exposure surface of the composite shrinks backward. The distance between the heating source and exposure surface is increasing with time. It results in decreasing the intensity of the incident heat flux and the temperature of pyrolysis zone. This causes less pyrolyzate to be generated. Secondly, melted fabric/foam forms an insulating layer, preventing heat transfer to the pyrolysis zone, and a barrier to the volatile passing through. It decreases the flow of volatile. The concentration of combustible gas is becoming lower by that time and never reaches the lower flammability limit.

5.3.2 Influence of fabric

Fabric 28 was described as a fire retardant fabric by the manufacturer. Its composite has a longer ignition time under the same incident irradiance compared with the other types of composites. It was reported (Eggestad and Johnsen 1987) that the cover fabric seems to make the greatest contribution to the ignitability of upholstered furniture. It is known that most of the fire retardant is accomplished by modification of the molecular structure during pyrolysis to produce a reduction in the fraction of flammable gases and tars (Alvares, 1976). It is probable that fire retardant chemicals will inhibit ignition in a similar manner.

Composite of Fabric 27 and foam has a longer ignition time under the same external heat flux. Fabric 27 is made of nylon face with cotton backing. Melted nylon charred and formed a barrier formation. It retarded the ignition time.

Matching Table 4-2 and Table 4-8, it was noted that the time to ignition of fabric/foam composite is related to mass per unit area of fabrics. The heavier fabrics require the longer ignition time. This is consistent with the previous research. It was also found that fabric composition, construction, colour and pattern significantly influence the ignitability of the composites.

5.3.3 Influence of air flow

The time to ignition is influenced by velocity of airflow in the test environment, as shown in Table 4-5. The convective heat transfer loss increases with the increasing of the air velocity around the surface. It decreases the rate of surface temperature rise. Additionally, the airflow velocity determines the concentration of oxygen and combustible volatities in the ignition boundary layer. The ignition time increases with the increasing of airflow velocity. A high velocity of airflow will delay the ignition or result in no ignition. It is obviously important that the air velocity of the test environment needs to be controlled properly as required by the standard.

5.4 Applicability of simple thermal theory

In this study, it was found that with the flux time product index, n=1, prediction of time-to-ignition shows a reasonably good comparison with the measured data, except when approaching the minimum heat flux. With n=2, the predictions are not as accurate as those are when n=1, as discussed in Section 4.4.3 and Section 4.4.4. This demonstrates that the thermally thin theory is applicable to predict the ignition time of the fabric-foam composites. It is expected and can be explained as follows.

It is assumed that ignition occurs when the surface reaches a material dependent temperature. This is commonly referred to as the critical surface temperature, as described previously. Several researchers have successfully correlated their data

using this technique. It is clear that this critical value is not only dependent on the material property, but also influenced by the heat transfer boundary conditions associated with the configuration of the sample. Usually, thermally thin means a sample thickness less than 1-2 mm (Mikkola and Wichman, 1989). The thickness of a fabric cover falls into this range. As the density of fabric is much higher than that of foam, the thermal conductivity of foam is much lower than that of a fabric. This produces a stratified material with a high - conductivity fabric at the surface and a low conductivity region inside. The foam inside behaves like an insulator for the thin fabric. Therefore, the composite material is ignited as thermally thin.

There are two alternatives to correlate and interpret data.

- There is a fundamental theory from which correlation formulas can be deduced.
- There is no presently fundamental theory from which correlation formulas can be deduced, so it is best to fit the data to an empirical formula.

For the first category, a fundamental formula is usually derived from a mathematical model, based on certain assumptions. Therefore, a theoretical formula has its limitation. When the limitations imposed by the theory are violated, the correlation will fail. For the second category, formulas may take advantage of some fundamental theory and need some modifications, but may go beyond the limitation. In this study, both of the methods were applied to correlate the ignition data. Prediction by using the linearized thermal ignition model falls into the first category. When the linear correlation achieves the highest R^2 value, the index n= best fit is obtained. This n value is an empirical constant. Predicting the ignition time by using the Flux Time Product theory falls into the second category. Fortunately, it is identical for the two methods when FTP index n=1, 2, as where the sample is expected to be thermally thin or thermally thick, respectively.

As we know, the typical value for FTP index is $1 \leq n \leq 2$. Some researchers have theoretically derived it. In this study, it was interesting to find that the linear correlation achieves best fit with $0.82 \leq n \leq 1.0$ for melting fabrics' composites. The n

value is beyond its typical range. It is because the theoretical models for $1 \leq n \leq 2$ has its limitations as follows.

- The mathematical models applied here, are only simple heat transfer models. They assume that heat flow in the solid is one-dimensional, i.e., perpendicular to the exposed surface. This is not a realistic situation. Heat transfer also occurs in the parallel direction to the exposed surface.

- Chemical effects prior to ignition are negligible. It assumes the solid is homogenous and chemically inert. It means that the gas and solid phase problems are greatly idealised. Gas phase complication, such as the interaction of incident radiance with volatile gases leaving the surface and the influences of gas motion along the surface, are ignored. Solid phase complication, such as variable radiant absorption thickness, variable thermal physical and thermal chemical properties, heat transfer and mass transfer in the decomposing solid, are ignored. An upholstered furniture composite consists of fabric cover and foam padding. It is not a homogenous solid. With a melting fabric, the fabric shrinks away from the heating source and exposes the foam to the incident irradiance. The exposure material changes from a fabric to foam. It follows that the thermal physical and thermal chemical properties of the material totally change. This would have significant influences on the heating process toward ignition.

- Convective heat transfer between the volatile gases and the solid is ignored.

- The material is opaque. It means all incident irradiance is absorbed by the exposure surface. Actually at the larger wavelengths, wave transparency occupies relatively high proportion of the irradiation and should not be ignored. It was reported that only about 20% of the incident radiant heat flux is absorbed by the fabric tested before charring begins, but up to 40% after charring (Zuber *et al*, 1973).

- The material is assumed to be grey body and Kirchoff's law is valid, ie, $\alpha=\varepsilon$. The material is idealised in the mathematical models.

- The value of α and ε are assumed to be constant between the start of exposure and the ignition. Actually, generated smoke obscures the incident irradiance. In-depth radiation effects and ambiguities resulting from the emission spectral characteristics of the material and the heat flux are not taken into account in the models. The value of α and ε are variable.

- The heat loss from the surface is assumed to consist of radiation, and convection with a constant convective heat transfer coefficient. This is not true. As the sample is exposed under a heat source, the surface temperature is changing as time passes, and the convective heat transfer coefficient is not a constant.

- For a thermally thin sample, the lumped heat capacity equation is applied, which assumes a uniform temperature across the sample thickness. Heat loss from the rear face and the effect of back material is ignored. For a thermally thick sample, it is assumed to behave as a semi-infinite solid, which means that there is not heat loss from the unexposed surface of the sample, and back material has no effect on the heat transfer of the sample. A pervious study shows that reducing heat losses from the rear of the sample will cause reducing ignition time (Thomson and Drysdale, 1988).

Based on the thermally thin theory and correlation data analysis in this study, it is reasonable to suggest that by applying n=0.9 (an average value of best-fit data for 7 melting fabrics) instead of n=1.0 when correlating the ignition data for the composites with a melting fabric. Use n=1.05 (an average value of best-fit data for 7 charring fabrics) as the flux time product index when correlating the ignition data of a charring fabric. As it is known that correlation of experimental data must have a firm theoretical foundation if they are to be useful. Therefore, this needs further verification by studying more fabrics.

No matter that the FTP index is 0.9 for melting fabric-foam composites and 1.05 for charring fabric-foam composites, both are reasonably close to 1.0. It is reasonable to approximate it as n=1.0 in a general engineering prediction of upholstered furniture. Therefore, it is suitable to simplify the sample as a thermally thin issue.

5.5 The critical heat flux, $\dot{q}''_{cr}$

5.5.1 The critical heat flux $\dot{q}''_{cr}$ and the minimum heat flux $\dot{q}''_{\min}$

As demonstrated previously, the heat flux required to cause ignition after an infinite length of time is defined as the critical heat flux. This is an idealised value for the minimum heat flux. The critical heat flux is a theoretical value derived from a correlation of experimental data. It is obvious that a different calculating method will yield different values of the critical heat flux with large and unreported margins of errors. The minimum heat flux obtained from the bench scale test has allowance for the uncertainty in the test. The critical heat flux from a good data correlation should be smaller than, but close to the minimum heat flux for the same material.

In this study, the critical heat flux obtained from correlation of the ignition data, has a relatively good agreement with the measured minimum heat flux as shown in Table 4-10 and Table 4-11, where the FTP index is equal to 1 or best fit, and satisfies the expectation of $\dot{q}''_{cr} < \dot{q}''_{\min}$. As indicated by Equation 4-16, the calculated critical value $\dot{q}''_{cr}$ is about 90% of the minimum heat flux $\dot{q}''_{\min}$. Literature (Drysdale, 1999) reported that for a wood product, a linear extrapolation of the plot of $t_{ig}^{-1/2}$ versus $\dot{q}''_e$ is likely to give a critical heat flux which is 70% of the true value – the minimum heat flux. This difference between the two results would be subject to the physical characteristic of the fuel and the test environment.

As shown in Table 4-10, calculation with n =best fit has a better prediction of critical heat flux than with n=1 in some degree. It is suggested, that n=0.9 be applied in a correlation for melting fabric-foam composites, and n=1.05 for charring fabric-foam composites if the characteristic is known beforehand. As these values are concluded from the tests of only 14 types of fabric/foam combinations in this study, further research is needed to verify this point, as demonstrated previously (Section 5.4).

Predicting ignition by using the thermally thin theory, where n=1.0 is suitable for engineering use. The predicted critical heat flux fits the measured minimum heat flux reasonably well. The main reason is the fabric cover is basically a thin material. The critical heat flux predicted by the thermally thick theory, where n=2, is again further

away from the measured value. It confirms that the fabrics are not thermally thick fuels.

5.5.2 Comparison with the Cone Calorimeter results

Some researchers have compared the ignitability with the ISO Ignitability Test and that with the Cone Calorimeter. One researcher (Mikkola, 1990) concluded that though ignition times in the Cone Calorimeter test are slightly higher than in the ISO Ignitability test, both tests can be used to measure ignitability. Another study (Östman and Taantaridis, 1990) found that for most materials the ISO Ignitability has greater slope of the linear correlation than the Cone Calorimeter. This means that the times to ignition are longer in the Cone Calorimeter. However, ignition data seem to agree fairly well or at least rank the different materials in approximately the same order. A good agreement was obtained from different researchers.

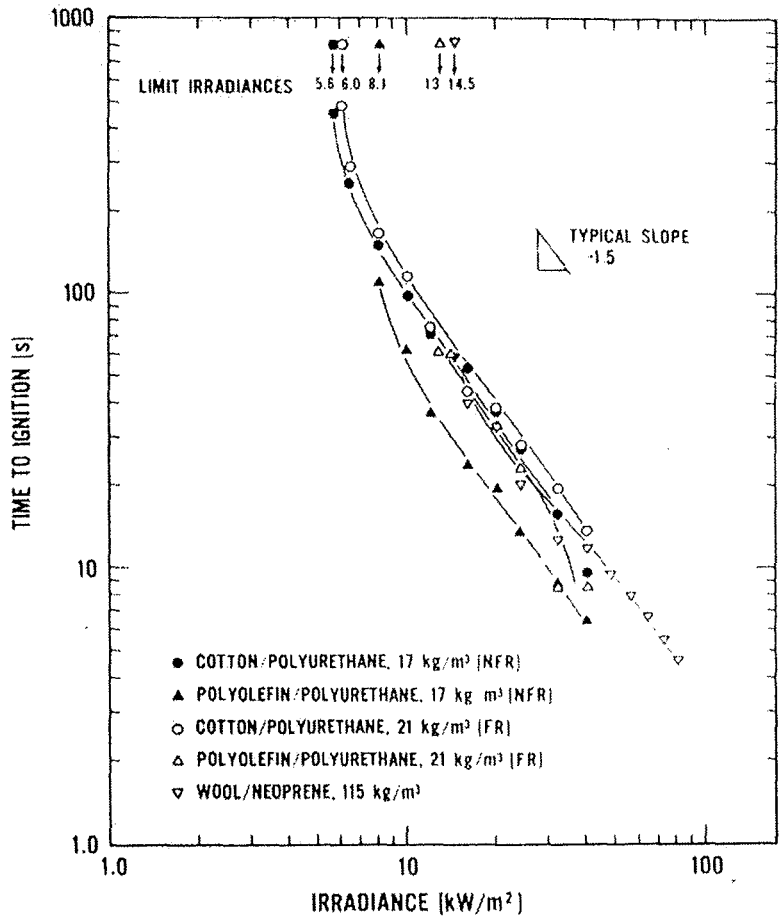

Figure 5-1 Ignitability curve for various fabric/foam assemblies (Babrauskas and Krasny, 1985)

The minimum heat fluxes obtained in this research for the 14 types of fabric-foam composites ranged from 6 to 17 kW/m^2, with 65% at 7 kW/m^2. Babrauskas conducted extensive investigation with the Cone Calorimeter in fabric/foam composites, which represented specimens taken from upholstered furniture in the U.S. (Babrauskas and Krasny, 1985). The irradiance, at which ignition occurred, ranged from 5.6 to 14.5 kW/m^2 as shown in Figure 5-1.

Comparative ignitability for the results with the ISO Apparatus and with the Cone Calorimeter is shown in Table 5-1. The two results are in a good agreement. This difference between the two results can be subject to the following factors.

Table 5-1 Comparative ignitability for the results with the ISO Apparatus and with the Cone Calorimeter

		The ISO Ignitability Apparatus	**The Cone Calorimeter**
Comparison 1			
Composite		Cotton (Fabric 28)/Foam	Cotton/Foam
composition	Fabric	Cotton (FR)	Cotton
	Foam	Polyurethane (27-29 kg/m^3)	Polyurethane (17 kg/m^3)
$\dot{q}''_{min}$ **(kW/m^2)**		**6.0 (6.5*)**	**5.6**
Comparison 2			
Composite		Polyolefin (Fabric 26) /Foam	Polyolefin/Foam
composition	Fabric	Polyolefin (100%)	Polyolefin
	Foam	Polyurethane (27-29 kg/m^3)	Polyurethane (17 kg/m^3)
$\dot{q}''_{min}$ **(kW/m^2)**		**8.0 (8.5*)**	**8.1**

* Bracket value of the test results

- Due to the limited time for testing, very detailed tests have not been done in this study. For example, tests for composites of Fabric 28 and foam were done under these external heat fluxes: 40, 35, 30, 25, 20, 15, 10, 8, 7, 6 kW/m^2. Under 7 kW/m^2, the composites were ignited. Then the testing heat flux went to the next heat flux level, 6 kW/m^2, at which no ignition happened. No more detail test was carried on the heat level between 6 to 7 kW/m^2. The minimum heat flux was determined as 6 kW/m^2. Actually, the minimum heat flux should be somewhere between 6 to 7 kW/m^2, and 6.5 kW/m^2 is a bracket value for this type of composite. So, the minimum heat flux for composite of Fabric 26 and foam is some value between 8 to 9 kW/m^2 with the bracket value of 8.5 kW/m^2.

- The density of polyurethane foam used in this study was 27 to 29 kg/m^3. The density of foam Babrauska used was 17 kg/m^3. Readers should keep in mind that density of the foam material could be a factor in determining its ignitability.

- This difference is subject to different test protocols. Specimens used in the ISO Ignitability Apparatus have a larger exposed surface area and larger thermal mass than the specimens used in the Cone Calorimeter.

- Physical properties of specimens used in the test, such as fabric weave, construction, colour and pattern, are different from lab to lab, though the composition of the fabric could be the same.

- The density of the backing insulation board used in the ISO Ignitability Apparatus was 825 kg/m^3, while the density of the fibre blanket used in the Cone Calorimeter was 65kg/m^3.

- The way of aluminium wrapping is different in the ISO Ignitability Test and the Cone Calorimeter. It could affect the ignitability of the samples.

5.5.3 The critical heat flux $\dot{q}''_{cr}$ versus material properties $\rho L_o c$

The prediction of the ignition is highly dependent upon the material properties, especially the product of density, thickness, and specific heat ($\rho L_o c$). In the matching of Table 4-8 and Table 4-10, it was found that the composite with Fabric 27 has the smallest value of $\rho L_o c$, but it has the highest critical/minimum heat flux. The composite with Fabric 28 has the biggest value of $\rho L_o c$, but it has the lowest critical/minimum heat flux.

The product of $\rho L_o c$ is a property of the composite of fabric and foam, which is considered as one fuel. Let us consider this item separately. The product of ρL_o [kg/m^2] is mass per unit area of the composite. (Notice should be taken here that this value is distinguished from the one in Table 4-8, which is mass per unit area of fabric only.). The product of $\rho L_o c$ (kJ/m^2 K] is actually the heat needed for a unit area of the material to rise one degree (K or °C) of its temperature. A smaller $\rho L_o c$ implies

that the material needs less heat for the same temperature rise. With the same incidence of heat flux, the temperature of the material rises higher. Consequently, the surface temperature of the material is higher. It results in more heat loss by both of radiative and convective heat transfer, of which the critical heat flux consists. This explains why the composite of Fabric 27 and foam, whose $\rho L_o c$ value is the lowest, has the highest critical heat flux and ignition temperature. The same explanation is suitable for the composite of Fabric 28 and foam has the lowest heat flux and the ignition temperature.

5.6 The effective ignition temperature T_{ig}

Analysis methods used in this study are based on the same fundamental assumption, that is, ignition occurs when the surface reaches a critical temperature. This critical temperature is the ignition temperature. Literature (Delichatsios *et al*, 1991) reported that the time to ignition for a fixed horizontal geometry corresponds very closely to the time at which the surface temperature reaches the pyrolysis temperature, which can be measured by a surface thermocouple. The ignition temperature can be understood as the lowest temperature of air passing around the fuel surface and causing it to produce combustible volatities at a rate, which is sufficiently high for ignition by a small electrical spark (Zuber *et al*, 1973). Ignition temperature has proved to be a useful ignition criterion for engineering purposes.

It was found that the 14 types of fabric/foam composites ignited between 250 °C and 300 °C (Table 4-12). It is lower compared with previous report (Zuber *et al*, 1973), where pilot ignition temperatures for fabric are considered to be between 300 °C to 390 °C. This difference may be subject to the following factors.

- Firstly, in this study the ignition temperatures between 250 °C and 300 °C are not measured values. They were calculated from the critical incident irradiance $\dot{q}''_{cr}$ by Equation 2-2, in which it is assumed the critical heat flux is the surface loss by radiative and convective heat transfer. It is an effective ignition temperature, which is subject to the error of the mathematical model in the correlation of ignition data. The reported ignition temperature 300 °C to 390 °C was a measured value, which is subject to uncertainty in the experiment.

- Secondly, this effective ignition temperature is not for the fabric cover only. It is a result of the fabric and foam composite. The interactions of fabrics and foams control the ignition, although the ignitability of the composites might be actually determined by the fabric alone, the foam initially acting as an insulating substitute. It might be argued that the above case is suitable for a composite with a charring fabric. For a composite with melting fabric cover, the fabric shrinks away and exposes the foam to the heat source. The ignitability of the composite may be more determined by the foam. Anyway, both agree on the combination result of fabric and foam.

- Thirdly, the reported ignition temperature 300 °C to 390 °C was obtained for fabric only from the Setchkin Furnace, where a fabric was heated convectively (Zuber *et al*, 1973). The composites in this study were heated up radiatively by a conical radiator.

The ignition of composite with Fabric 27 always occurred after flame flashes. This can be explained by the analogy with combustible liquids of the flash point and the fire point. The flash point is its temperature (presumed to be uniform) at which the volatile and air mixture lying just above its surface is capable of marginally supporting a momentarily flashing propagation of a flame when prompted by a pilot spark. The fire point is very similar to the flash point, except that the flame does not merely flash and cease, but must also be marginally self-sustained so as to continue burning (SFPE Handbook, 1995). Obviously the flash point is lower that the fire point. For Fabric 27, the difference of the flash point and the fire point would have been greater than that of other fabrics. It takes a longer time for the temperature to rise from its flash point to the fire point. The time difference is long enough for it to be observed visually.

Fabric 27 consists of nylon face and cotton backing. It has the highest ignition temperature. One factor is that it has the lowest $\rho L_o c$ value. It was explained in Section 5.5.3. Another factor is that it has high ratio of cotton. The pile fabrics' ignition time appeared to be longer at higher rayon/cotton ratios (Hilado and Brauer, 1979).

The composite with Fabric 28, which is nominated as a fire retardant fabric by manufacturer, has the lowest ignition temperature. It can be explained that fire retardant addition reduces the decomposition temperature of cotton and the amount of retardant was insufficient to provide self-extinguishing properties. Sufficient retardant has to be added to make the fabric self extinguishing (Reeves and Smitherman, 1978). The reduced decomposition temperature makes the fuel generate a sufficient amount of pyrolyzates to cause ignition at a lower temperature than would have been available without the retardant.

The effective ignition temperature is a derived temperature from an approximate model. As long as the piloting conditions and models of ignition are consistent with an inert solid, it is probably a good general value to use. As the ignition temperature is a surrogate condition for a gas-phase flammable limit, it is probably dependent on sample size, orientation and oxygen concentration (Quintiere and Harkleroad, 1985).

Though the ignition temperature is a useful criterion for engineering purposes, it is necessary to keep in mind that there are circumstances when the use of this criterion will predict ignition, but in fact ignition will not occur. As the case described in Section 5.3.1, a specimen was exposed for a prolonged period of time to a flux approaching to the minimum heat flux for piloted ignition and no ignition occurs. The solid fuel will become fully exhausted and develop a thick layer of char. A subsequent increase in the incidence of heat flux might cause the surface temperature to rise above the critical value, but ignition may occur.

5.7 Engineering application

The objective of this project is to evaluate the ignitability of New Zealand upholstered furniture. It aims to predict the time to ignition of the furniture. In practice, it is difficult to estimate the ignition of furniture for various designs and various compositions. It would be significant to have a general prediction of the time to ignition in the engineering design.

As demonstrated in Sections 4.4.2, the time-to-ignition is given by Equation 2-8 as:

$$t_{ig} = \rho\, cL_0 \frac{(T_{ig} - T_0)}{(\dot{q}''_e - \dot{q}''_{cr})}$$

Equation 4-9,Equation 4-15 and Equation 4-19 give as:

$$\rho\, L_0 c = 1.30 \pm 0.29 \quad (\text{kW/m}^2\,\text{K})$$

$$\dot{q}''_{cr} = 7.8 \qquad (\text{kW/m}^2)$$

$$(6.1 \le \dot{q}''_{cr} \le 16.1\ \text{kW/m}^2)$$

$$T_{ig}=280\pm40\ ^{\circ}\text{C}$$

By substituting these mean values into Equation 2-8, assuming T_o=20°C, it gives Equation 5-1, which estimates the ignitability of a fabric-foam composite.

$$t_{ig} = \frac{338}{(\dot{q}''_e - 7.8)}\ (\text{s}) \qquad \textbf{Equation 5-1}$$

When applying Equation 5-1, it should be noticed that the values of ignition temperature T_{ig}, the critical heat flux $\dot{q}''_{cr}$ and the property of composites $\rho L_o c$ are mean values with variations. Large uncertainties in the calculation are included. It is suggested to be used when sufficient information is unavailable. However, it is suitable in engineering application.

5.8 Effect of specimen orientation

In this particular study, the ignition of the specimen using the ISO Ignitability Apparatus was only in a horizontal orientation (the exposure surface facing up). Previous research (Shields *et al*, 1993) indicated that for wood based specimens in a ceiling orientation (the exposure surface facing down) or vertical orientation, the mean times to ignition have significantly greater than those obtained for specimens in the horizontal orientation. This effect would be valid for fabric/foam composite. Fortunately, the results from this study, which is in the horizontal orientation, are on the conservative side.

5.9 Uncertainty of the test

It was noticed that, some researchers reported that the times to ignition in the Cone Calorimeter are shorter (Shields *et al,* 1993, Babraukas and Parker, 1987), while some others demonstrated that the ignition times in the Cone Calorimeter test are slightly higher than in the ISO ignitability test (Mikkola, 1991). This indicates that the two test methods are subject to some uncertainty and it can not be concluded by some simple comparisons.

In pursuing a general comparison of the times-to-ignition obtained with the ISO Apparatus or a Cone Calorimeter, some external physical factors which may generate uncertainties of the tests must be considered:

- Test environment. This includes ambient temperature and relative humidity, and airflow velocity. This may be different from one lab to another.
- The material properties of the backing boards. Conductivity of the board, which will affect heat transfer in the specimen, is dependent on the density of the material. So, the density of backing material in service needs proper control.
- Operation protocol of tests should be strictly followed.
- The calibration of the ignition apparatus has influence on the ignition result. It is important to allow the apparatus to heat up to equilibrium. When the heater attained a specified temperature, it was found that the reading of the millivolt-measuring device exhibited a cycle variation. It is suggested that calibration period be long enough to eliminate the effect of these cycles.
- As each ISO Ignitability Apparatus is constructed individually, its elements and wiring of electrical and control circuit would change from lab to another.
- Uncertainty might be caused from operation of different individuals, electrical interference, size of spark and so on.

Chapter Six

CONCLUSIONS

- Characterising the heating process leading up to ignition, fabrics can be mainly divided into two categories - charring and melting. This characteristic of a fabric is dependent on its composition and content. A fabric containing cotton and/or viscose behaves as a charring material. A fabric consisting of nylon, polyester, polyolefin, polypropylene and/or acrylic behaves as a melting material.

- It is applicable to use the thermally thin theory to predict the ignition time of the fabric/foam composites in the engineering calculation. The foam behaves like an insulating substrate for the thin fabric. Before sufficient research are carried out, the use of the thermally thin theory is recommended to predict the ignitability of upholstered furniture for engineering design. The thermally thick theory is not suitable in predicting the ignitability of the composites of upholstered furniture.

- Plotting $t_{ig}^{-1/n}$ versus $\dot{q}_e''$, the best fit to ignition data is achieved when the Flux Time Product index is $0.82 \leq n \leq 1.0$ for melting fabric/foam composites and $1.16 \geq n \geq 1.0$ for composites with charring fabrics, respectively. In general, the best fit is achieved when n=0.9 for melting fabrics/foam composites correlation, and n=1.05 for charring fabrics/foam composites correlation.

- The calculated critical value $\dot{q}_{cr}''$ from mathematical models is approximately 90% of the minimum heat flux $\dot{q}_{\min}''$ from bench scale tests. Their relationship can simplified as:

$$\dot{q}_{\min}'' = 1.1 * \dot{q}_{cr}''$$

- The minimum heat fluxes for upholstered furniture composite range from 6 kW/m^2 to 17 kW/m^2. The minimum heat fluxes of over 65% of composites were 7 kW/m^2. With 95% confidence, the critical heat flux for the composites of New Zealand upholstered furniture can be predicted as:

$$\dot{q}''_{cr} = 7.8 \qquad \text{kW/m}^2$$

$$(6.1 \leq \dot{q}''_{cr} \leq 16.1 \text{ kW/m}^2)$$

- Most ignition temperatures of the composites are predicted to be between 250 °C to 300 °C. Composites of fire retardant fabric and foam obtained a relative lower ignition temperature than those without treatments. The predicted ignition temperature for the composites of New Zealand upholstered furniture is:

$$T_{ig}=280\pm40 \text{ °C}$$

- When insufficient information is available, the following relationship can be used as an estimation of ignitability of fabric/foam composites.

$$t_{ig} = \frac{338}{(\dot{q}''_e - 7.8)} \qquad \text{(s)}$$

- With an incident heat flux approaching to the minimum heat flux, ignition is expected in less than 4 minutes for the composites with a melting fabric. With a charring fabric, ignition of composites is expected in a much longer time. It is dependent upon the physical and chemical properties of the materials. Ignition time of 13 minutes was observed.

- Test results with the ISO Ignitabiliy Apparatus have slightly smaller standard deviation value as an average. It is recommended the ISO Apparatus with electrical spark be used in an ignitability test. The test results in this study are comparable to those with the Cone Calorimeter. It shows a good comparison between the two methods.

- The airflow velocity of the test environment has significant influence on the ignitability of fabric-foam composites. Even low velocity airflow will delay ignition or results in no ignition.

Chapter Seven

RECOMMENDATIONS FOR FURTHER WORK

- More tests are recommended as a part of this project, including testing the ignitability of the foam block without fabric cover by using the ISO Ignitability Apparatus for comparison with the results in this study.

- In this research, only one type of polyurethane foam is investigated. The influences of the density and the fire retardant addition of the foam on the ignitability of upholstered furniture composite need to be further studied.

- More tests are recommended as another part of this project. Test the ignitability of the composites of the fabric and an insulating material backing, by using the ISO Ignitability Test. A study could then be carried out as to whether the foam performs the same as an insulating material.

REFERENCES

Alvares, N.J. (1976), Ignition Inhibitors for Cellulosic Materials, University of California.

Atreya, A. (1995), 'Convective heat transfer'. In SFPE Handbook of Fire Protection Engineering. 2nd Ed., National Fire Protection Association, Massachusetts. pp 1-39-64.

Babraukas, V, and Parker, W.J. (1987) Ignitability Measurements with the Cone Calorimeter, *Fire and Materials*, Vol. 11, 31-43.

Babraukas, V. and Krasny, J.F. (1991) 'Upholstered Furniture and Mattresses'. In: *Fire Protection Handbook.* 17th Edition. Ed: A.E. Cote. The National Fire Protection Association. pp 3/123-132.

Babrauskas, V. and Krasny, J.F. (1985), Fire Behaviour of Upholstered Furniture, NBS Monograph 173 (U.S.), National Bureau of Standards.

British Standard BS 476; Part 13: 1987. *Method of Measuring the Ignitability of Products Subjected to Thermal Irradiance*, Fire Tests on Building Materials and Structures.

BS 476: Part 13:1987, Method of Measuring the Ignitability of Products subjected to Thermal irradiance, Fire Tests on Building Materials and Structures. *British Standard.*

Delichatsios, M.A., Panagiotou, T. and Kiley, F. (1991), The Use of Time to Ignition Data for Characterising the Thermal Inertial and the Minimum (Critical) Heat Flux for Ignition or Pyrolysis, *Combustion and Flame*, Vol. 84, 323-332.

Denize, H.R. (2000) *The Combustion Behaviour of Upholstered Furniture Materials in New Zealand*, ME thesis, The University of Canterbury.

Drysdale, D. (1999), *An Introduction to Fire Dynamics*. Second edition. John Wiley and Sons Ltd, Chichester, pp 212-222.

Effestad, J. and Johnsen, A.C. (1987), Effects of Interliners on the Ignitability of Upholstered Furniture, *Journal of Fire Science*, Vol. 5, 152-161.

Hilado, C.J. and Brauer, D.P. (1979), Ignitability of Furniture Upholstery Fabrics: Effects of Fibre Composition, Fabric Construction, and Backcoating, *Journal of Coated Fabrics*, Vol. 8, 205-225.

Janssens, M. (1991), A Thermal Model for Piloted Ignition of Wood Including Variable Thermophysical Properties, *Fire Safety Science* 3, 167-176.

Mikkola, E. (1991) Ignitability Comparison between the ISO Ignitability Test and the Cone Calorimeter, Journal of Fire Science, Vol. 9, July/August, 276-284.

Mikkola, E. and Wichman, I.S. (1989) On the Thermal Ignition of Combustible Materials, *Fire and Materials*, Vol. 14, 87-96.

Östman, B.A.L. and Taantaridis, L.D. (1990), Ignitability in the Cone Calorimeter and the ISO Ignitability Test, *Interflame '90*, Swedish Institute for Wood Technology Research, Sweden.

Paul, K.T. (1986) Fire and Upholstered Furniture, *Fire and Materials*, Vol 10, 29-39.

Quintiere, J.G. and Harkleroad, M.T. (1985), New Concepts for Measuring Flame Spread Properties, *Fire Safety: Science and Engineering*, ASTM STP882, T.Z. Harmathy, Ed., American Society or Testing and Materials, Philadelphia, 239-267.

Reeves, W.A. and Smitherman, J.E. (1978), Ignition Characteristics of Fire Retardant Cotton and Polyester/Cotton Fabrics, American Dyestuff Reporter, Vol. 67, No. 9, 64-85.

SFPE, *Fire Engineering Guide*: *Piloted Ignition of Solid Materials Under Radiant Exposure*, Society of Fire Protection Engineers, 2001.

Shields, T.J., Silcock, G.W. and Murray, J.J. (1993) The Effects of Geometry and Ignition Mode on Ignition Times Obtained Using a Cone Calorimeter and ISO Ignitability Apparatus, *Fire and Materials*, Vol. 17, 25-32.

Shields, T.J., Silcock, G.W. and Murray, J.J. (1994) Evaluating Ignition Data Using the Flux Time Product, *Fire and Materials*, Vol. 18, 243-254.

Simms, D.L. (1960) Ignition of cellulosic materials by radiation, *Comb. and Flame*, Vol. 4, 293-300.

Tewarson, A. (1995), ' Generation of Heat and Chemical Compounds in Fires'. In SFPE Handbook of Fire Protection Engineering. 2nd Ed, National Fire Protection Association, Massachusetts. Pp 3-53-124.

Thomson, H.E. and Drysdale, D.D. (1988), An Experimental Evaluation of Critical Surface Temperature as a Criterion for Piloted Ignition of Solid Fuels, Fire Safety Journal, Vol. 13, 185-196.

Toal, B.R., Silcock, G.H. and Shields, T.J. (1989) An Examination of Piloted Ignition Characteristics of Cellulosic Materials Using the ISO Ignitability Test, *Fire and Materials*, Vol. 14, 97-106.

APPENDICES

Appendix A Fourteen Fabric Samples

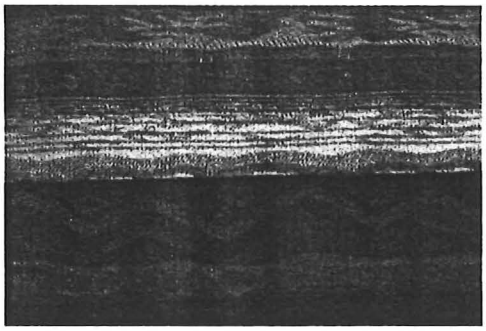

Fabric 23

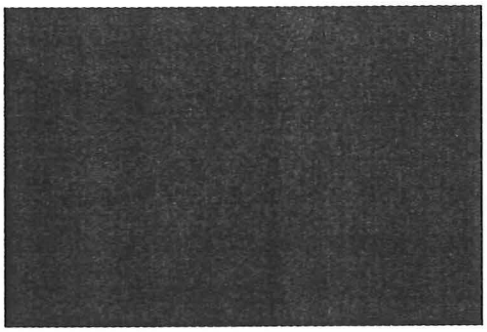

Fabric 24

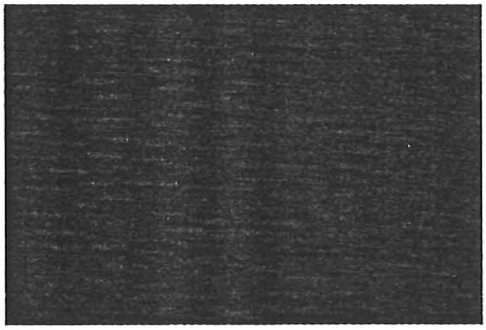

Fabric 25

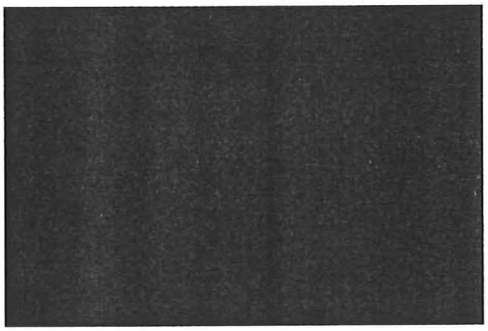

Fabric 26

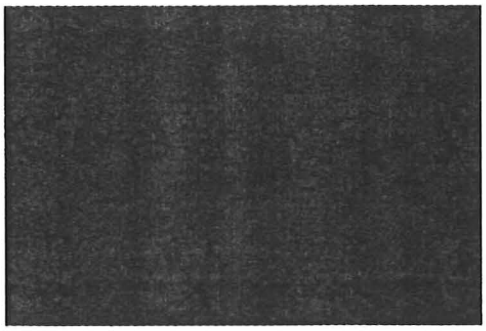

Fabric 27

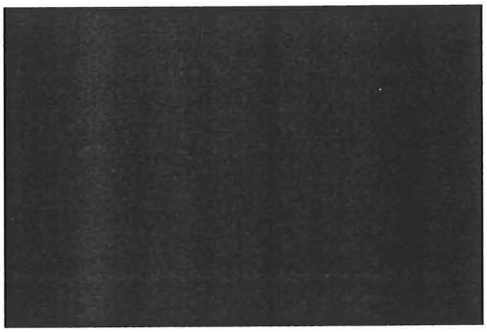

Fabric 28

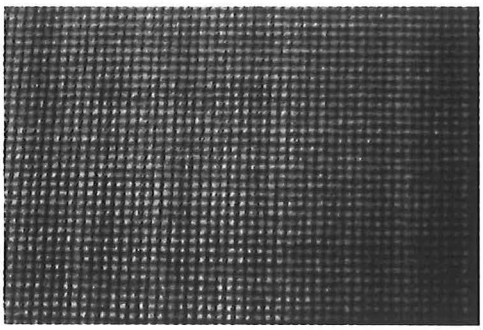

Fabric 29

Fabric 30

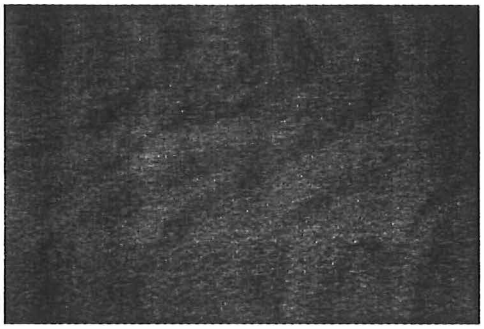

Fabric 31

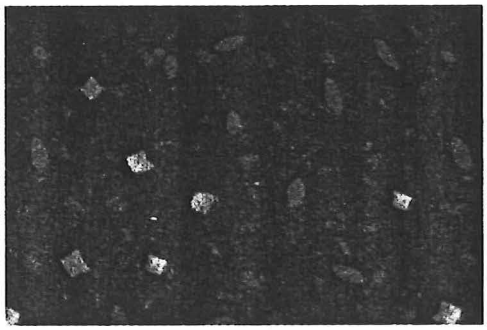

Fabric 32

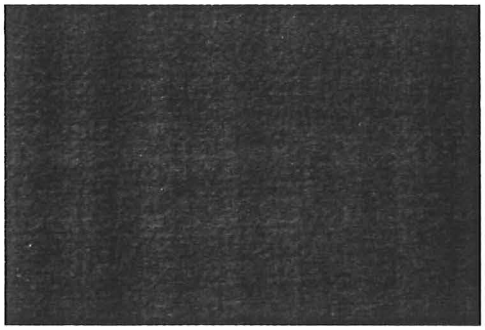

Fabric 33

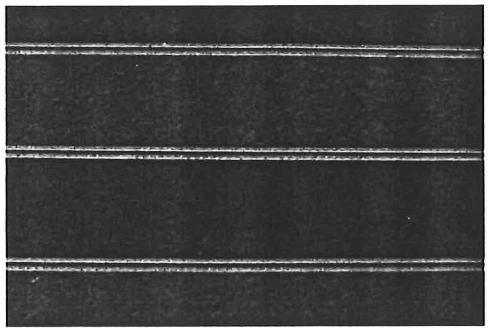

Fabric 34

Fabric 35

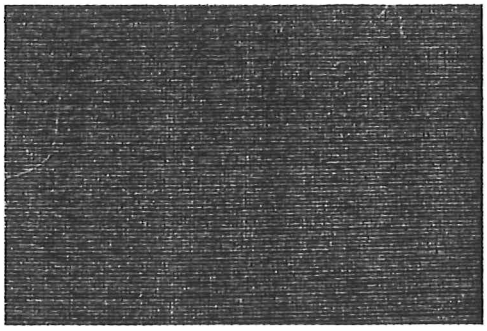

Fabric 36

Appendix B

The ISO Ignitability Test Results

(Composites weights and the times to ignition)

Note:

- Data with shadow were not used in the calculation in this study. The reason is:
  - a The airflow velocity was higher that 0.2 m/s.
  - b The test were repeated.

- SD = standard deviation

Table B - 1 Test data for Fabric 23/foam composites

Incident irradiance q_e (kW/m^2)	Sample No.	Specimen mass m (g)	time to ignition t_{ig} (s)	mass (mean) m^* (g)	mass (SD) (g)	time to ignition (mean) $t_{ig,mean}$ (s)	time to ignition (max) $t_{ig,max}$ (s)	time to ignition (min) $t_{ig,min}$ (s)	time to ignition SD (s)	time to ignition ratio of SD/mean
10[a]	1	56.47	NI	55.81	0.55	127	NI	127	-	-
	2	56.1	NI							
	3	55.52	NI							
	4	55.9	NI							
	5	55.05	127							
40[b]	6	55.67	11.8	55.72	0.28	10.1	11.8	8.0	1.5	0.15
	7	55.26	11.2							
	8	55.89	9.7							
	9	55.99	8							
	10	55.78	9.9							
40	11	55.71	8.2	55.42	0.36	8.1	8.5	7.3	0.5	0.06
	12	55.68	8							
	13	54.96	7.3							
	14	55.12	8.4							
	15	55.65	8.5							
35	16	56.33	9.6	56.19	0.22	9.32	10	8.2	0.7	0.07
	17	56.34	9.2							
	18	56.06	9.6							
	19	56.37	8.2							
	20	55.86	10							
30	21	55.78	12.2	55.02	0.53	11.68	12.8	10.7	0.9	0.07
	22	54.53	10.7							
	23	54.62	11.7							
	24	55.32	12.8							
	25	54.83	11							
25	26	56.12	15.6	55.33	0.72	15	15.6	14.4	0.5	0.03
	27	54.42	15							
	28	55.02	14.7							
	29	56.02	14.4							
	30	55.08	15.3							
20	31	55.37	18.6	55.27	0.85	19.7	21.4	17.1	1.8	0.09
	32	54.93	21.4							
	33	56.64	17.1							
	34	55.03	21							
	35	54.36	20.4							
15	36	54.89	31.5	55.33	0.50	31.42	34.6	28	2.3	0.07
	37	55.11	31.8							
	38	56.18	34.6							
	39	55.23	28							
	40	55.23	31.2							
10	41	54.87	84.4	55.24	0.26	88.08	103.6	71.9	13.4	0.15
	42	55.15	NI							
	43	55.55	71.9							
	44	55.38	103.6							
	45	55.25	92.4							
8	46	55.55	NI	55.71	0.39	189	189	189	-	-
	47	55.37	NI							
	48	56.27	NI							
	49	55.96	189							
	50	55.42	NI							
7	51	56.49	NI	55.75	0.73	NI	-	-	-	-
	52	56.41	NI							
	53	55.84	NI							
	54	54.96	NI							
	55	55.04	NI							

Table B - 2 Test data for Fabric 24/foam composites

Incident irradiance q_e (kW/m^2)	Sample No.	Specimen mass m (g)	time to ignition t_{ig} (s)	mass (mean) m^* (g)	mass (SD) (g)	time to ignition (mean) $t_{ig,mean}$ (s)	time to ignition (max) $t_{ig,max}$ (s)	time to ignition (min) $t_{ig,min}$ (s)	time to ignition SD (s)	time to ignition ratio of SD/mean
10[a]	1	60.48	155	60.46	0.14	155	NI	155	-	-
	2	60.26	NI							
	3	60.42	NI							
	4	60.65	NI							
	5	60.51	NI							
40[b]	6	60.78	11.7	60.45	0.30	11.2	11.7	10.8	0.4	0.03
	7	60.53	11.3							
	8	60.05	10.8							
	9	60.24	10.9							
	10	60.65	11.1							
40	11	60.08	10.4	60.21	0.26	9.7	10.4	9.0	0.6	0.06
	12	60.48	9							
	13	60	9.8							
	14	60.5	9.2							
	15	60	10							
35	16	60.16	12.2	60.58	0.28	11.5	12.2	10.8	0.7	0.06
	17	60.92	10.8							
	18	60.66	10.9							
	19	60.66	11.6							
	20	60.51	12.1							
30	21	59.57	14.9	59.98	0.33	14.7	15	14.1	0.4	0.03
	22	60.19	14.9							
	23	60.11	15							
	24	59.71	14.1							
	25	60.33	14.5							
25	26	60.06	18.2	60.32	0.26	19.0	20.6	18.2	0.9	0.05
	27	60.46	18.6							
	28	60.59	18.7							
	29	60.48	20.6							
	30	60.03	19							
20	31	60	23.9	60.36	0.46	23.9	25.1	23.2	0.7	0.03
	32	60.23	23.7							
	33	59.96	23.8							
	34	61.07	25.1							
	35	60.56	23.2							
15	36	61.01	37.3	60.75	0.35	38.3	39.4	36.8	1.1	0.03
	37	60.18	36.8							
	38	60.92	39							
	39	60.99	38.8							
	40	60.66	39.4							
10	41	60.18	104.8	60.27	0.51	109.0	121.7	104.7	8.5	0.08
	42	59.52	NI							
	43	60.17	121.7							
	44	60.67	104.7							
	45	60.82	104.8							
9	46	60.92	NI	60.43	0.30	NI	-	-	-	-
	47	60.46	NI							
	48	60.38	NI							
	49	60.13	NI							
	50	60.24	NI							

Table B - 3 Test data for Fabric 25/foam composites

Incident irradiance q_e (kW/m^2)	Sample No.	Specimen mass m (g)	time to ignition t_{ig} (s)	mass (mean) $\dot{m}$ (g)	mass (SD) (g)	time to ignition (mean) $t_{ig,mean}$ (s)	time to ignition (max) $t_{ig,max}$ (s)	time to ignition (min) $t_{ig,min}$ (s)	time to ignition SD (s)	time to ignition ratio of SD/mean
10[a]	1	60.81	NI	60.59	0.15	178	NI	178	-	-
	2	60.39	178							
	3	60.58	NI							
	4	60.63	NI							
	5	60.55	NI							
40	6	61.07	10.5	60.35	0.62	10.3	10.5	9.9	0.2	0.02
	7	60.81	10.3							
	8	59.93	9.9							
	9	60.4	10.3							
	10	59.56	10.4							
35	11	60.33	11.2	60.66	0.60	11.7	11.9	11.2	0.3	0.02
	12	60.39	11.7							
	13	60.51	11.8							
	14	60.34	11.9							
	15	61.73	11.8							
30	16	60.53	14.8	60.40	0.24	15.6	17.7	13.9	1.5	0.10
	17	60.61	15							
	18	60.48	17.7							
	19	60	13.9							
	20	60.39	16.7							
25	21	59.95	19.3	60.34	0.23	20.1	23.5	18.5	2.0	0.10
	22	60.36	23.5							
	23	60.4	19.9							
	24	60.56	19.4							
	25	60.45	18.5							
20	26	60.66	35.4	60.39	0.52	28.3	35.4	24.6	4.2	0.15
	27	60.9	27.6							
	28	59.77	26.2							
	29	60.72	24.6							
	30	59.89	27.8							
15	31	60.55	38.6	60.76	0.22	39.1	42.2	37.9	1.8	0.04
	32	60.79	37.9							
	33	60.54	38.2							
	34	61.06	38.6							
	35	60.88	42.2							
10	36	61.16	123.5	60.77	0.42	133.75	170.8	115.1	25.1	0.19
	37	60.1	170.8							
	38	60.85	125.6							
	39	60.68	NI							
	40	61.08	115.1							
9	41	60.79	NI	60.81	0.26	156	165.3	146.7	13.2	0.08
	42	60.55	165.3							
	43	60.56	NI							
	44	61.15	146.7							
	45	60.98	NI							
8	46	60.44	NI	60.75	0.48	NI	-	-	-	-
	47	60.09	NI							
	48	60.86	NI							
	49	61.22	NI							
	50	61.13	NI							

Table B - 4 Test data for Fabric 26/foam composites

Incident irradiance q_e (kW/m^2)	Sample No.	Specimen mass m (g)	time to ignition t_{ig} (s)	mass (mean) m^* (g)	mass (SD) (g)	time to ignition (mean) $t_{ig,mean}$ (s)	time to ignition (max) $t_{ig,max}$ (s)	time to ignition (min) $t_{ig,min}$ (s)	time to ignition SD (s)	time to ignition ratio of SD/mean
10[a]	1	52.1	150	53.09	0.58	138.25	155	119	17.1	0.12
	2	53.61	129							
	3	53.35	119							
	4	53.27	155							
	5	53.14	NI							
40[b]	6	53.09	10.1	52.94	0.28	13.2	19.7	9.5	4.1	0.31
	7	53.05	9.5							
	8	53.02	12.5							
	9	52.45	19.7							
	10	53.1	14.3							
40	11	52.17	9.1	52.23	0.26	8.5	12.0	6.0	2.2	0.26
	12	52.68	12							
	13	52.2	6							
	14	52	7.6							
	15	52.09	7.8							
35	16	53	8.4	52.44	0.71	9.8	12	8.4	1.6	0.16
	17	51.65	8.9							
	18	52	8.8							
	19	52.19	12							
	20	53.36	11							
30	21	52.15	16.1	52.33	0.23	13.3	16.1	10.4	2.6	0.20
	22	52.66	10.7							
	23	52.48	14.1							
	24	52.15	10.4							
	25	52.21	15.1							
25	26	51.76	13.4	52.43	0.46	14.1	16	12.3	1.4	0.10
	27	52.42	14.2							
	28	52.3	14.5							
	29	53.01	16							
	30	52.65	12.3							
20	31	52.8	21.4	52.45	0.34	17.2	21.4	14.7	2.5	0.15
	32	52.75	15.9							
	33	52.1	17							
	34	52.11	17							
	35	52.47	14.7							
15	36	53.57	25	53.24	0.26	27.8	36.5	25	5.0	0.18
	37	53.32	25							
	38	53.09	25.1							
	39	53.34	27.4							
	40	52.88	36.5							
10	41	52.36	NI	52.38	0.27	80.65	85.9	74.9	4.9	0.06
	42	52.24	78.5							
	43	52.56	74.9							
	44	52.72	83.3							
	45	52.04	85.9							
9	46	53.01	132	52.82	0.12	121.5	132	113.9	9.4	0.08
	47	52.85	113.9							
	48	52.76	NI							
	49	52.68	118.7							
	50	52.79	NI							
8	51	53	NI	52.59	0.25	NI	-	-	-	-
	52	52.6	NI							
	53	52.34	NI							
	54	52.43	NI							
	55	52.6	NI							

Table B - 5 Test data for Fabric 27/foam composites

Incident irradiance q_e (kW/m^2)	Sample No.	Specimen mass m (g)	time to ignition t_{ig} (s)	mass (mean) $\dot{m}$ (g)	mass (SD) (g)	time to ignition (mean) $t_{ig,mean}$ (s)	time to ignition (max) $t_{ig,max}$ (s)	time to ignition (min) $t_{ig,min}$ (s)	time to ignition SD (s)	time to ignition ratio of SD/mean
10[a]	1	58.14	NI	57.39	0.62	NI	-	-	-	-
	2	57.11	NI							
	3	57.3	NI							
	4	57.85	NI							
	5	56.57	NI							
15[a]	6	57.98	NI	56.99	0.56	NI	-	-	-	-
	7	56.7	NI							
	8	56.85	NI							
	9	56.67	NI							
	10	56.74	NI							
40	11	56.81	12.2	56.9	0.15	13.2	15.1	11	1.6	0.12
	12	57.14	11							
	13	56.84	13.9							
	14	56.75	13.7							
	15	56.96	15.1							
35	16	57.62	17	56.988	0.37	16.9	19.3	15.8	1.4	0.09
	17	56.71	19.3							
	18	56.96	16							
	19	56.73	16.2							
	20	56.92	15.8							
30	21	56.63	20	56.99	0.30	21.1	22.8	19.8	1.2	0.06
	22	56.96	21.5							
	23	56.97	19.8							
	24	56.93	21.2							
	25	57.46	22.8							
25	26	57.64	32.1	57.346	0.28	30.4	32.1	28.7	1.5	0.05
	27	57.25	30.5							
	28	57.28	31.6							
	29	57.6	29.3							
	30	56.96	28.7							
20	31	56.77	50.9	57.23	0.32	53.9	57.4	50.9	2.8	0.05
	32	57.62	55.1							
	33	57.39	57.4							
	34	57.23	51.3							
	35	57.14	54.8							
18	36	57.7	67.1	57.32	0.30	69.9	73.6	67.1	3.3	0.05
	37	57.38	NI							
	38	56.9	NI							
	39	57.42	69							
	40	57.2	73.6							
17	41	57.73	NI	57.672	0.24	NI	-	-	-	-
	42	57.65	NI							
	43	57.98	NI							
	44	57.7	NI							
	45	57.3	NI							
15	46	57.19	NI	57.434	0.22	NI	-	-	-	-
	47	57.65	NI							
	48	57.53	NI							
	49	57.21	NI							
	50	57.59	NI							

Table B - 6 Test data for Fabric 28/foam composites

Incident irradiance q_e (kW/m^2)	Sample No.	Specimen mass m (g)	time to ignition t_{ig} (s)	mass (mean) $\dot{m}$ (g)	mass (SD) (g)	time to ignition (mean) $t_{ig,mean}$ (s)	time to ignition (max) $t_{ig,max}$ (s)	time to ignition (min) $t_{ig,min}$ (s)	time to ignition SD (s)	time to ignition ratio of SD/mean
10[a]	1	63.78	220	63.27	0.73	223.8	236	202	13.5	0.06
	2	63.81	202							
	3	63.66	231							
	4	62.98	230							
	5	62.11	236							
40	6	62.92	13.4	63.06	0.48	15.4	18.0	13.4	1.7	0.11
	7	62.98	14.4							
	8	62.67	16							
	9	62.86	18							
	10	63.89	15.1							
35	11	63.37	17.6	63.51	0.20	17.44	18.4	15.5	1.1	0.06
	12	63.69	18.4							
	13	63.6	17.8							
	14	63.65	17.9							
	15	63.24	15.5							
30	16	63.7	21.4	63.39	0.33	21.96	23.5	19.9	1.5	0.07
	17	63.58	23.2							
	18	63.01	19.9							
	19	63.6	23.5							
	20	63.06	21.8							
25	21	63.74	29.3	63.31	0.61	27.54	29.3	25.6	1.4	0.05
	22	62.53	26.9							
	23	63.03	28							
	24	64.09	27.9							
	25	63.14	25.6							
20	26	63.22	35.6	63.38	0.20	36	41.5	32	3.5	0.10
	27	63.22	34.6							
	28	63.32	41.5							
	29	63.43	36.3							
	30	63.7	32							
15	31	63.04	65.4	63.58	0.41	56.46	66.4	46	9.0	0.16
	32	64.1	46							
	33	63.36	66.4							
	34	63.82	51.2							
	35	63.58	53.3							
10	36	64.03	205.2	64.03	0.35	180.2	205.2	149.2	22.7	0.13
	37	63.57	178.7							
	38	64.11	198.8							
	39	64.54	149.2							
	40	63.92	169.1							
8	41	62.81	350	63.20	0.42	360	373	350	8.9	0.02
	42	63.01	364							
	43	63.9	355							
	44	63.22	358							
	45	63.04	373							
7	46	63	NI	63.45	0.51	736	736	736	-	-
	47	63.61	NI							
	48	64.05	NI							
	49	63.75	NI							
	50	62.84	736							
6	51	62.8	NI	62.80	-	NI	-	-	-	-
	52	-	-							
	53	-	-							
	54	-	-							
	55	-	-							

Table B - 7 Test data for Fabric 29/foam composites

Incident irradiance q_e (kW/m^2)	Sample No.	Specimen mass m (g)	time to ignition t_{ig} (s)	mass (mean) $\dot{m}$ (g)	mass (SD) (g)	time to ignition (mean) $t_{ig,mean}$ (s)	time to ignition (max) $t_{ig,max}$ (s)	time to ignition (min) $t_{ig,min}$ (s)	time to ignition SD (s)	time to ignition ratio of SD/mean
10[a]	1	57.96	NI	57.68	0.17	NI	-	-	-	-
	2	57.65	NI							
	3	57.68	NI							
	4	57.63	NI							
	5	57.48	NI							
40	6	57.86	10	57.83	0.18	9.7	10.3	9.1	0.5	0.05
	7	57.88	9.8							
	8	58.1	10.3							
	9	57.71	9.5							
	10	57.62	9.1							
35	11	57.16	10.9	57.87	0.57	10.9	11.1	10.7	0.2	0.02
	12	57.34	11.1							
	13	58.19	10.9							
	14	58.36	11.1							
	15	58.3	10.7							
30	16	57.33	13.5	57.42	0.22	14.0	15.2	12.4	1.1	0.08
	17	57.58	14.8							
	18	57.73	15.2							
	19	57.25	13.9							
	20	57.23	12.4							
25	21	57.6	17.3	57.41	0.27	16.76	17.3	15.8	0.7	0.04
	22	57	17.3							
	23	57.49	17.2							
	24	57.3	16.2							
	25	57.67	15.8							
20	26	57.36	22	57.11	0.43	22	22.8	20.9	0.7	0.03
	27	56.66	22.8							
	28	56.78	20.9							
	29	57.03	22.2							
	30	57.72	22.1							
15	31	58.16	35.5	57.88	0.22	36.3	38.8	34.1	1.7	0.05
	32	57.99	36.6							
	33	57.92	34.1							
	34	57.6	36.5							
	35	57.74	38.8							
10	36	57.05	97.6	57.60	0.63	103.8	112.6	97.6	6.3	0.06
	37	58	NI							
	38	56.79	103							
	39	58.03	101.9							
	40	58.14	112.6							
9	41	58.1	NI	58.22	0.32	133.6	135.3	131.5	1.9	0.01
	42	58.31	135.3							
	43	58.7	NI							
	44	58.13	134							
	45	57.84	131.5							
8	46	58.03	NI	57.38	0.49	NI	-	-	-	-
	47	57.67	NI							
	48	57.37	NI							
	49	56.81	NI							
	50	57.02	NI							

Table B - 8 Test data for Fabric 30/foam composites

Incident irradiance q_e (kW/m^2)	Sample No.	Specimen mass m (g)	time to ignition t_{ig} (s)	mass (mean) $\dot{m}$ (g)	mass (SD) (g)	time to ignition (mean) $t_{ig,mean}$ (s)	time to ignition (max) $t_{ig,max}$ (s)	time to ignition (min) $t_{ig,min}$ (s)	time to ignition SD (s)	time to ignition ratio of SD/mean
10[a]	1	56.18	300	55.68	0.36	399.67	456	300	86.6	0.22
	2	55.21	NI							
	3	55.59	NI							
	4	55.85	456							
	5	55.55	443							
40	6	56.28	9.1	56.06	0.69	10.2	11.6	9.1	0.9	0.09
	7	56.75	11.6							
	8	56.6	10.1							
	9	55.13	10.2							
	10	55.56	10.2							
35	11	55.58	11.6	55.66	0.51	12.06	13.2	11.5	0.7	0.06
	12	55.23	11.9							
	13	55.42	11.5							
	14	56.53	13.2							
	15	55.54	12.1							
30	16	56.58	17.3	55.95	0.41	16.14	17.9	14.2	1.5	0.09
	17	56.17	16							
	18	55.64	14.2							
	19	55.7	17.9							
	20	55.66	15.3							
25	21	56.15	20.8	56.06	0.38	19.26	20.8	17.5	1.3	0.07
	22	55.78	18.7							
	23	55.79	19.3							
	24	56.69	17.5							
	25	55.88	20							
20	26	56.26	23.9	55.87	0.41	25.98	28.9	23.3	2.3	0.09
	27	55.31	27							
	28	55.91	28.9							
	29	56.25	23.3							
	30	55.64	26.8							
15	31	56.34	40.8	56.34	0.15	42.06	49.6	39.6	4.2	0.10
	32	56.59	40.1							
	33	56.23	39.6							
	34	56.32	40.2							
	35	56.24	49.6							
10	36	55.81	274.1	55.74	0.40	210.34	274.1	150.3	55.2	0.26
	37	56.11	150.3							
	38	55.31	155.9							
	39	56.14	247							
	40	55.33	224.4							
8	41	55.94	517	56.04	0.23	553.4	622	495	50.4	0.09
	42	56.01	580							
	43	56	622							
	44	56.43	553							
	45	55.81	495							
7	46	55.62	NI	56.09	0.40	NI	-	-	-	-
	47	55.71	NI							
	48	56.32	NI							
	49	56.32	NI							
	50	56.49	NI							

Table B - 9 Test data for Fabric 31/foam composites

Incident irradiance q_e (kW/m^2)	Sample No.	Specimen mass m (g)	time to ignition t_{ig} (s)	mass (mean) m^* (g)	mass (SD) (g)	time to ignition (mean) $t_{ig,mean}$ (s)	time to ignition (max) $t_{ig,max}$ (s)	time to ignition (min) $t_{ig,min}$ (s)	time to ignition SD (s)	time to ignition ratio of SD/mean
10[a]	1	53.04	NI	53.50	0.27	157	157	157	-	-
	2	53.47	NI							
	3	53.59	NI							
	4	53.67	NI							
	5	53.71	157							
40	6	53.85	8.1	53.49	0.75	8.3	9.2	7.8	0.6	0.07
	7	53.77	7.8							
	8	52.73	8							
	9	54.41	8.5							
	10	52.71	9.2							
35	11	54.56	9.8	53.86	0.47	9.44	10.9	8.3	1.0	0.11
	12	53.39	9.4							
	13	53.55	8.8							
	14	53.68	10.9							
	15	54.11	8.3							
30	16	53.78	11.5	53.42	0.34	12.08	12.8	11.3	0.7	0.06
	17	53.73	12.8							
	18	53.28	12.7							
	19	52.96	12.1							
	20	53.37	11.3							
25	21	53.43	16	53.15	0.35	14.34	16	13.7	0.9	0.07
	22	52.82	13.9							
	23	52.81	13.7							
	24	53.58	13.9							
	25	53.12	14.2							
20	26	53.54	17.4	53.57	0.21	17.76	18.6	16.9	0.8	0.04
	27	53.56	18.6							
	28	53.74	17.3							
	29	53.78	18.6							
	30	53.24	16.9							
15	31	53.87	30.7	54.07	0.33	30.18	31.7	27.8	1.5	0.05
	32	54.55	27.8							
	33	54.14	29.9							
	34	54.14	30.8							
	35	53.67	31.7							
10	36	53.61	84.1	53.43	0.22	88.86	94.7	84.1	4.8	0.05
	37	53.37	92.8							
	38	53.08	84.3							
	39	53.49	94.7							
	40	53.59	88.4							
8	41	53.57	NI	53.69	0.35	117	190	81	49.4	0.42
	42	54.16	190							
	43	53.95	81							
	44	53.5	98							
	45	53.29	99							
7	46	53.04	NI	53.28	0.37	NI	-	-	-	-
	47	53.87	NI							
	48	53.29	NI							
	49	52.91	NI							
	50	53.3	NI							

Table B - 10 Test data for Fabric 32/foam composites

Incident irradiance q_e (kW/m^2)	Sample No.	Specimen mass m (g)	time to ignition t_{ig} (s)	mass (mean) $\dot{m}$ (g)	mass (SD) (g)	time to ignition (mean) $t_{ig,mean}$ (s)	time to ignition (max) $t_{ig,max}$ (s)	time to ignition (min) $t_{ig,min}$ (s)	time to ignition SD (s)	time to ignition ratio of SD/mean
10[a]	1	61.79	325	62.04	1.05	296	325	273	21.6	0.07
	2	61.34	291							
	3	61.31	273							
	4	61.88	NI							
	5	63.86	295							
15[a]	6	61.14	59	61.52	0.34	68.6	76.0	59.0	7.1	0.10
	7	62.03	75							
	8	61.33	65							
	9	61.47	76							
	10	61.61	68							
40	11	61.38	11.2	61.58	0.15	10.76	11.6	10.1	0.6	0.06
	12	61.71	10.4							
	13	61.46	10.1							
	14	61.68	11.6							
	15	61.65	10.5							
35	16	61.68	12	61.49	0.22	12.12	13	11.5	0.6	0.05
	17	61.4	12.4							
	18	61.74	13							
	19	61.21	11.5							
	20	61.41	11.7							
30	21	61.1	15.5	61.19	0.45	17.36	19	15.5	1.5	0.09
	22	61.7	19							
	23	60.52	17.2							
	24	61.14	18.8							
	25	61.47	16.3							
25	26	61.11	20.7	61.37	0.28	20.48	21.8	19.4	1.0	0.05
	27	61.5	21.8							
	28	61.12	21							
	29	61.37	19.5							
	30	61.77	19.4							
20	31	61.48	30.4	61.26	0.23	29.48	30.4	28.2	0.9	0.03
	32	61.51	28.2							
	33	60.99	29							
	34	61.12	30.1							
	35	61.18	29.7							
15	36	61.94	62.8	61.45	0.66	59.74	64	54.9	4.0	0.07
	37	61.72	60.6							
	38	60.43	64							
	39	62	54.9							
	40	61.17	56.4							
10	41	60.87	204.6	61.62	0.46	181.7	204.6	167.1	14.2	0.08
	42	61.75	177.9							
	43	62.12	174.5							
	44	61.78	167.1							
	45	61.6	184.4							
8	46	60.97	463	61.16	0.13	512.12	576	460	52.0	0.10
	47	61.27	576							
	48	61.17	509.3							
	49	61.11	460							
	50	61.27	552.3							
7	51	61.62	NI	61.14	0.42	NI	-	-	-	-
	52	60.55	NI							
	53	61.29	NI							
	54	61.33	NI							
	55	60.89	NI							

Table B - 11 Test data for Fabric 33/foam composites

Incident irradiance q_e (kW/m^2)	Sample No.	Specimen mass m (g)	time to ignition t_{ig} (s)	mass (mean) $\bar{m}$ (g)	mass (SD) (g)	time to ignition (mean) $t_{ig,mean}$ (s)	time to ignition (max) $t_{ig,max}$ (s)	time to ignition (min) $t_{ig,min}$ (s)	time to ignition SD (s)	time to ignition ratio of SD/mean
10[a]	1	57.93	NI	57.66	0.26	137	137	137	-	-
	2	57.68	NI							
	3	57.57	NI							
	4	57.27	137							
	5	57.83	NI							
15[a]	6	56.96	39	57.52	0.39	39.0	46.0	33.0	4.7	0.12
	7	57.93	40							
	8	57.76	46							
	9	57.3	37							
	10	57.67	33							
40	11	57.48	10.3	57.43	0.42	8.78	10.3	8.2	0.9	0.10
	12	56.75	8.9							
	13	57.51	8.2							
	14	57.49	8.2							
	15	57.91	8.3							
35	16	57.2	9.2	57.63	0.32	9.94	11.2	9.2	0.8	0.08
	17	57.66	11.2							
	18	57.46	9.7							
	19	58.01	10							
	20	57.83	9.6							
30	21	57.95	16	57.85	0.29	12.675	16	10.8	2.4	0.19
	22	58.01	11.2							
	23	57.82								
	24	58.11	10.8							
	25	57.38	12.7							
25	26	57.94	15.9	57.50	0.60	14.82	15.9	14.1	0.7	0.05
	27	57.67	14.4							
	28	57.79	14.1							
	29	56.45	14.9							
	30	57.66	14.8							
20	31	57.41	22.7	57.84	0.31	19.88	22.7	18	1.9	0.09
	32	58.11	20.4							
	33	57.88	18.4							
	34	57.66	19.9							
	35	58.15	18							
15	36	56.81	30	57.38	0.49	31.28	34	30	1.6	0.05
	37	58.05	34							
	38	57.16	31.5							
	39	57.19	30.7							
	40	57.67	30.2							
10	41	57.92	83.4	57.45	0.40	84.05	97.6	73.2	10.1	0.12
	42	57.18	82							
	43	57.32	73.2							
	44	57.8	NI							
	45	57.01	97.6							
8	46	57.69	184	57.77	0.30	179	184	174	7.1	0.04
	47	57.79	174							
	48	57.76	NI							
	49	58.22	NI							
	50	57.37	NI							
7	51	57.44	NI	57.86	0.40	NI	-	-	-	-
	52	57.45	NI							
	53	57.98	NI							
	54	58.33	NI							
	55	58.1	NI							

Table B - 12 Test data for Fabric 34/foam composites

Incident irradiance q_e (kW/m^2)	Sample No.	Specimen mass m (g)	time to ignition t_{ig} (s)	mass (mean) $\dot{m}$ (g)	mass (SD) (g)	time to ignition (mean) $t_{ig,mean}$ (s)	time to ignition (max) $t_{ig,max}$ (s)	time to ignition (min) $t_{ig,min}$ (s)	time to ignition SD (s)	time to ignition ratio of SD/mean
10[a]	1	54.75	239	54.69	0.17	278	317	239	55.2	0.20
	2	54.52	NI							
	3	54.57	NI							
	4	54.68	NI							
	5	54.94	317							
40	6	54.77	10.7	55.13	0.21	8.8	10.7	7.4	1.4	0.16
	7	55.31	8							
	8	55.19	7.4							
	9	55.26	9.8							
	10	55.13	8.2							
35	11	54.31	9.3	54.58	0.57	10.44	11.8	9.3	1.1	0.11
	12	54.26	11							
	13	54.01	11.8							
	14	55.43	9.3							
	15	54.89	10.8							
30	16	54.97	10	55.20	0.45	11.84	13.9	10	1.7	0.15
	17	55.83	13.9							
	18	55.36	12.3							
	19	55.23	12.9							
	20	54.62	10.1							
25	21	54.34	18.6	54.70	0.35	17.94	19.2	15.4	1.5	0.08
	22	54.47	18.5							
	23	54.77	19.2							
	24	54.67	18							
	25	55.26	15.4							
20	26	55	27.3	55.29	0.33	21.4	27.8	15.7	5.7	0.27
	27	54.89	18.4							
	28	55.67	15.7							
	29	55.45	27.8							
	30	55.45	17.8							
15	31	55.06	28.4	54.96	0.23	35.68	43.4	27.3	7.3	0.21
	32	54.94	39.3							
	33	54.88	43.4							
	34	55.26	27.3							
	35	54.65	40							
10	36	54.8	198	54.90	0.37	158.9	198	113.3	36.5	0.23
	37	55.42	113.3							
	38	54.83	136.3							
	39	55.06	193.3							
	40	54.4	153.6							
8	41	54.54	167	54.71	0.25	219	299	167	50.3	0.23
	42	54.4	210							
	43	54.8	299							
	44	55.03	190							
	45	54.8	229							
7	46	54.43	NI	54.74	0.36	NI	-	-	-	-
	47	55.2	NI							
	48	54.48	NI							
	49	54.53	NI							
	50	55.05	NI							

Table B - 13 Test data for Fabric 35/foam composites

Incident irradiance q_e (kW/m^2)	Sample No.	Specimen mass m (g)	time to ignition t_{ig} (s)	mass (mean) m^* (g)	mass (SD) (g)	time to ignition (mean) $t_{ig,mean}$ (s)	time to ignition (max) $t_{ig,max}$ (s)	time to ignition (min) $t_{ig,min}$ (s)	time to ignition SD (s)	time to ignition ratio of SD/mean
10[a]	1	62.04	573	62.58	0.61	332.6	573	168	203.8	0.61
	2	63.38	537							
	3	62.53	182							
	4	61.95	168							
	5	63	203							
15[a]	6	62.26	61	62.47	0.34	56.6	61.0	46.0	6.3	0.11
	7	62.28	56							
	8	62.12	59							
	9	62.83	61							
	10	62.84	46							
40	11	63.29	11.2	62.71	0.64	11.74	12.7	10.8	0.9	0.07
	12	63.24	10.8							
	13	62.77	12.6							
	14	62.52	11.4							
	15	61.71	12.7							
35	16	62.7	11.7	62.74	0.48	12	12.7	11.3	0.5	0.04
	17	63.58	12.1							
	18	62.4	12.7							
	19	62.47	12.2							
	20	62.56	11.3							
30	21	62.45	16.2	62.72	0.71	17.14	21	13.9	2.6	0.15
	22	63.18	21							
	23	63.06	13.9							
	24	63.31	17.8							
	25	61.59	16.8							
25	26	63.6	20.7	63.66	0.37	20.96	22.7	19.4	1.2	0.06
	27	64.09	19.4							
	28	63.96	20.7							
	29	63.42	22.7							
	30	63.21	21.3							
20	31	63.59	23.6	63.47	0.15	28	30.9	23.6	2.7	0.10
	32	63.61	30.9							
	33	63.49	29							
	34	63.41	28							
	35	63.23	28.5							
15	36	62.96	50.1	63.18	0.30	44.18	50.1	41.4	3.4	0.08
	37	63.08	43.1							
	38	62.87	41.4							
	39	63.47	42.6							
	40	63.52	43.7							
10	41	62.62	109.4	62.85	0.28	112.88	120.9	106	6.9	0.06
	42	63.2	106							
	43	63.05	108.4							
	44	62.84	119.7							
	45	62.54	120.9							
8	46	63.97	NI	63.45	0.40	695.0	777.8	652.6	56.9	0.08
	47	62.98	652.6							
	48	63.11	777.8							
	49	63.62	685.6							
	50	63.59	663.8							
7	51	62.83	NI	62.73	0.52	NI	-	-	-	-
	52	63.15	NI							
	53	63.06	NI							
	54	62.75	NI							
	55	61.85	NI							

Table B - 14 Test data for Fabric 36/foam composites

Incident irradiance q_e (kW/m^2)	Sample No.	Specimen mass m (g)	time to ignition t_{ig} (s)	mass (mean) $\dot{m}$ (g)	mass (SD) (g)	time to ignition (mean) $t_{ig,mean}$ (s)	time to ignition (max) $t_{ig,max}$ (s)	time to ignition (min) $t_{ig,min}$ (s)	time to ignition SD (s)	ratio of SD/mean
10[a]	1	60.54	388	61.00	0.40	318.4	418	220	82.1	0.26
	2	60.63	286							
	3	61.25	220							
	4	61.13	418							
	5	61.45	280							
15[a]	6	61.58	74	61.83	0.58	68.8	74.0	62.0	5.9	0.09
	7	61.5	63							
	8	62.86	74							
	9	61.55	62							
	10	61.66	71							
40	11	61.37	10.8	61.40	0.49	11.24	12.1	10.7	0.6	0.05
	12	60.69	10.7							
	13	61.95	12.1							
	14	61.22	11.4							
	15	61.75	11.2							
35	16	60.97	11.8	61.22	0.40	12.38	13	11.8	0.6	0.05
	17	60.98	13							
	18	61.84	12							
	19	60.9	13							
	20	61.4	12.1							
30	21	61.22	16	61.23	0.26	16.36	17.5	15.8	0.7	0.04
	22	61.38	17.5							
	23	60.84	15.8							
	24	61.17	16							
	25	61.53	16.5							
25	26	62.23	19.4	61.69	0.35	21.46	22.6	19.4	1.2	0.06
	27	61.36	21.8							
	28	61.52	21.4							
	29	61.85	22.6							
	30	61.47	22.1							
20	31	62.46	32.7	61.84	0.69	30	32.7	26.8	2.6	0.09
	32	60.83	26.8							
	33	61.42	32.5							
	34	62.26	30							
	35	62.23	28							
15	36	60.69	44	60.52	0.26	48.96	55	40.8	6.4	0.13
	37	60.24	54.9							
	38	60.25	40.8							
	39	60.61	50.1							
	40	60.82	55							
10	41	60.99	173.3	61.24	0.37	177.24	202.3	163	15.0	0.08
	42	61.4	177.8							
	43	61.16	163							
	44	60.87	202.3							
	45	61.8	169.8							
8	46	61.01	440	61.68	0.53	413.16	447	314	56.4	0.14
	47	62.4	420.8							
	48	61.4	447							
	49	61.65	314							
	50	61.92	444							
7	51	61.24	NI	61.28	0.15	NI	-	-	-	-
	52	61.41	NI							
	53	61.35	NI							
	54	61.03	NI							
	55	61.36	NI							

Appendix C

Correlation of Time to Ignition Data

Fabric 23

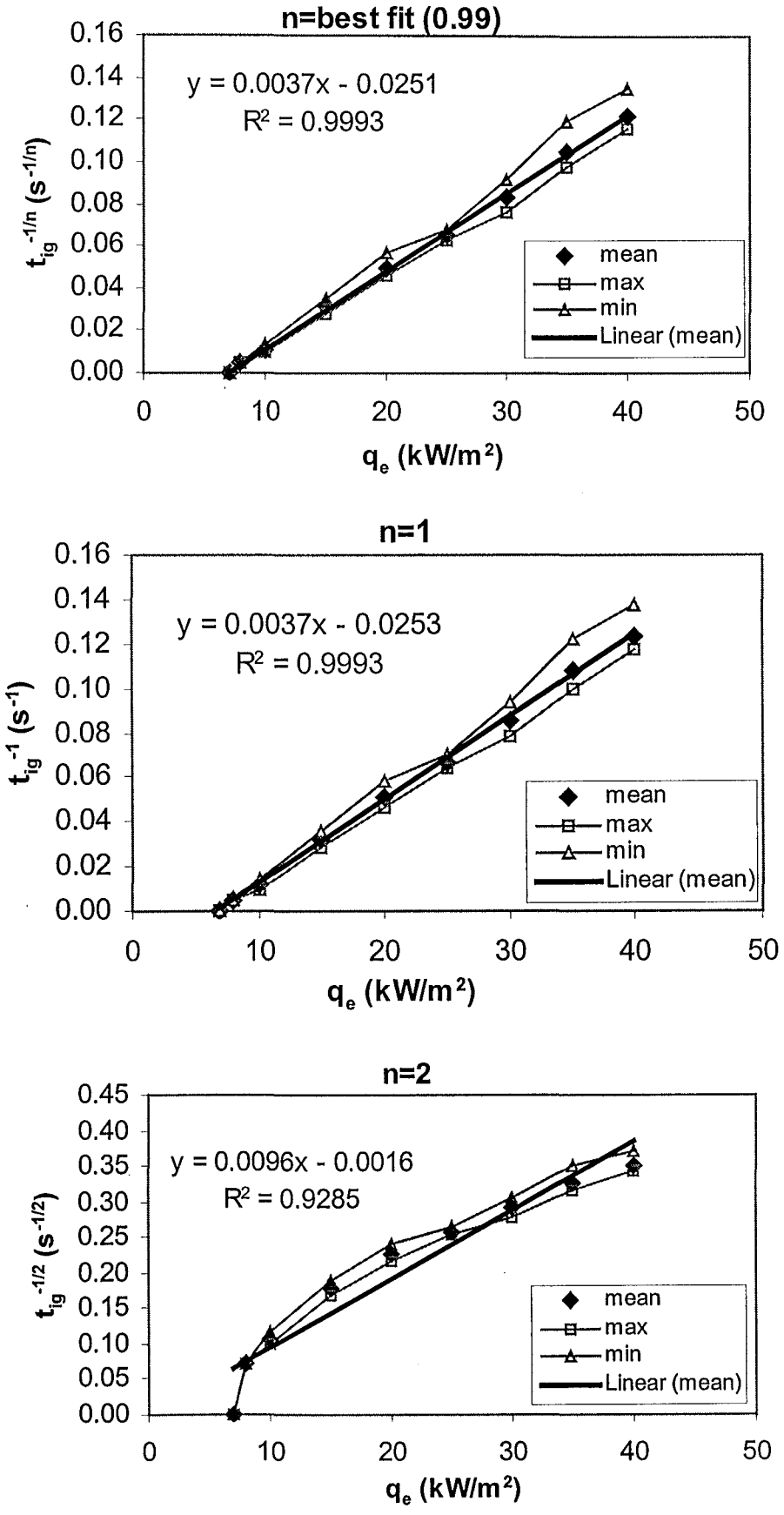

Figure C - 1 Linear correlation for Fabric 23

Fabric 24

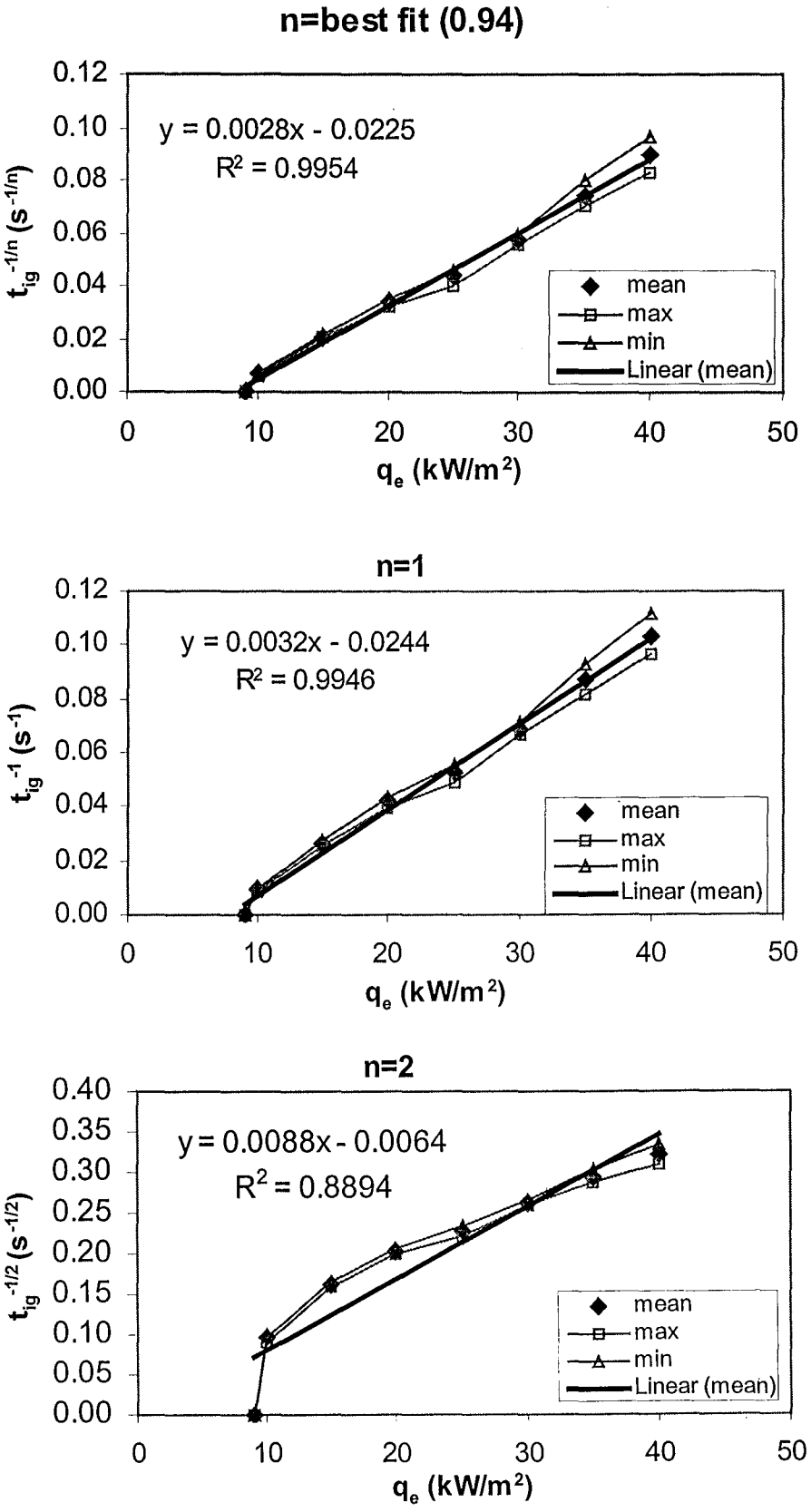

Figure C - 2 Linear correlation for Fabric 24

Fabric 25

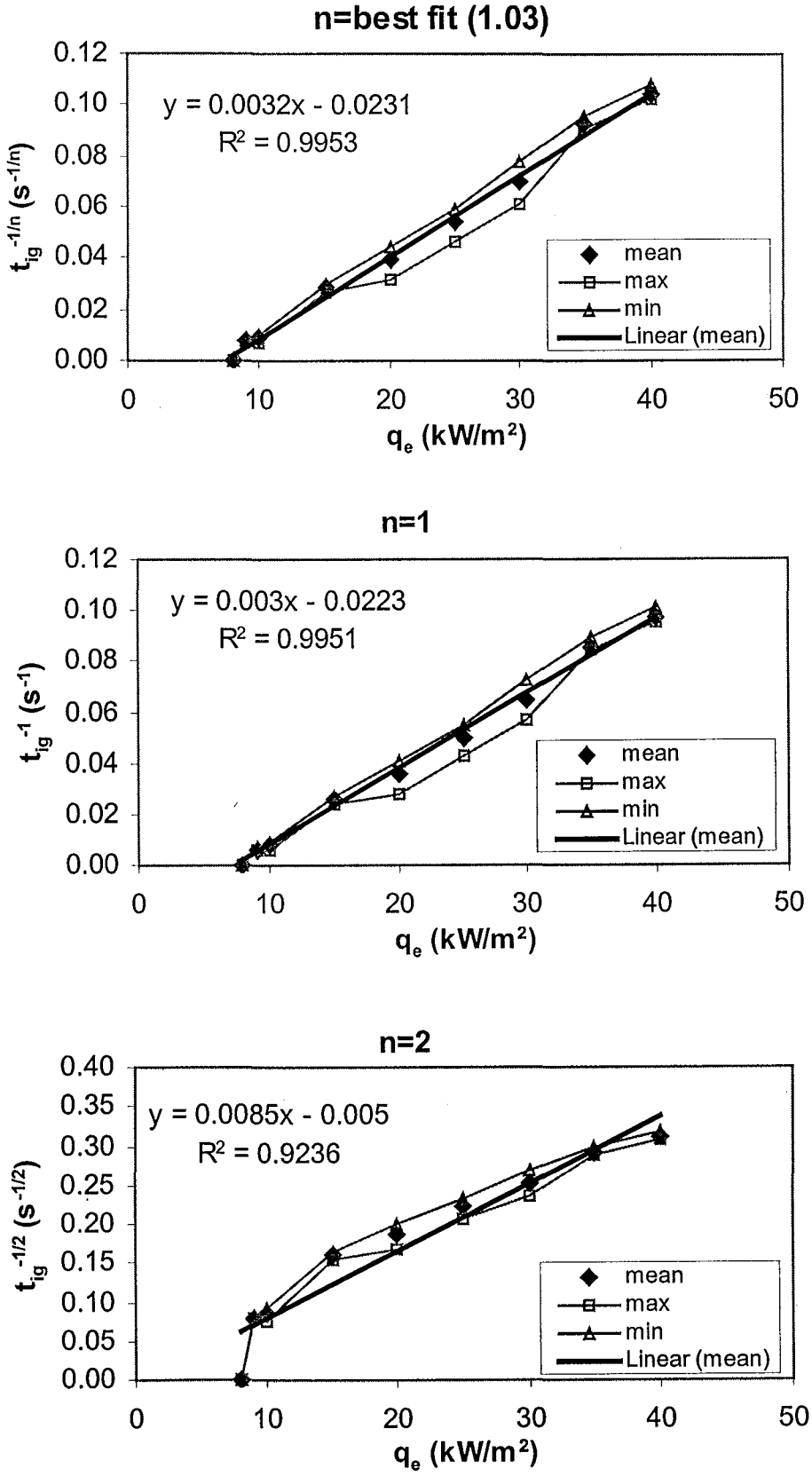

Figure C - 3 Linear correlation for Fabric 25

Fabric 26

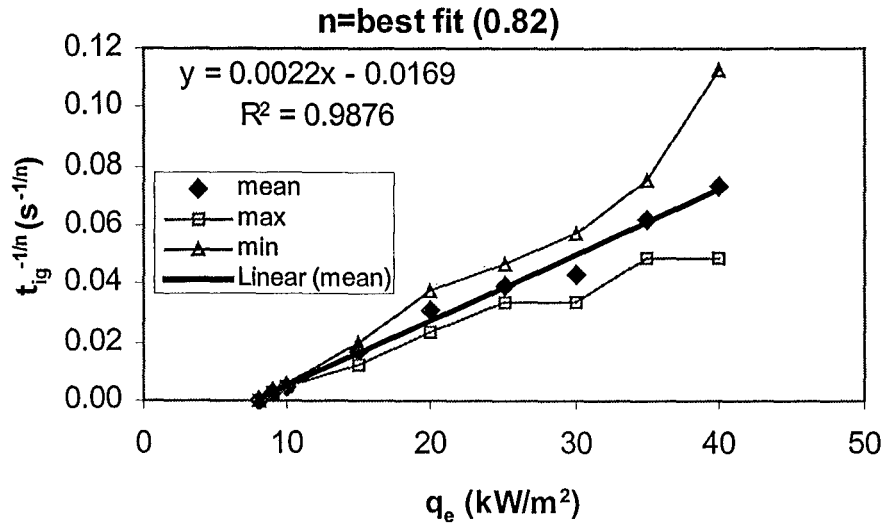

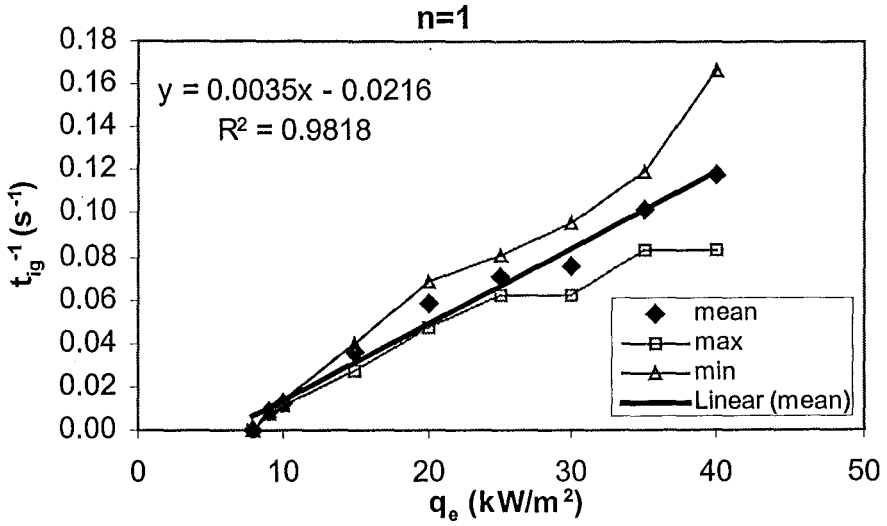

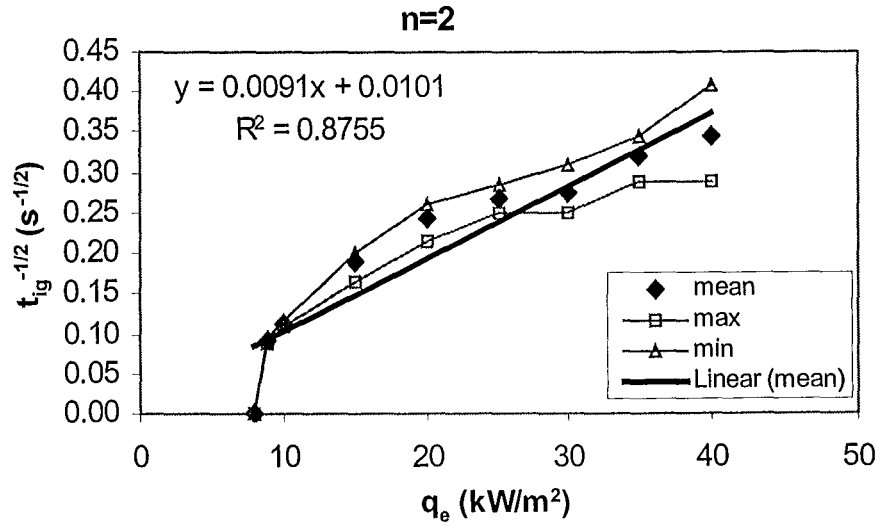

Figure C - 4 Linear correlation for Fabric 26

Fabric 27

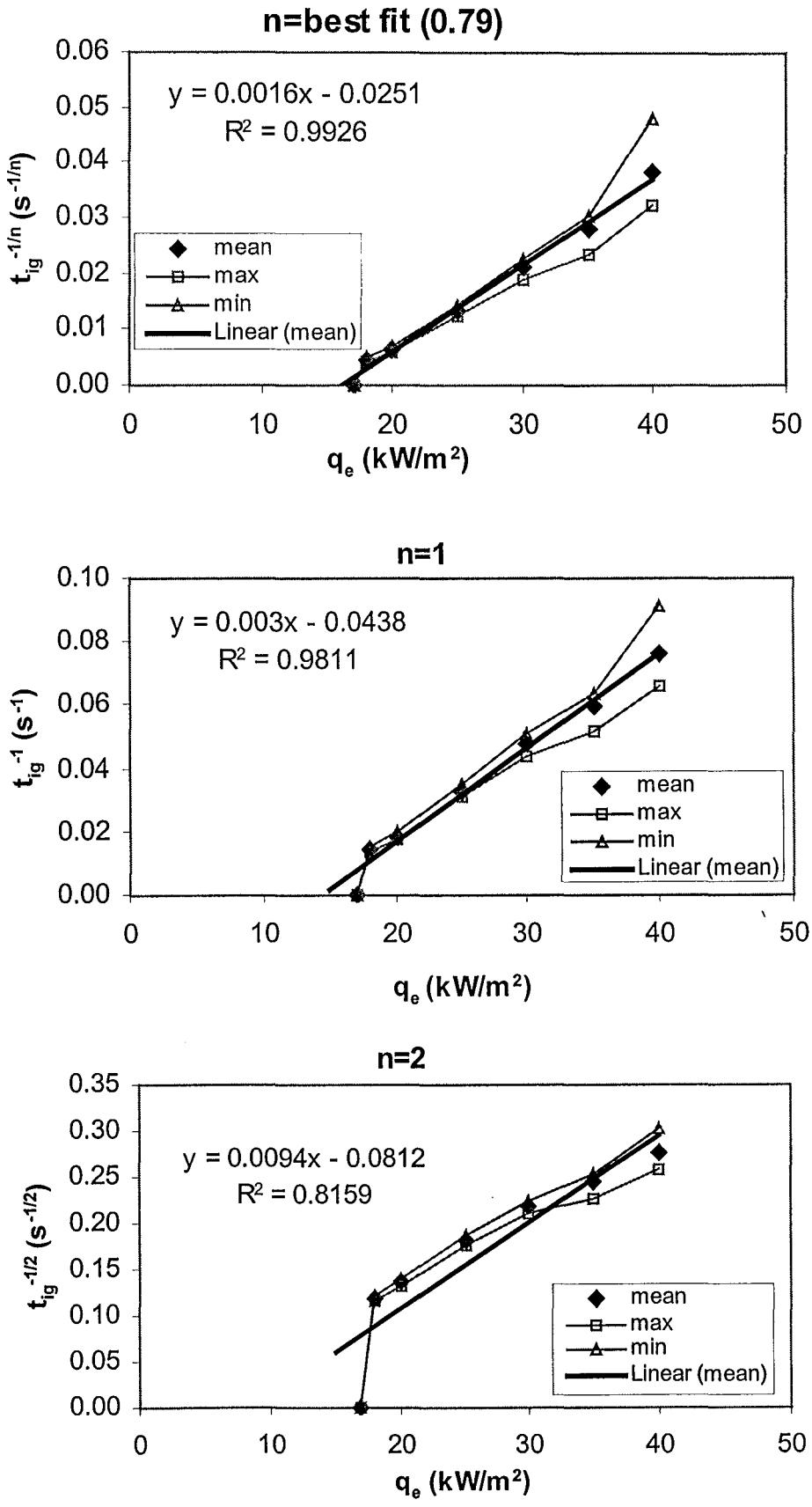

Figure C - 5 Linear correlation for Fabric 27

Fabric 28

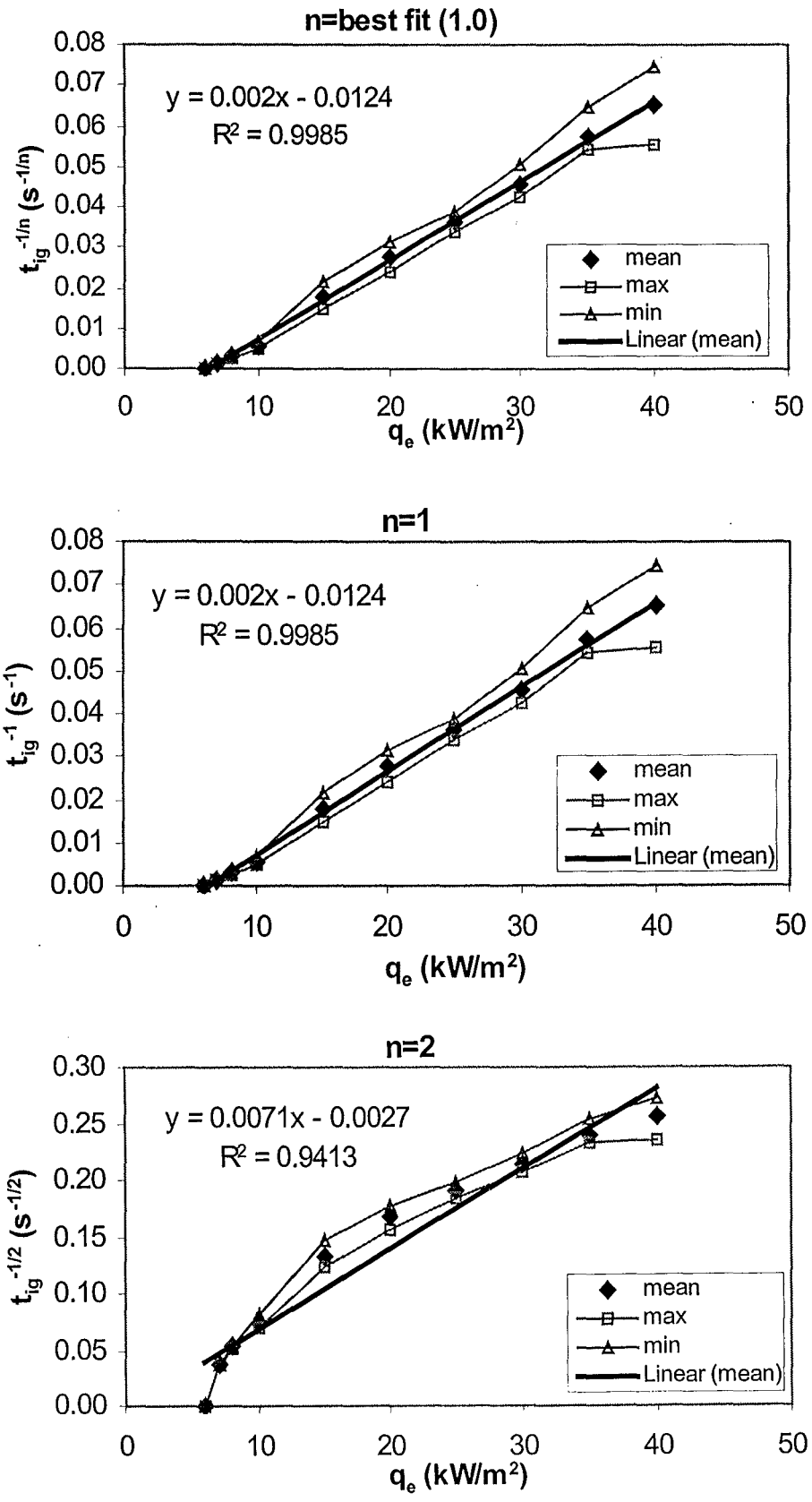

Figure C - 6 Linear correlation for Fabric 28

Fabric 29

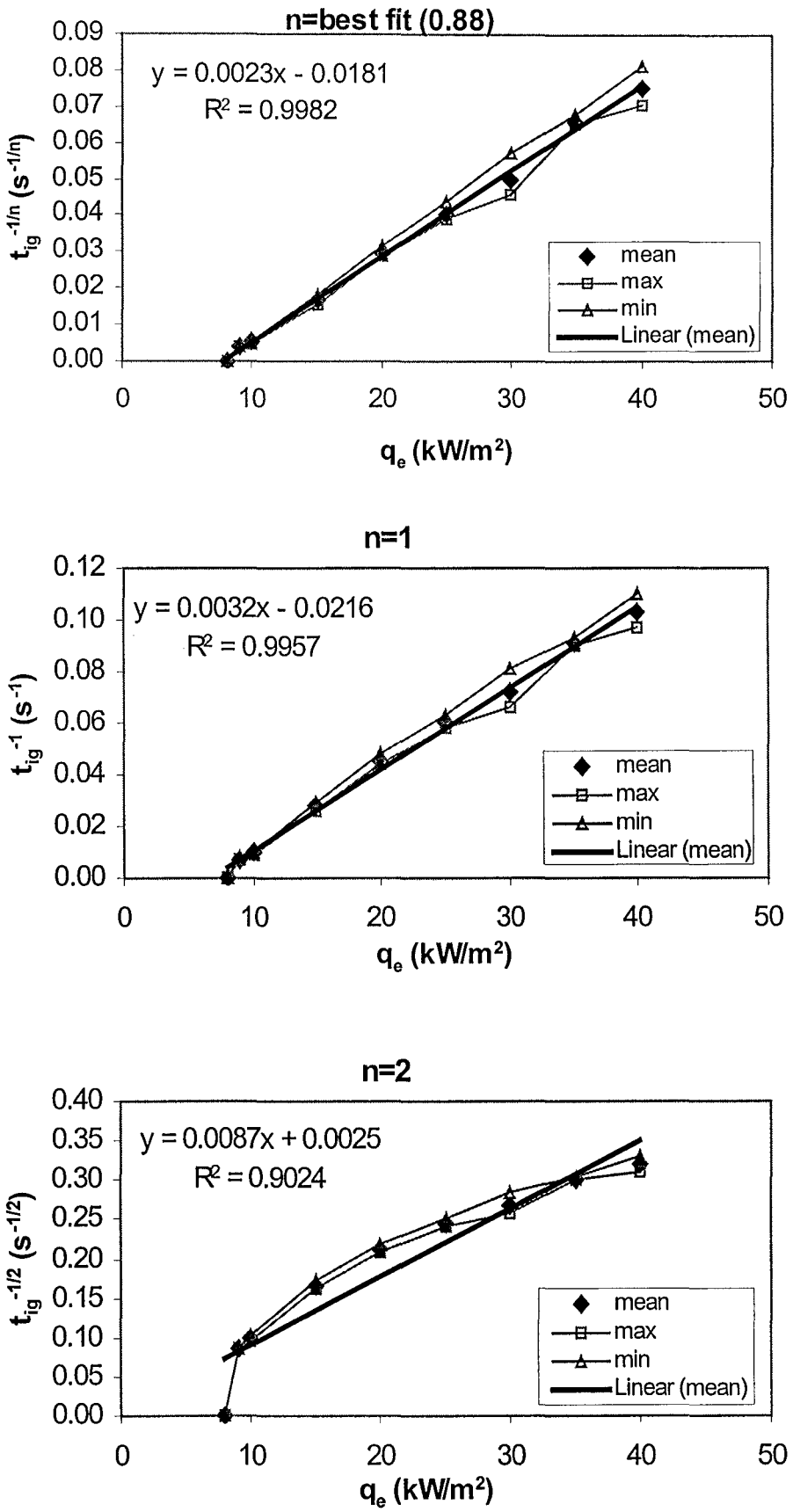

Figure C - 7 Linear correlation for Fabric 29

Fabric 30

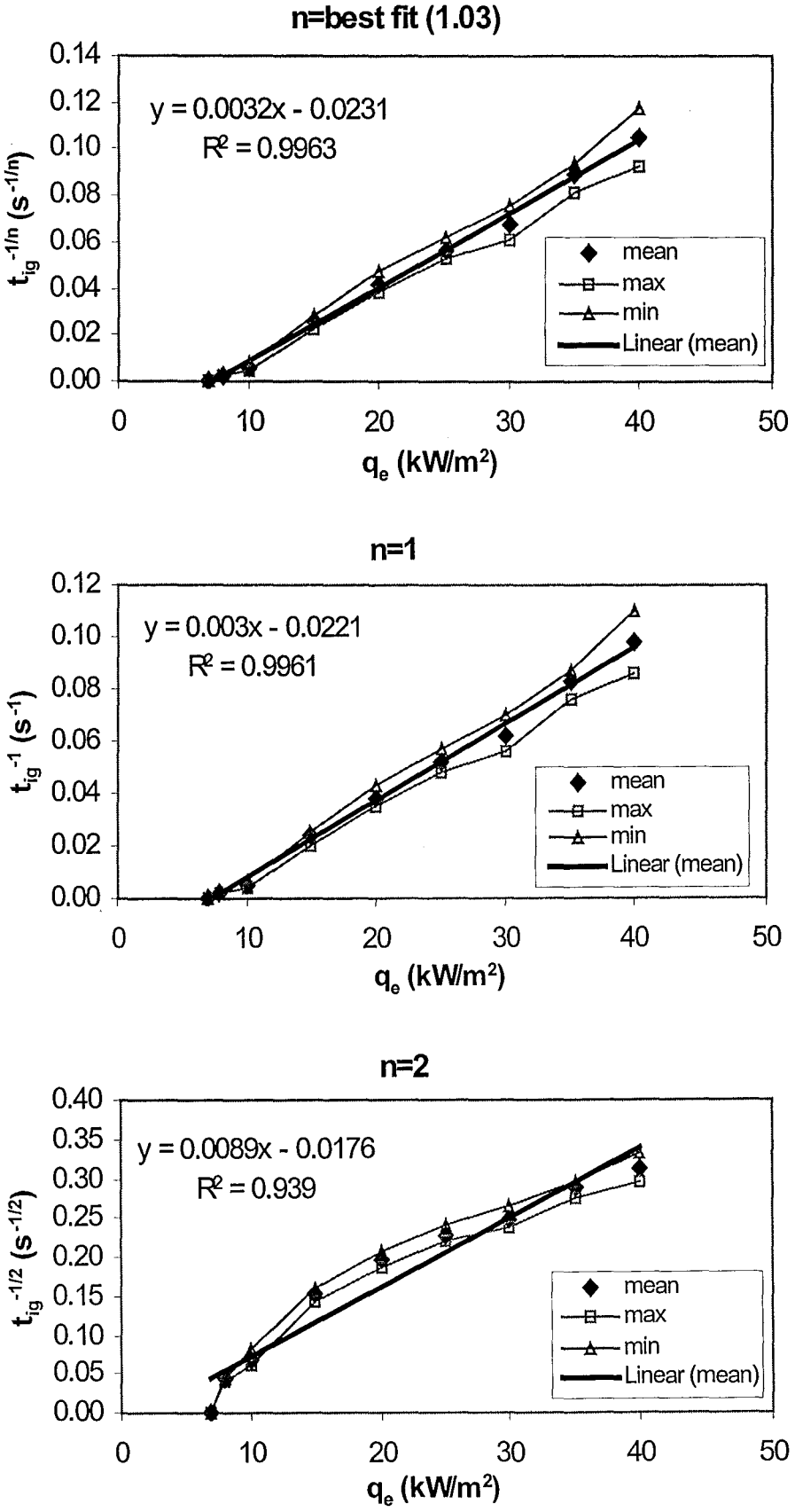

Figure C - 8 Linear correlation for Fabric 30

Fabric 31

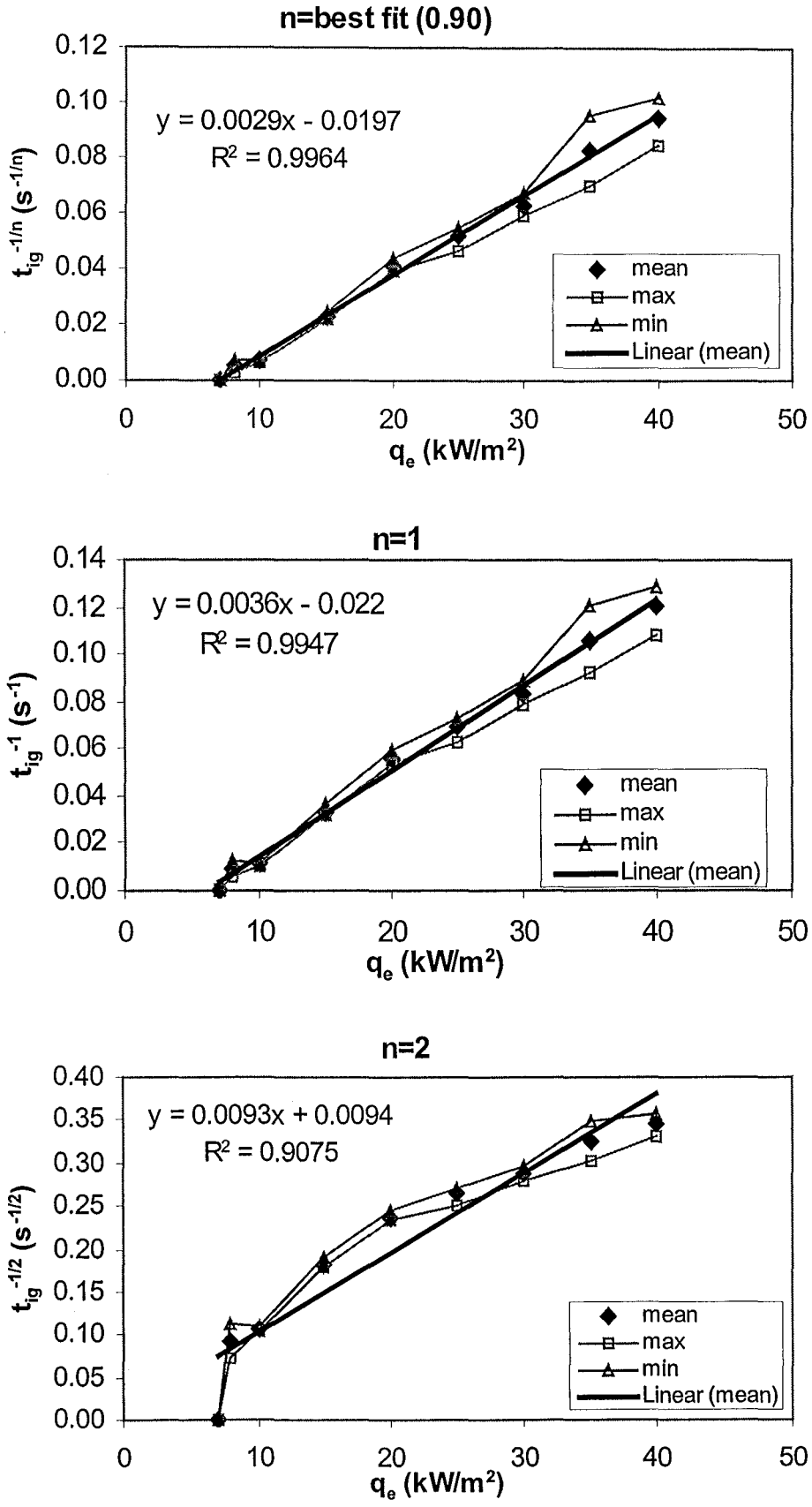

Figure C - 9 Linear correlation for Fabric 31

Fabric 32

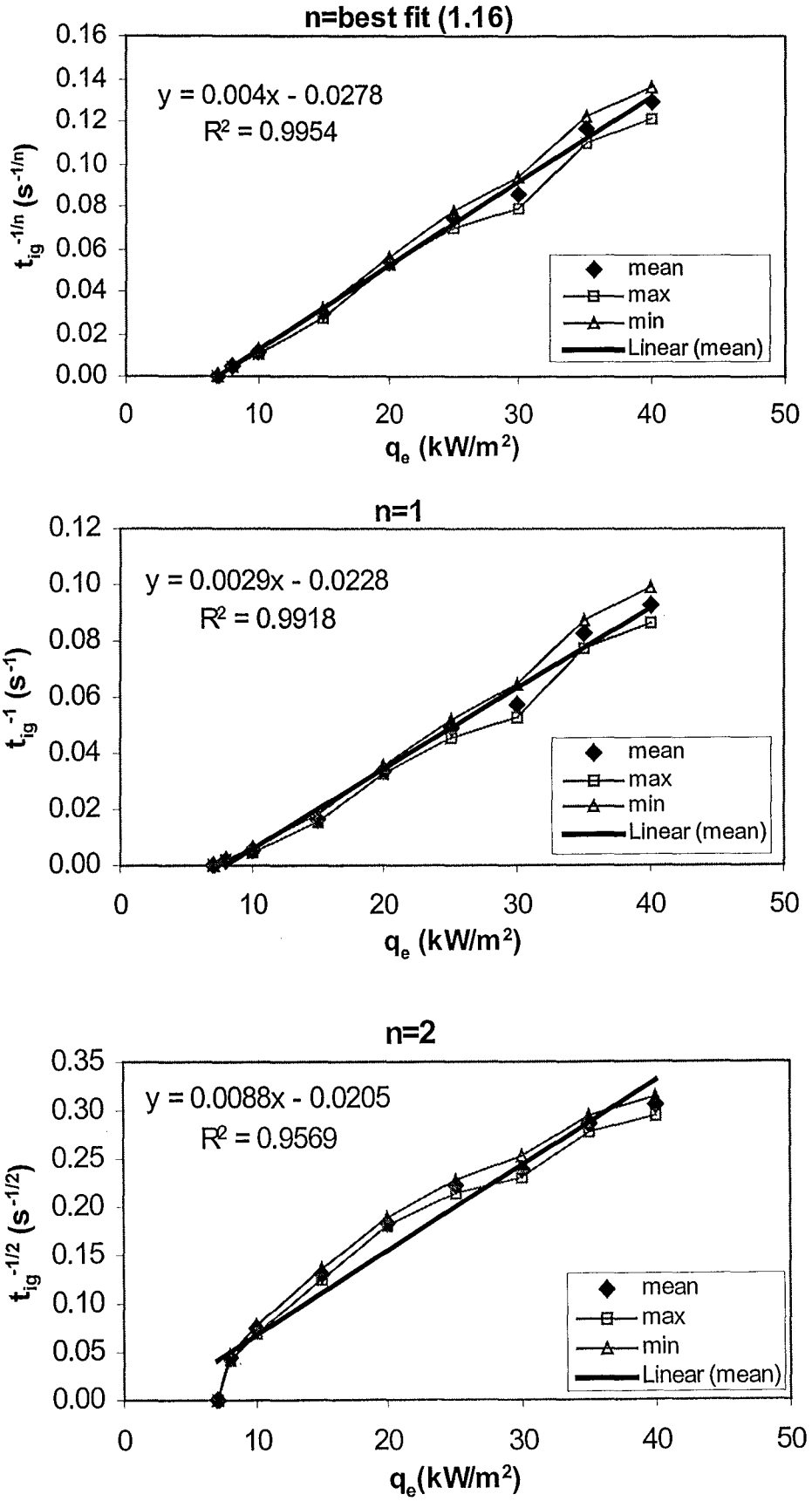

Figure C - 10 Linear correlation for Fabric 32

Fabric 33

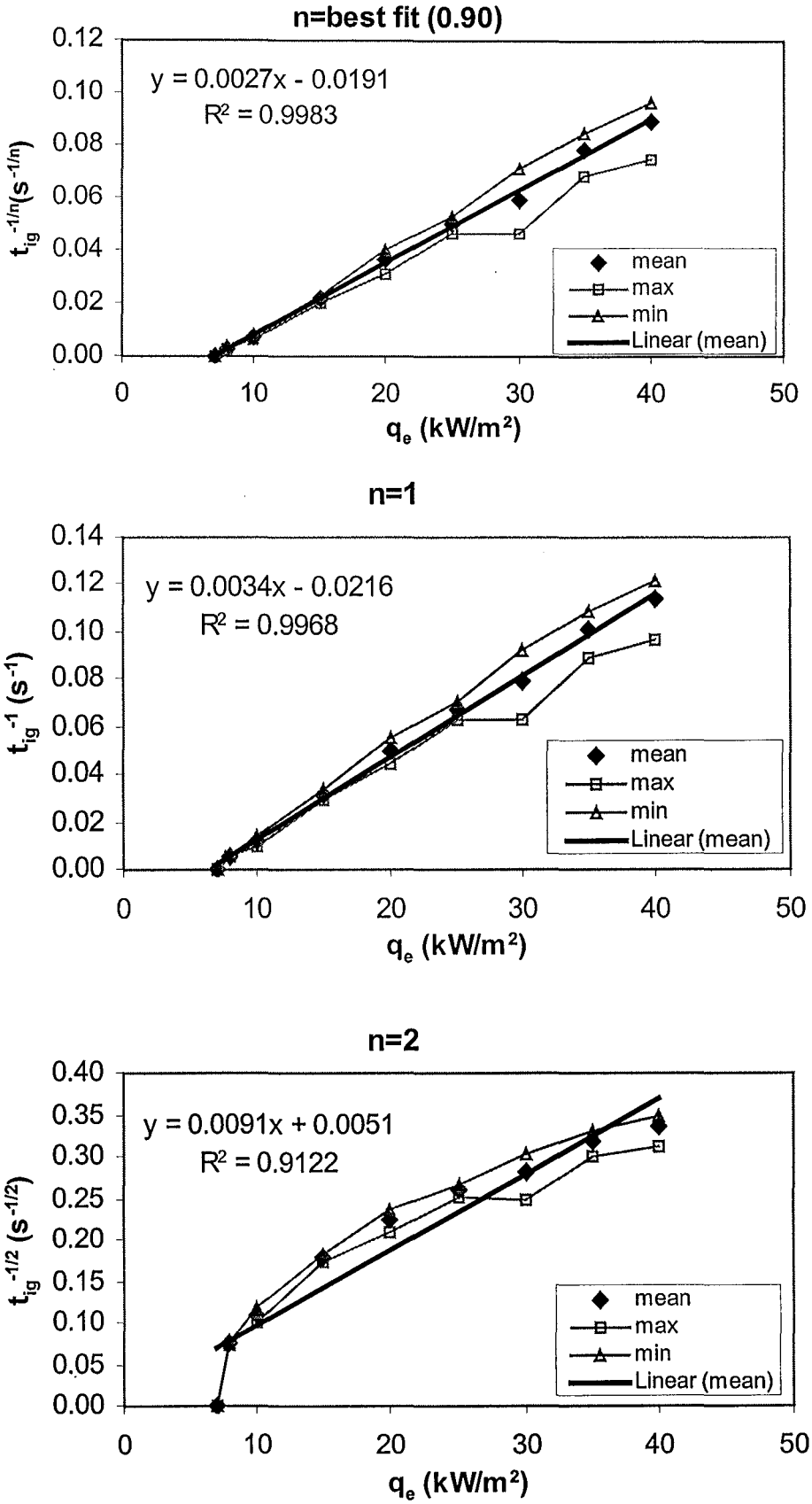

Figure C - 11 Linear correlation for Fabric 33

Fabric 34

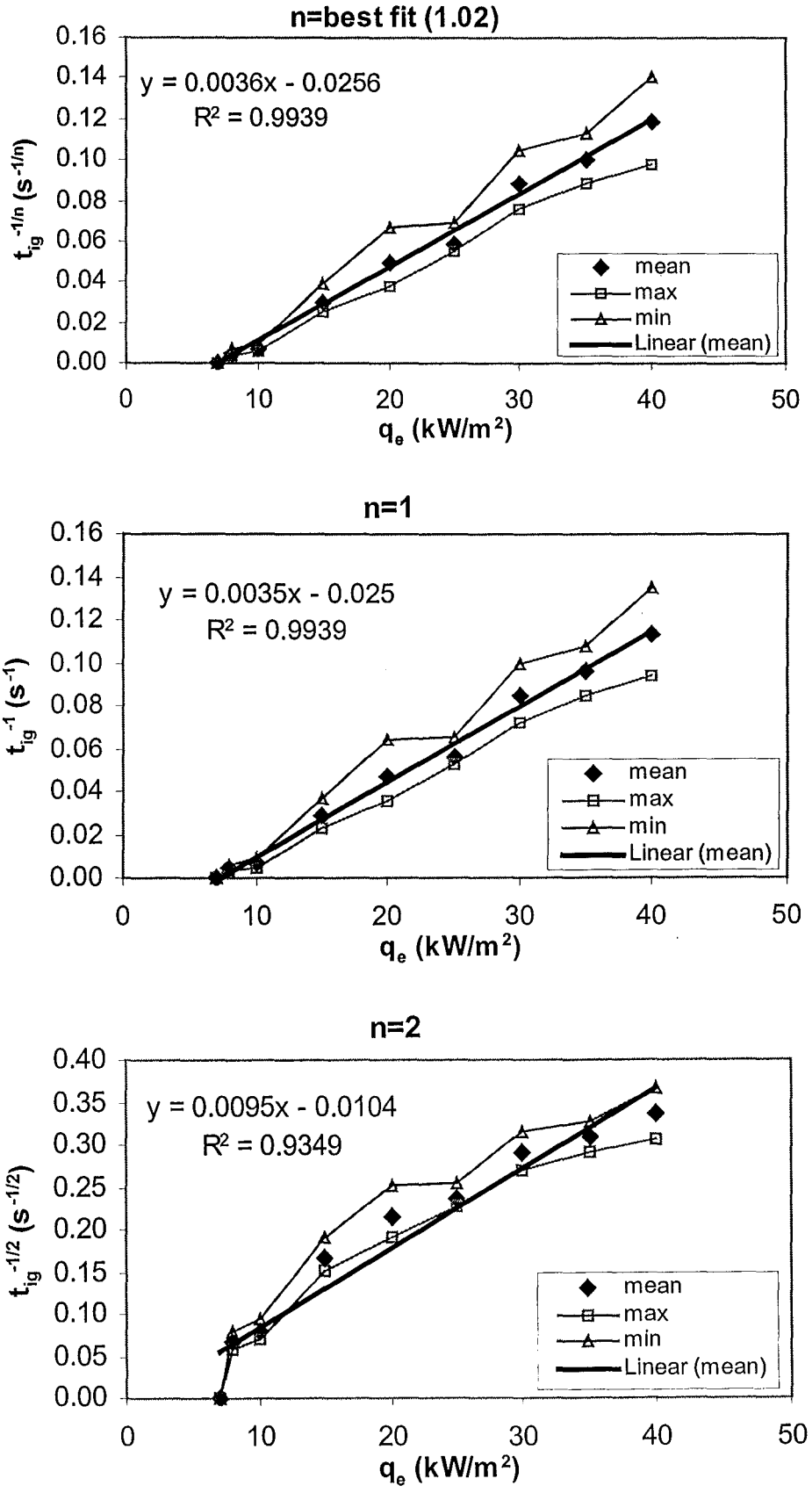

Figure C - 12 Linear correlation for Fabric 34

Fabric 35

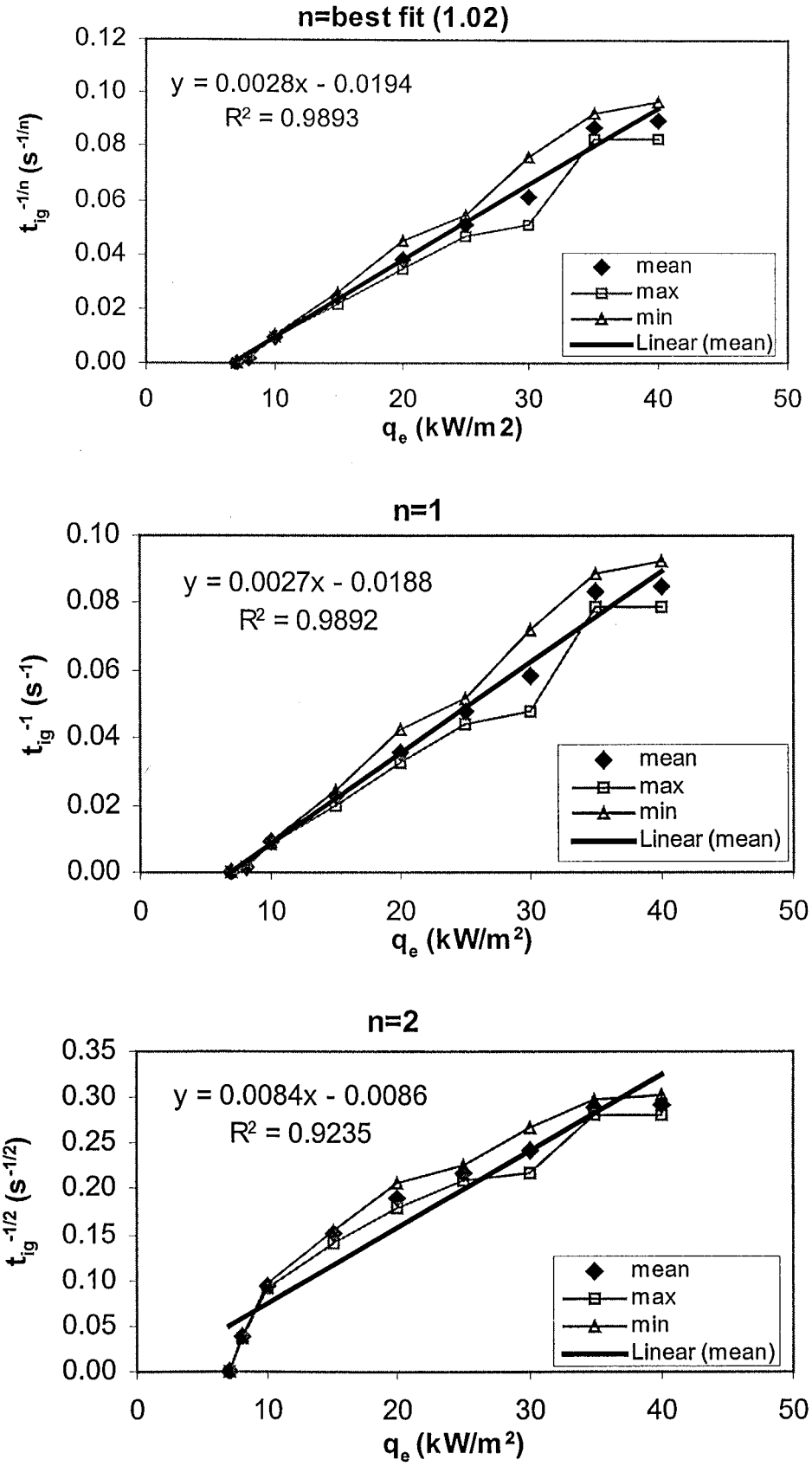

Figure C - 13 Linear correlation for Fabric 35

Fabric 36

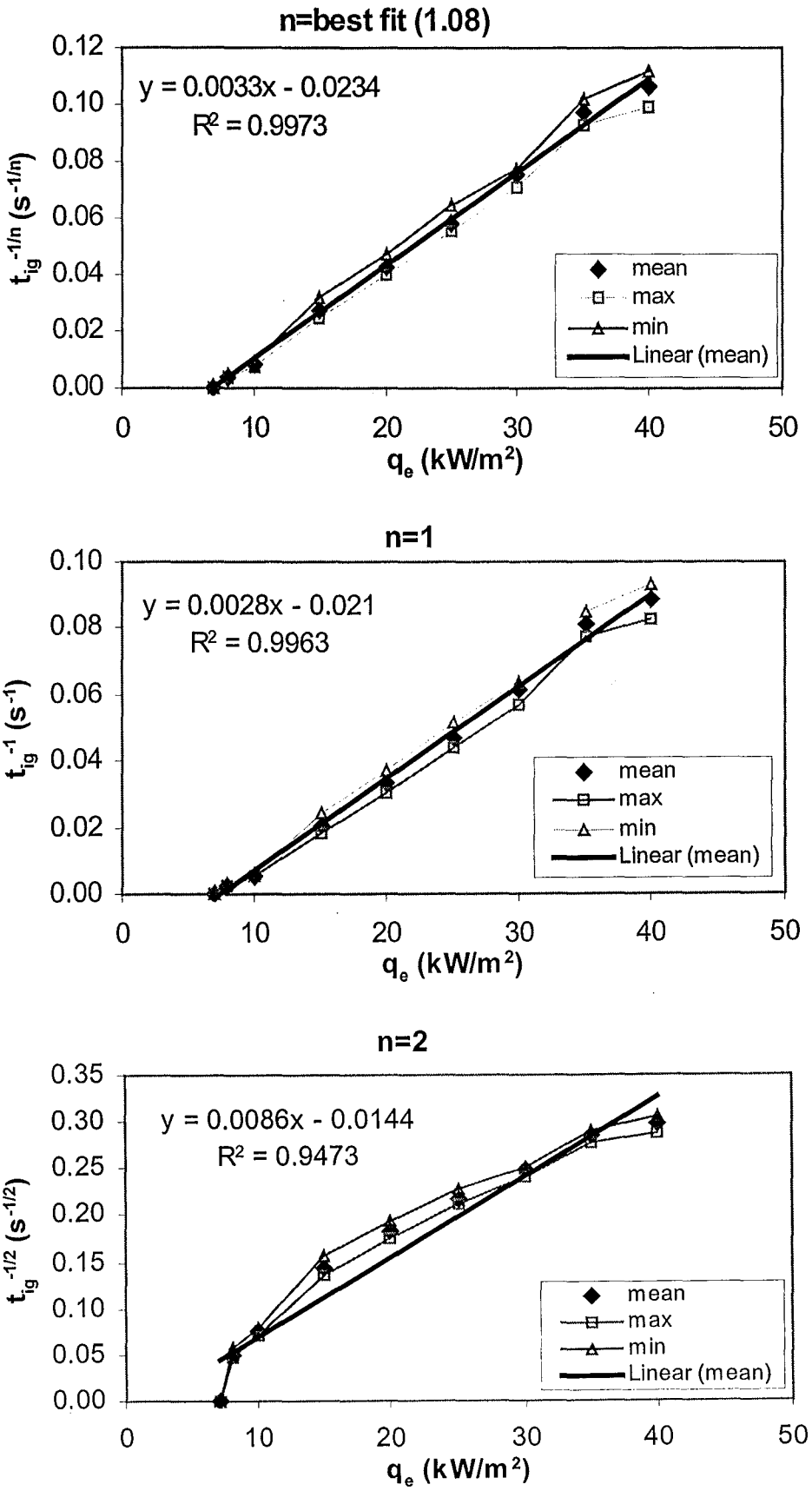

Figure C - 14 Linear correlation for Fabric 36

Appendix D

Prediction Results for Time-to-ignition

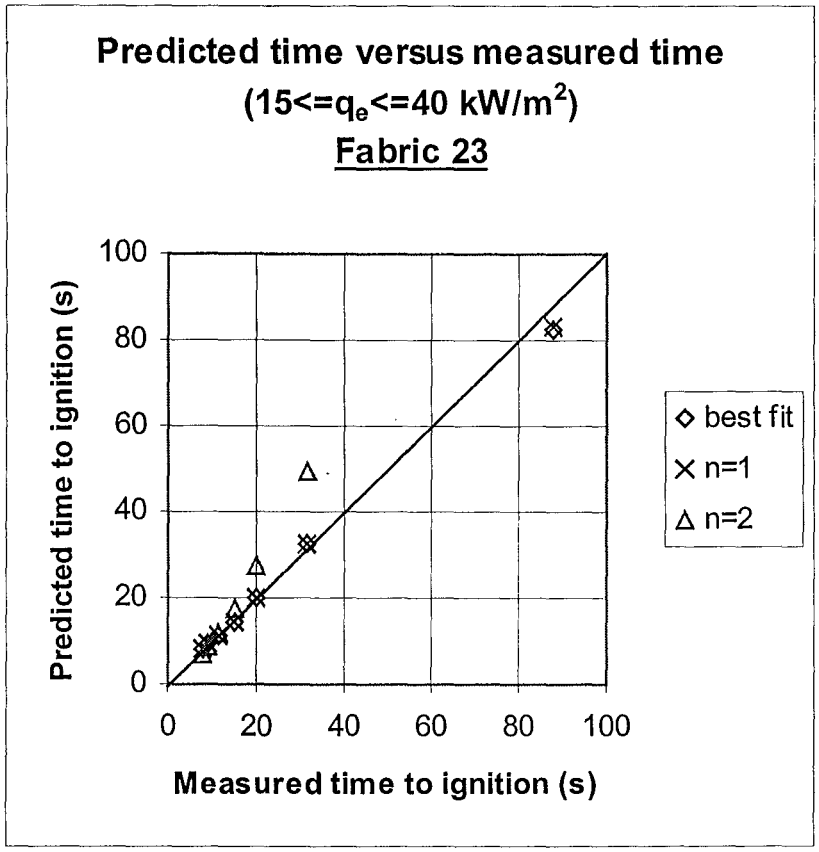

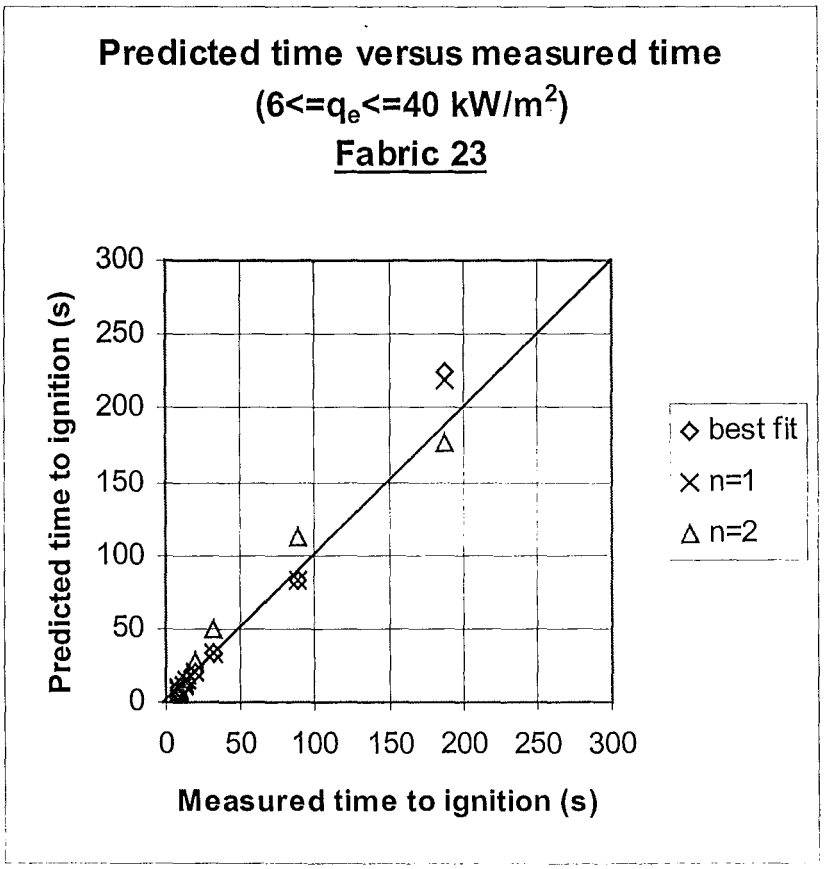

Figure D - 1 Comparative plot of the measured time to ignition versus the predicted for fabric 23

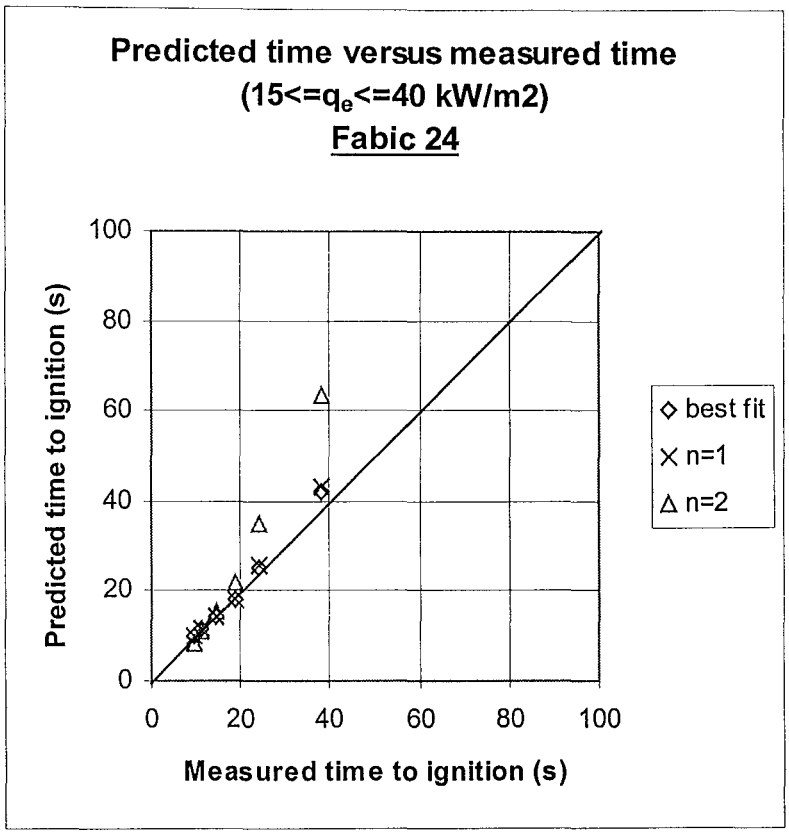

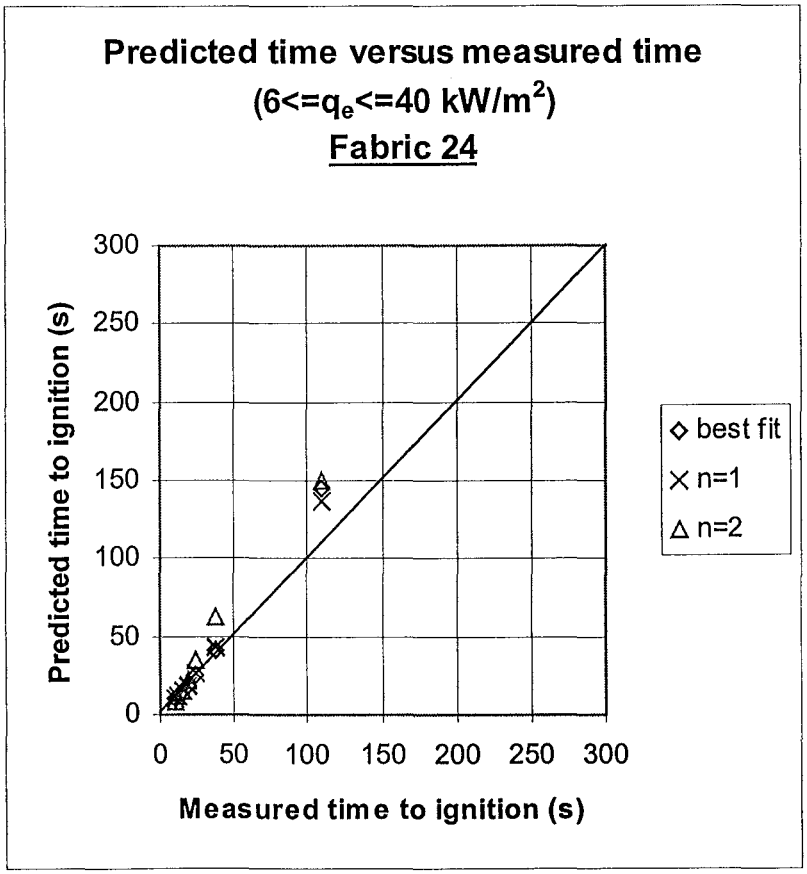

Figure D - 2 Comparative plot of the measured time to ignition versus the predicted for fabric 24

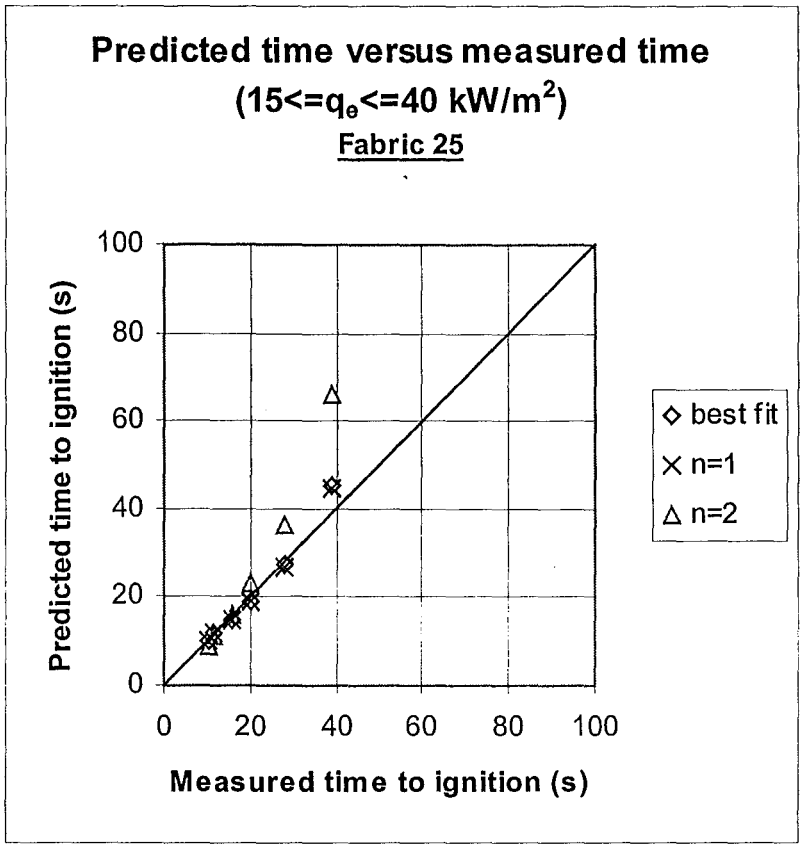

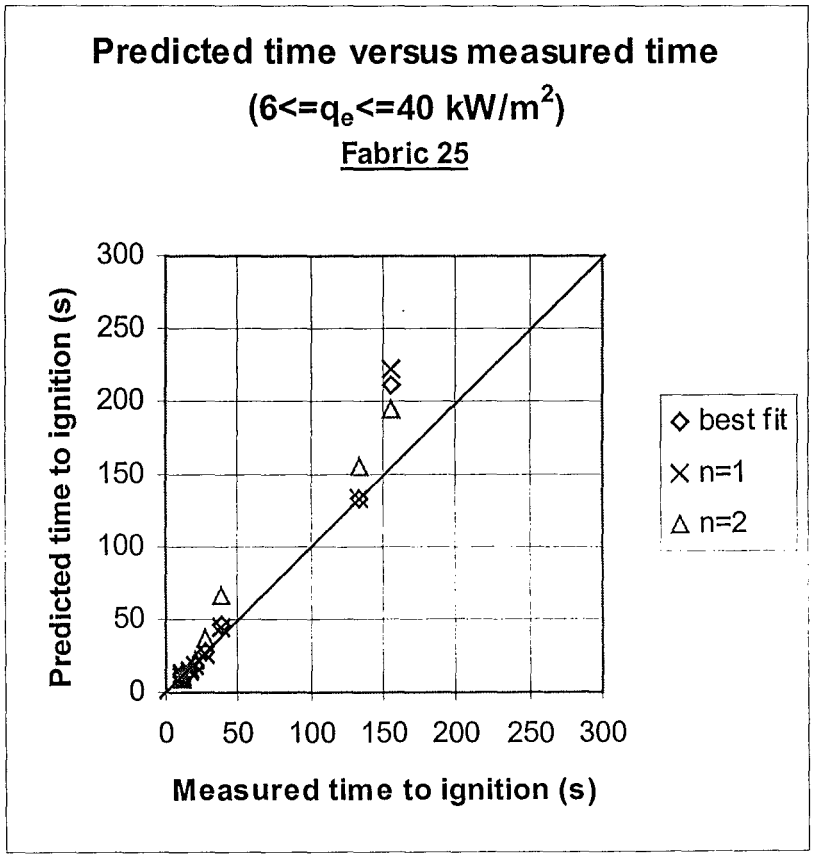

Figure D - 3 Comparative plot of the measured time to ignition versus the predicted for fabric 25

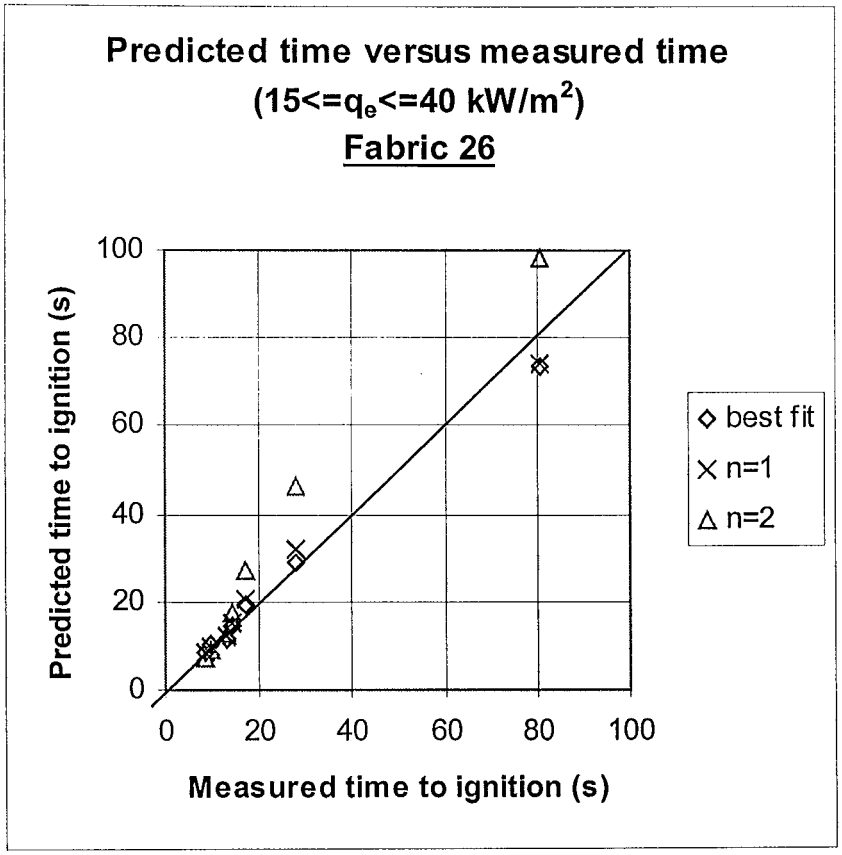

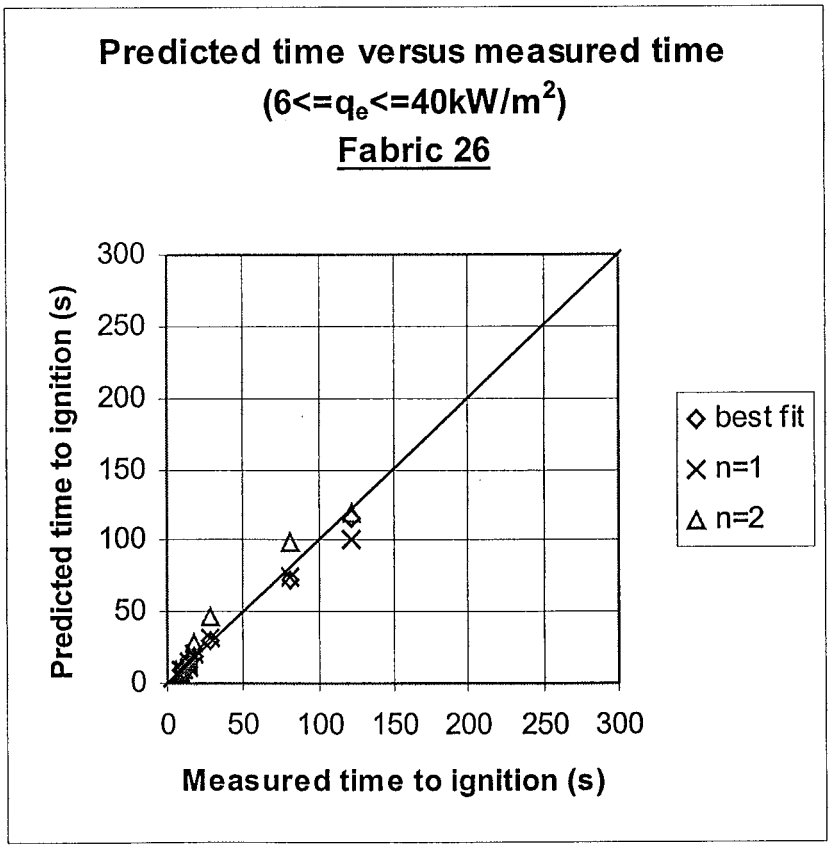

Figure D - 4 Comparative plot of the measured time to ignition versus the predicted for fabric 26

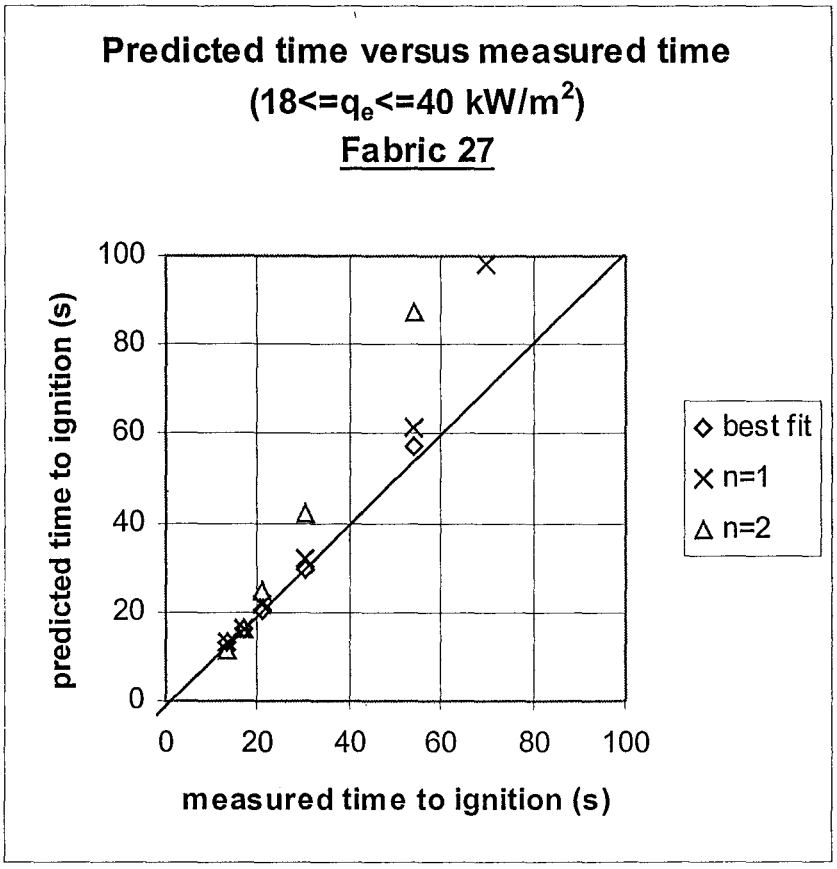

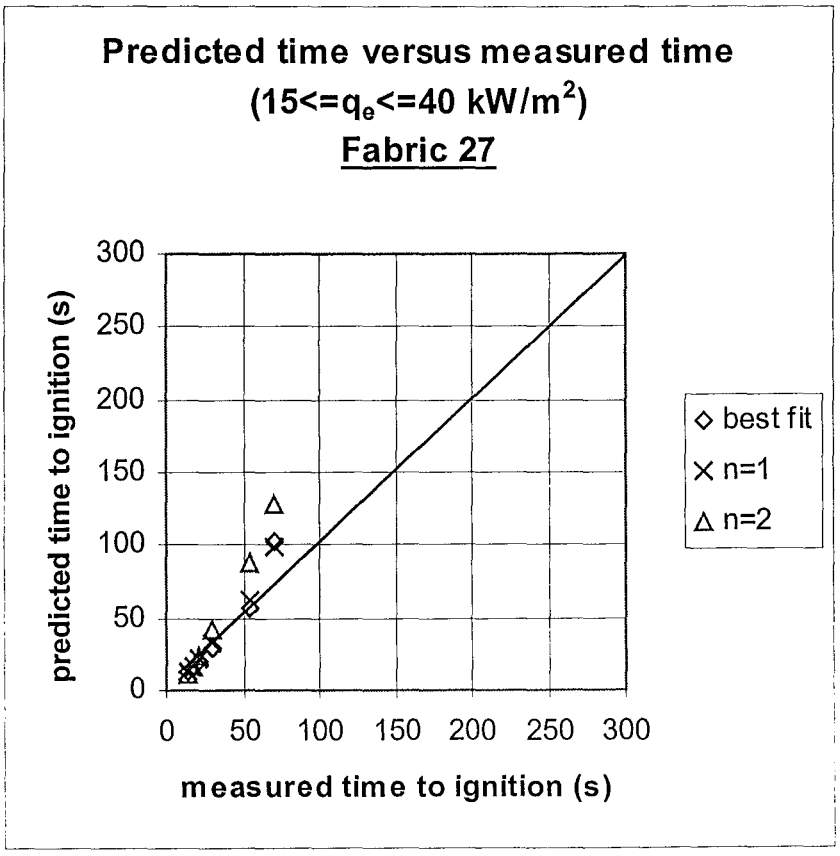

Figure D - 5 Comparative plot of the measured time to ignition versus the predicted for fabric 27

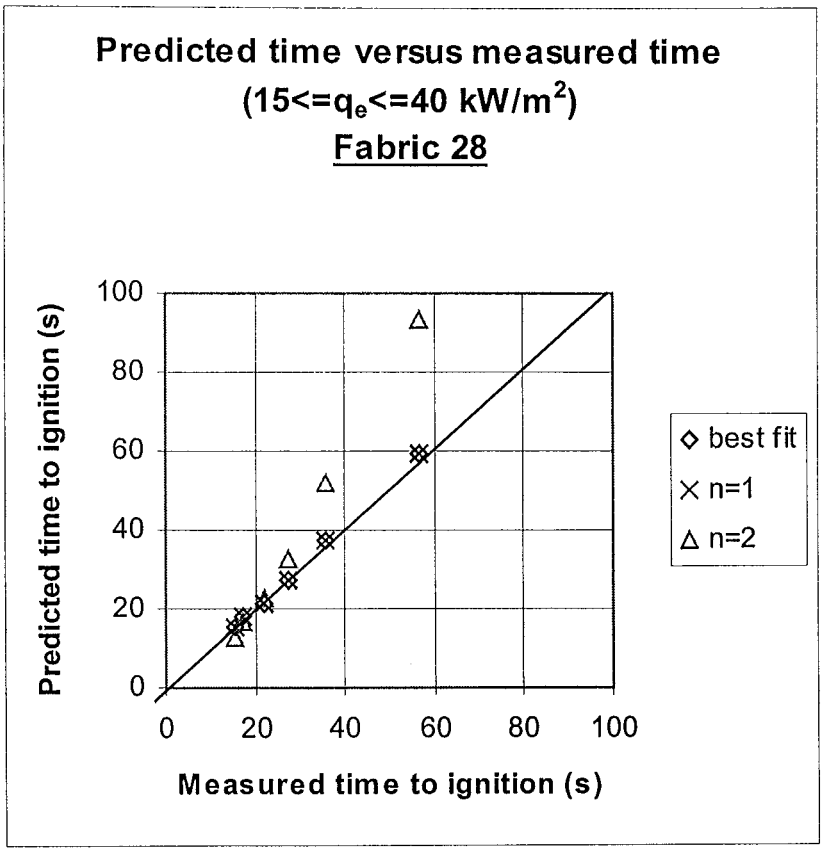

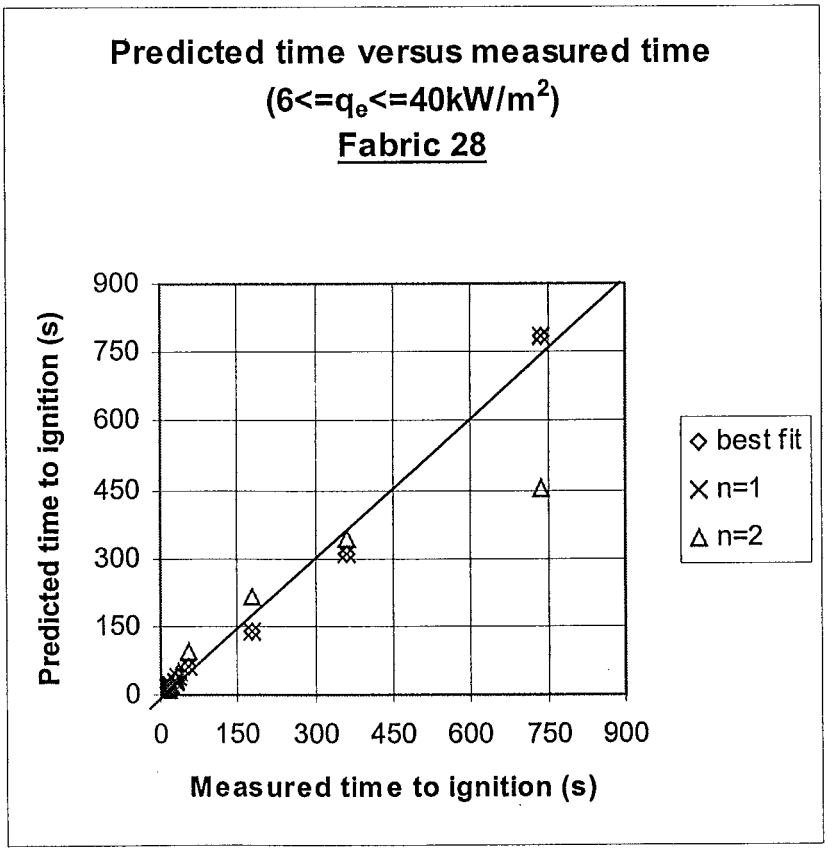

Figure D - 6 Comparative plot of the measured time to ignition versus the predicted for fabric 28

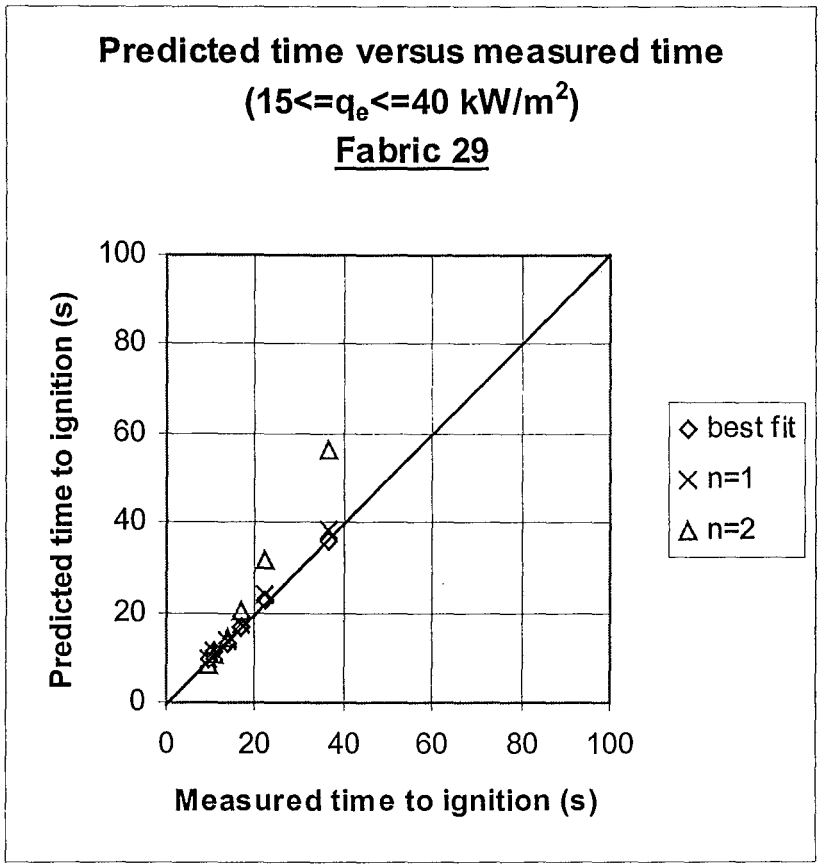

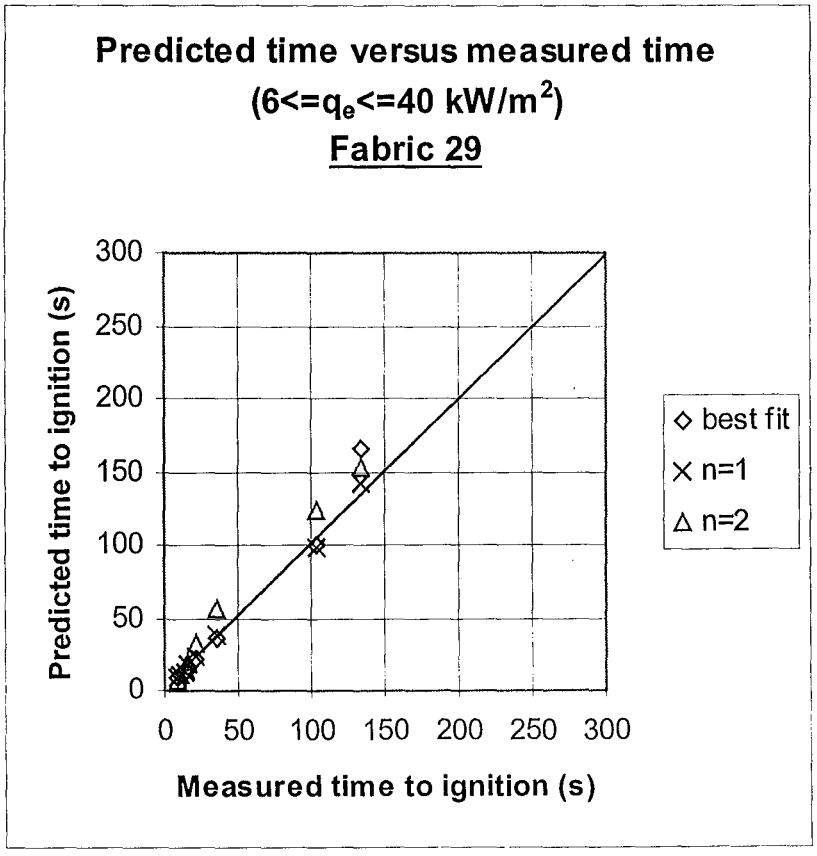

Figure D - 7 Comparative plot of the measured time to ignition versus the predicted for fabric 29

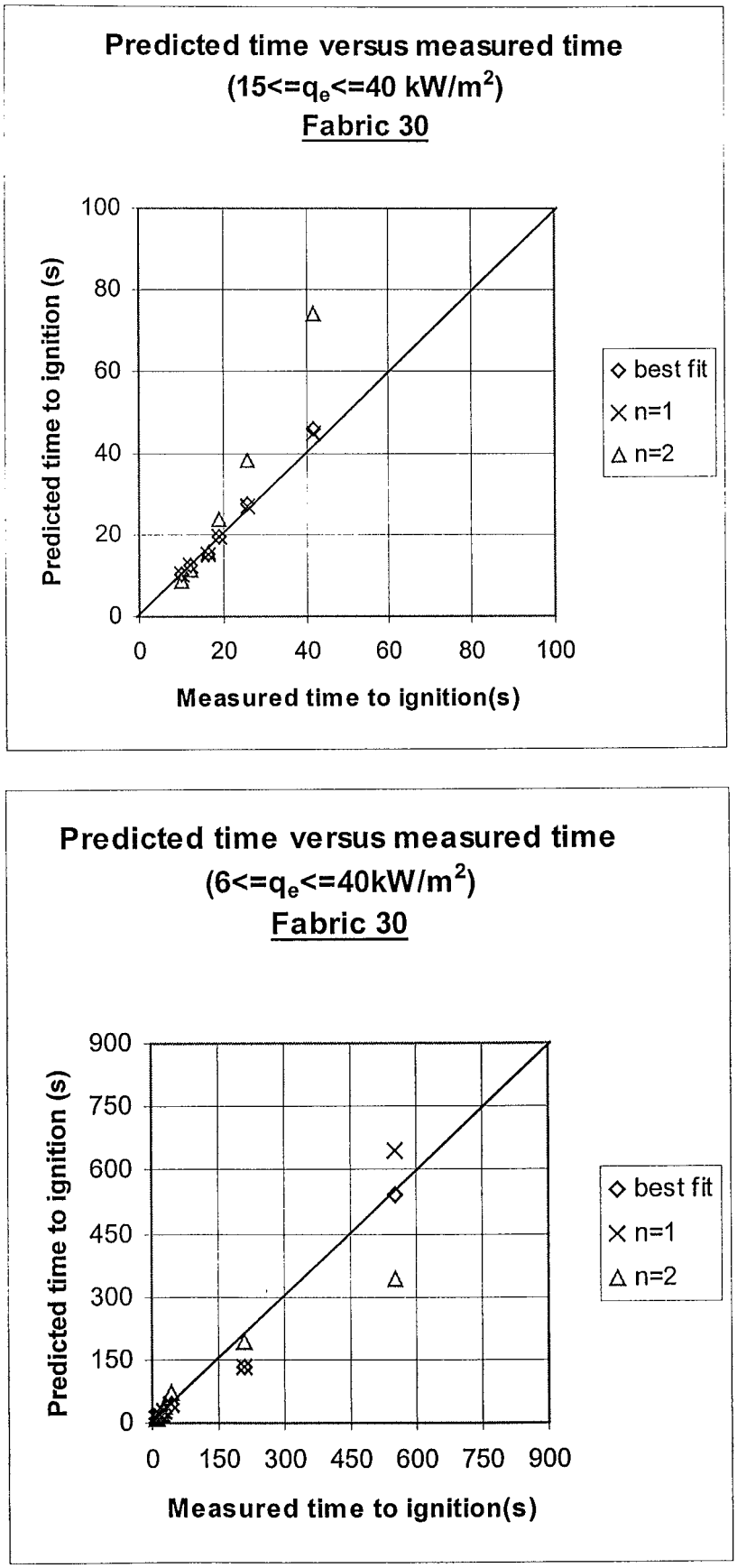

Figure D - 8 Comparative plot of the measured time to ignition versus the predicted for fabric 30

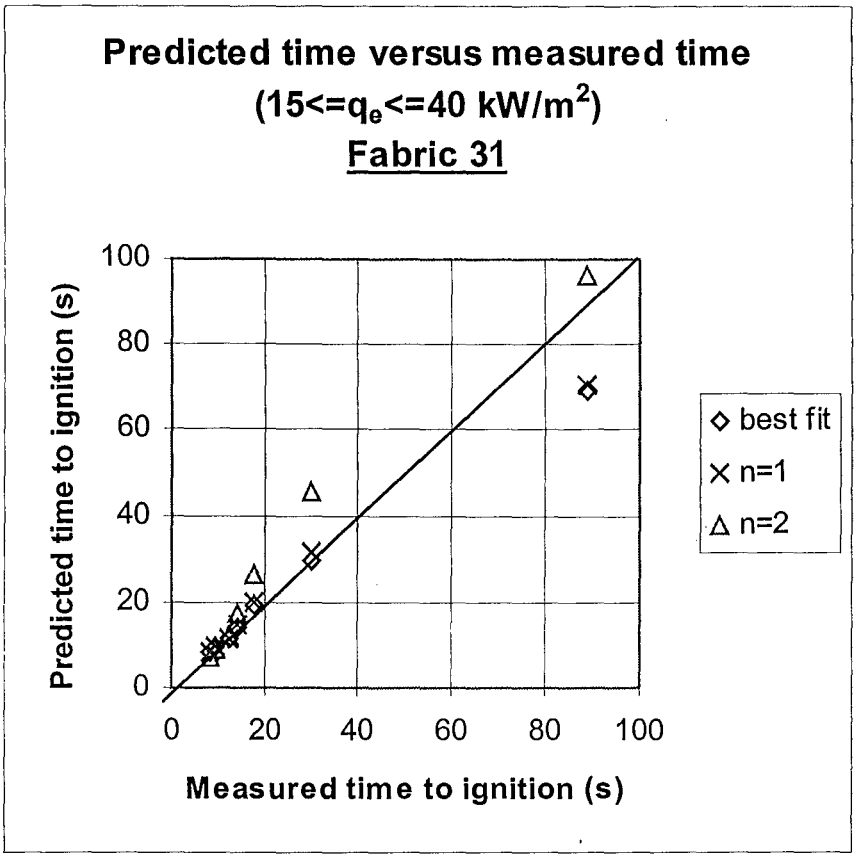

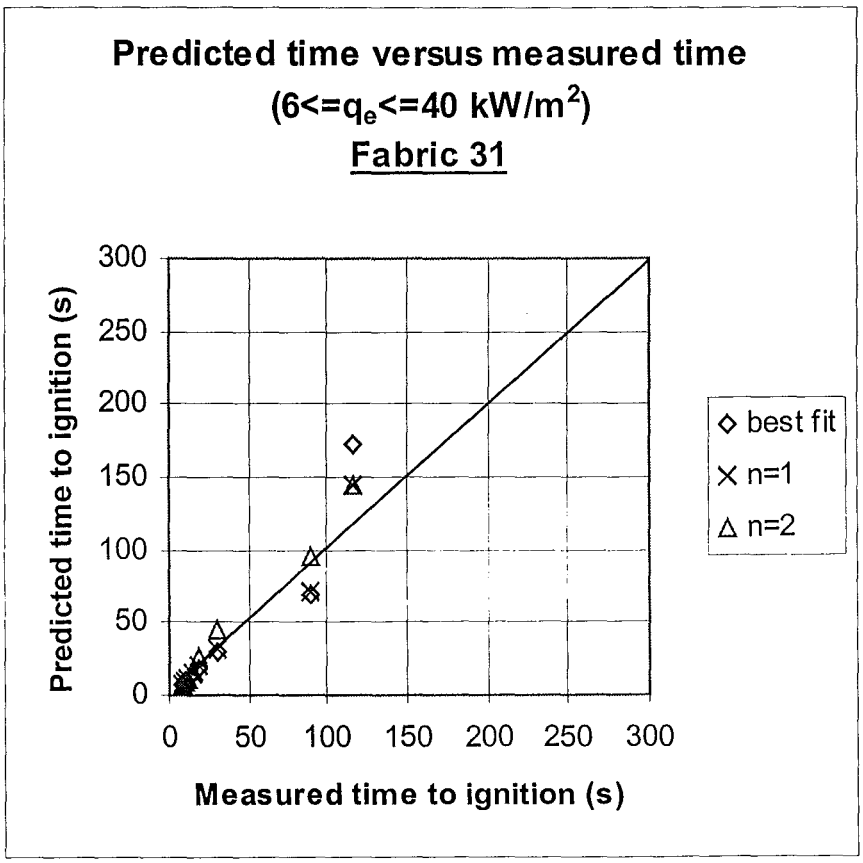

Figure D - 9 Comparative plot of the measured time to ignition versus the predicted for fabric 31

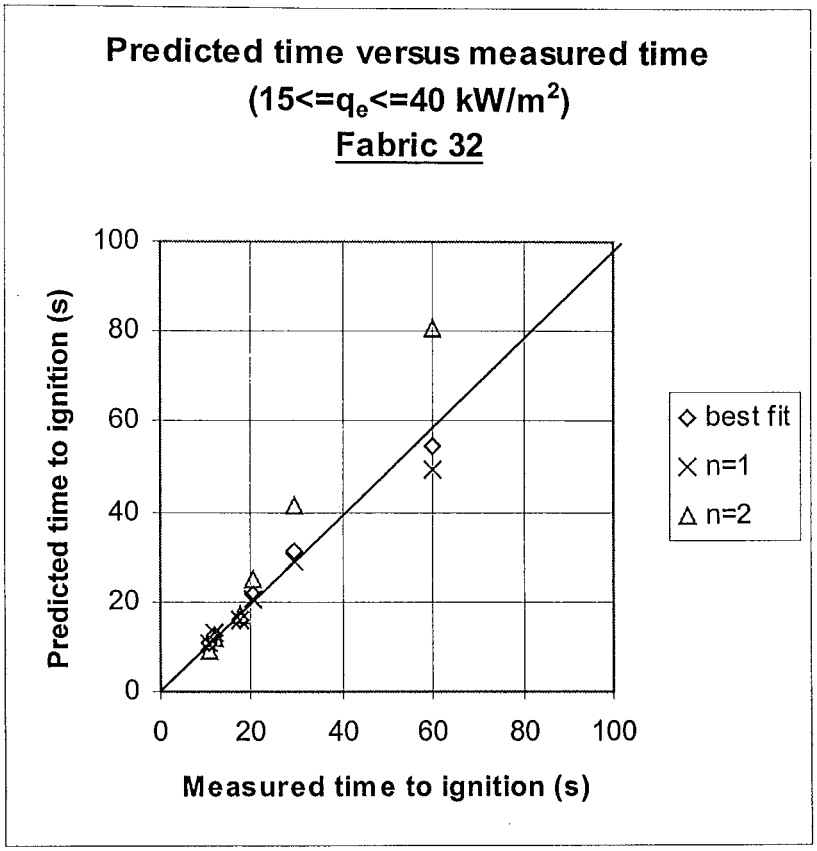

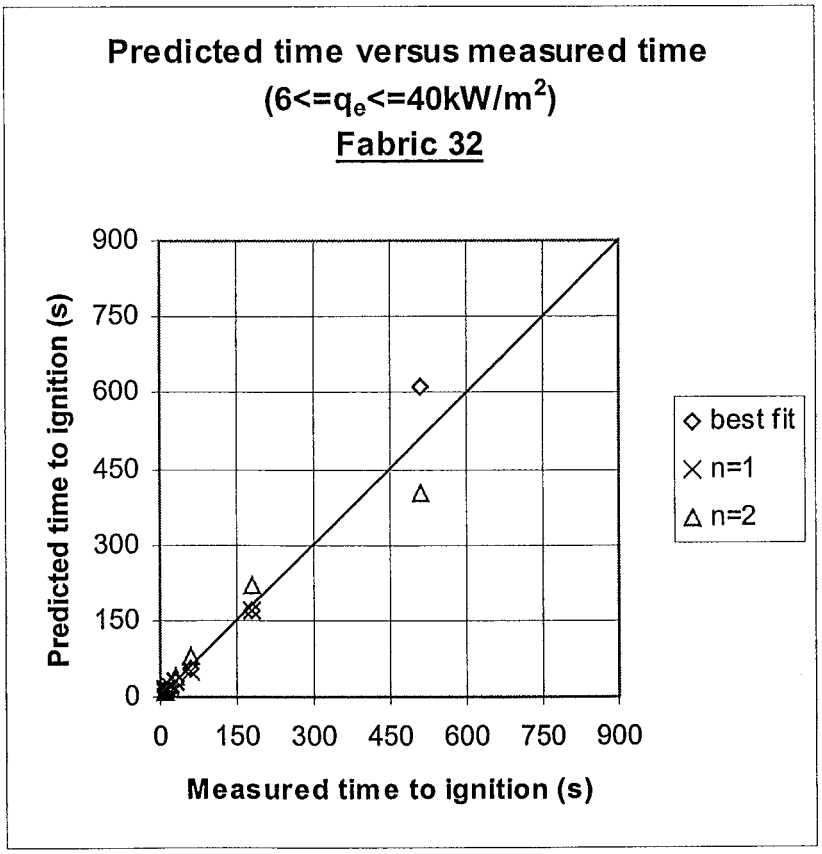

Figure D - 10 Comparative plot of the measured time to ignition versus the predicted for fabric 32

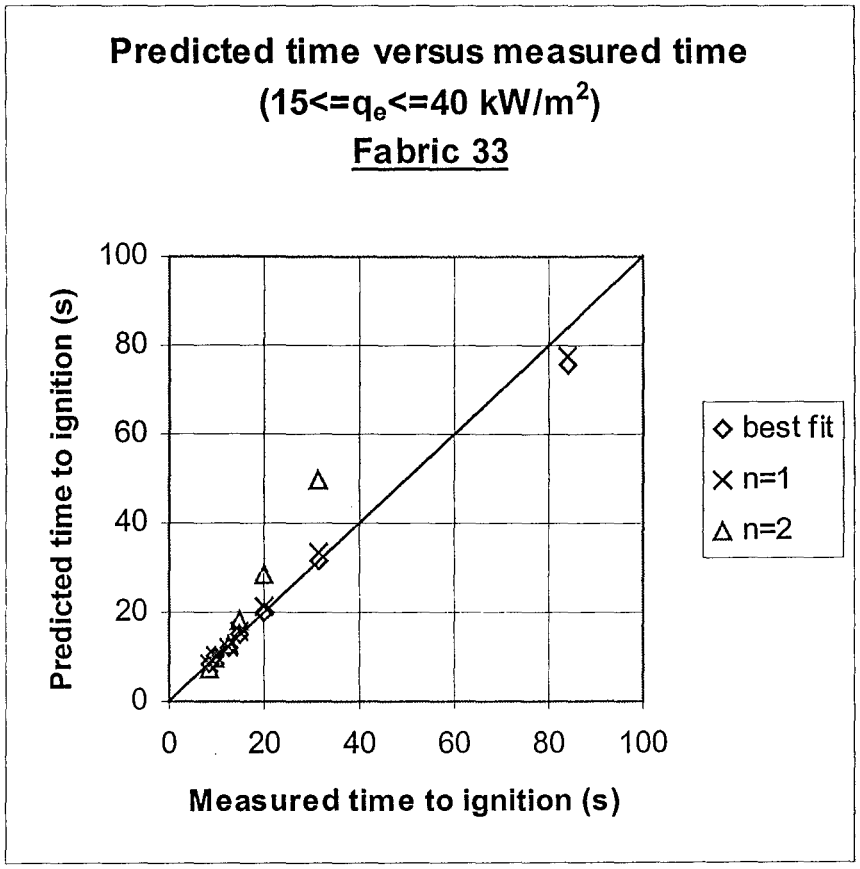

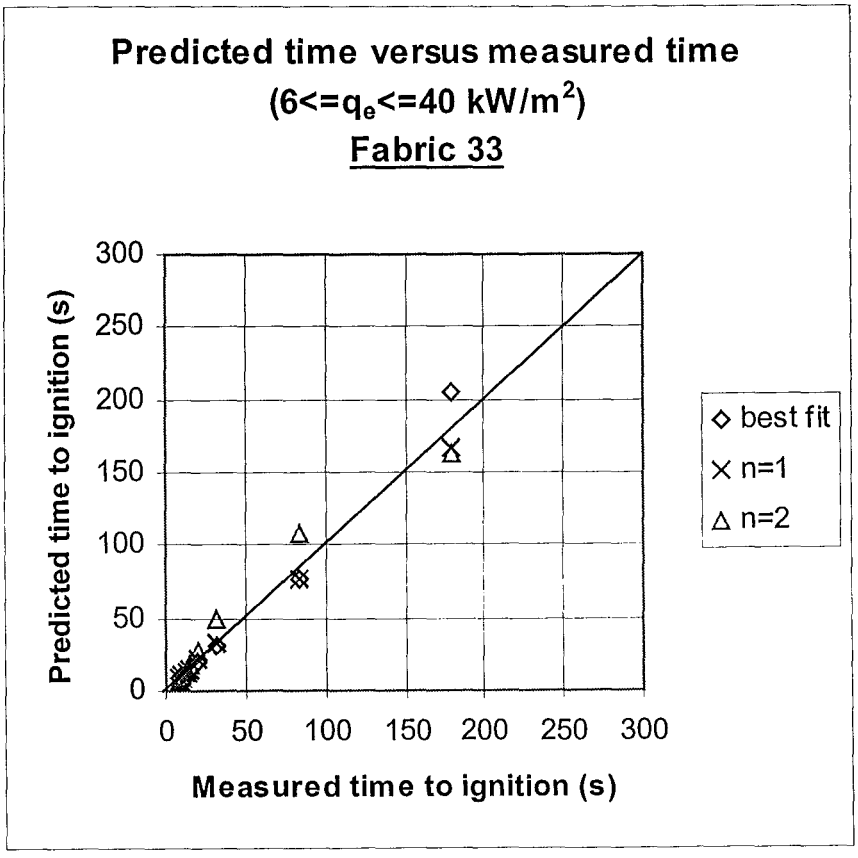

Figure D - 11 Comparative plot of the measured time to ignition versus the predicted for fabric 33

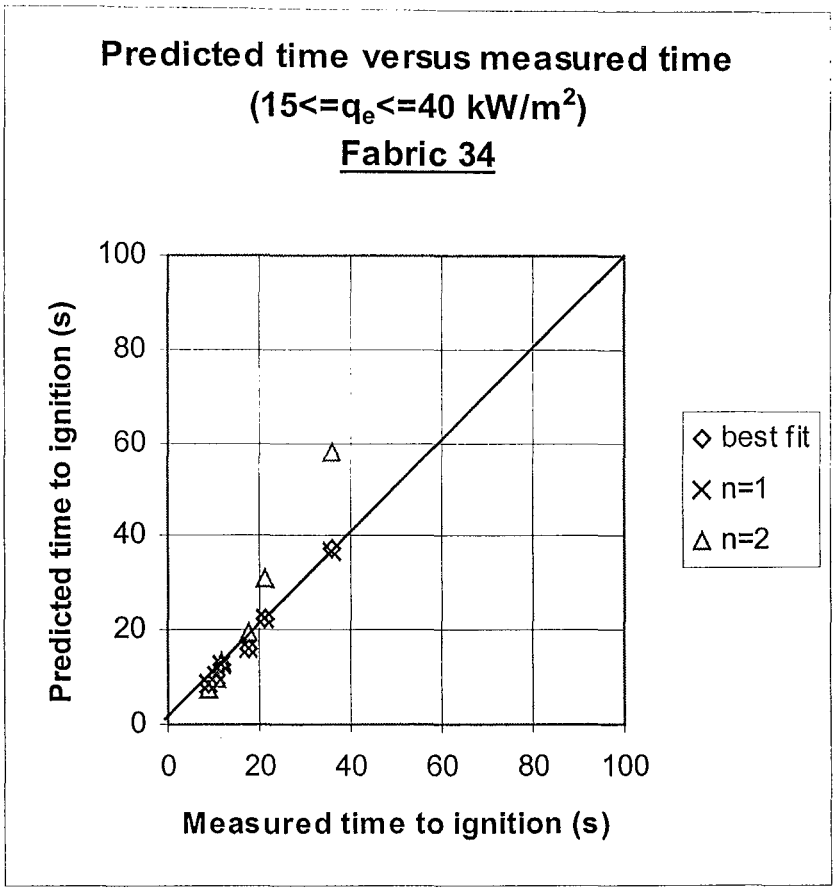

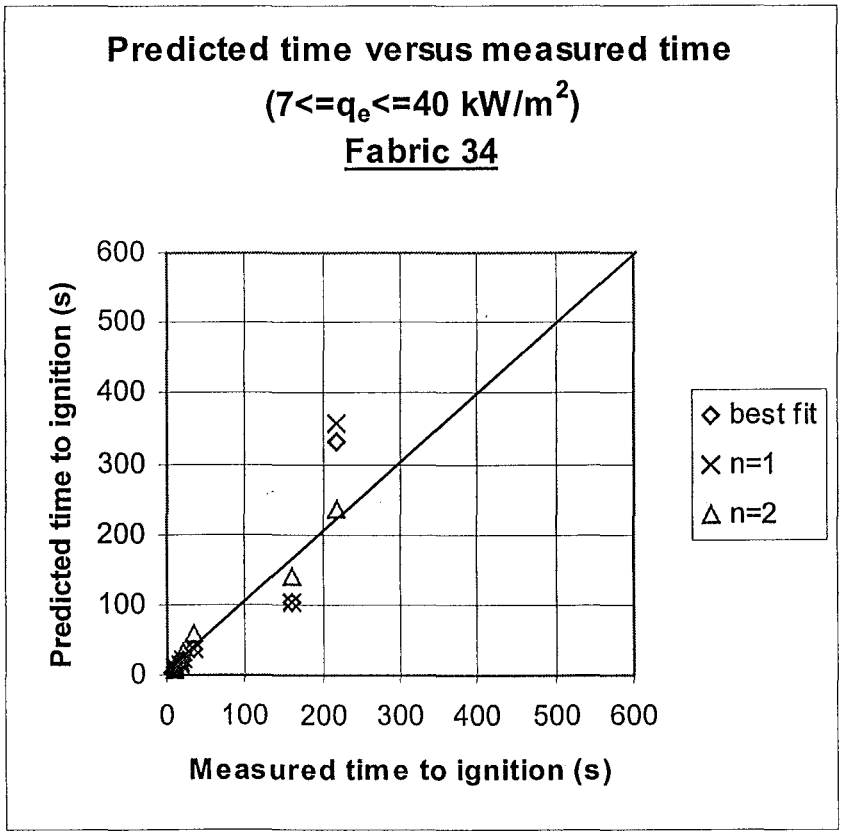

Figure D - 12 Comparative plot of the measured time to ignition versus the predicted for fabric 34

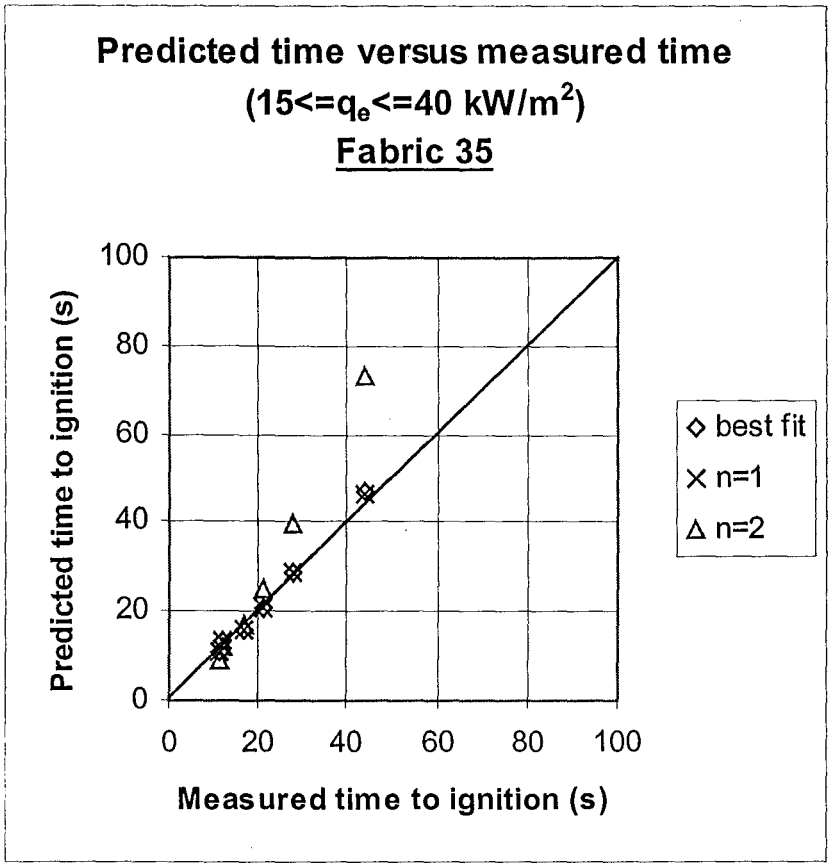

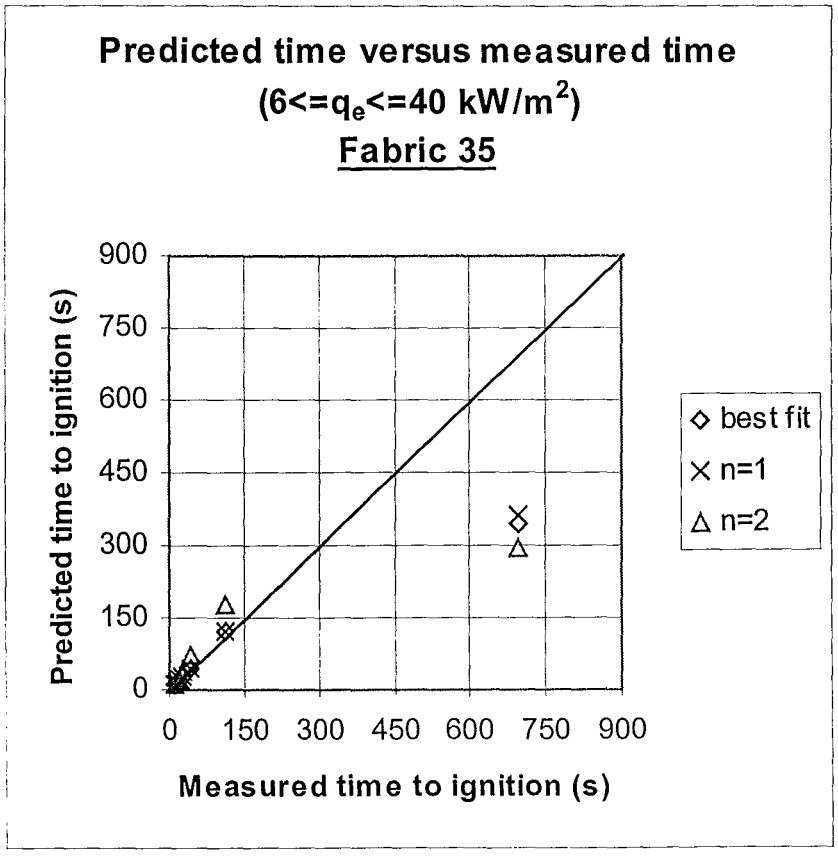

Figure D - 13 Comparative plot of the measured time to ignition versus the predicted for fabric 35

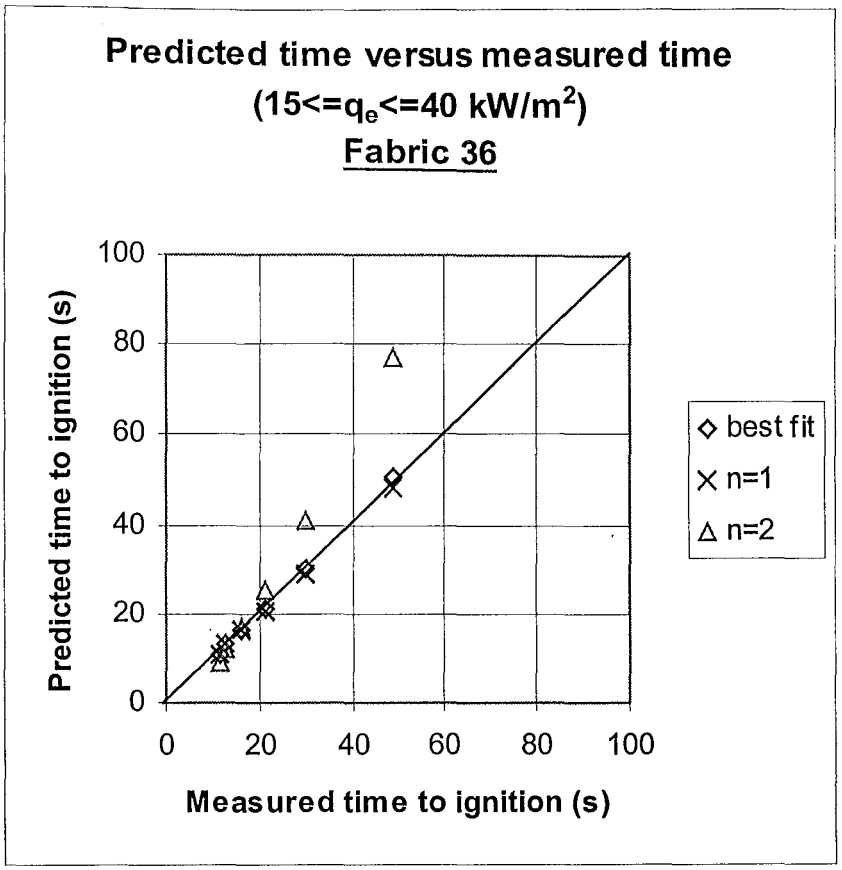

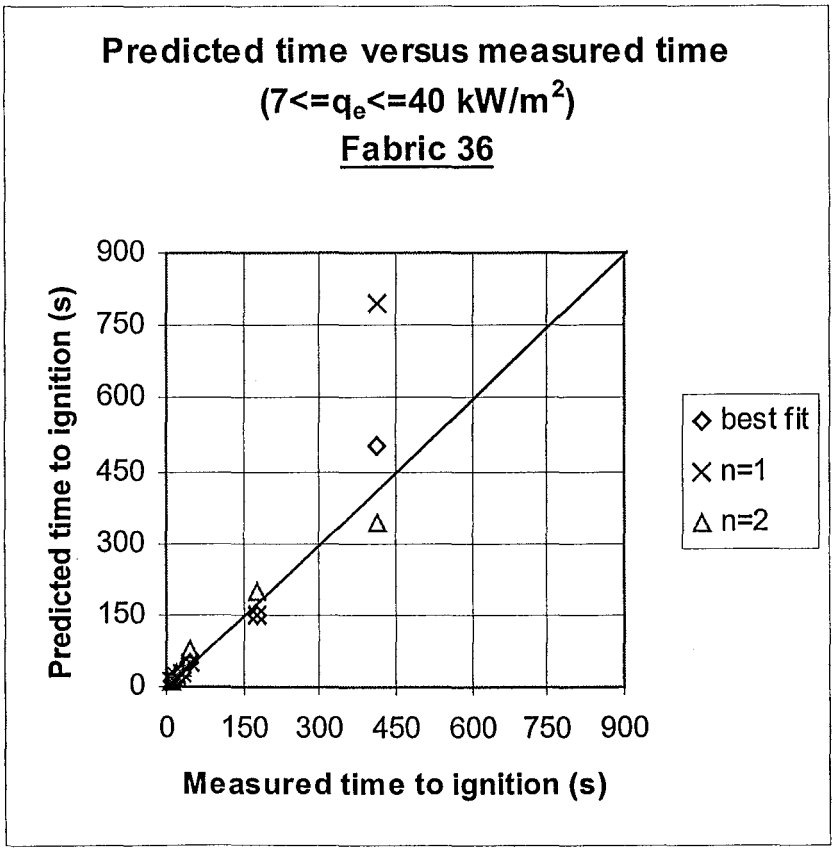

Figure D - 14 Comparative plot of the measured time to ignition versus the predicted for fabric 36

FIRE ENGINEERING RESEARCH REPORTS

95/1	Full Residential Scale Backdraft	I B Bolliger
95/2	A Study of Full Scale Room Fire Experiments	P A Enright
95/3	Design of Load-bearing Light Steel Frame Walls for Fire Resistance	J T Gerlich
95/4	Full Scale Limited Ventilation Fire Experiments	D J Millar
95/5	An Analysis of Domestic Sprinkler Systems for Use in New Zealand	F Rahmanian
96/1	The Influence of Non-Uniform Electric Fields on Combustion Processes	M A Belsham
96/2	Mixing in Fire Induced Doorway Flows	J M Clements
96/3	Fire Design of Single Storey Industrial Buildings	B W Cosgrove
96/4	Modelling Smoke Flow Using Computational Fluid Dynamics	T N Kardos
96/5	Under-Ventilated Compartment Fires - A Precursor to Smoke Explosions	A R Parkes
96/6	An Investigation of the Effects of Sprinklers on Compartment Fires	M W Radford
97/1	Sprinkler Trade Off Clauses in the Approved Documents	G J Barnes
97/2	Risk Ranking of Buildings for Life Safety	J W Boyes
97/3	Improving the Waking Effectiveness of Fire Alarms in Residential Areas	T Grace
97/4	Study of Evacuation Movement through Different Building Components	P Holmberg
97/5	Domestic Fire Hazard in New Zealand	KDJ Irwin
97/6	An Appraisal of Existing Room-Corner Fire Models	D C Robertson
97/7	Fire Resistance of Light Timber Framed Walls and Floors	G C Thomas
97/8	Uncertainty Analysis of Zone Fire Models	A M Walker
97/9	New Zealand Building Regulations Five Years Later	T M Pastore
98/1	The Impact of Post-Earthquake Fire on the Built Urban Environment	R Botting
98/2	Full Scale Testing of Fire Suppression Agents on Unshielded Fires	M J Dunn
98/3	Full Scale Testing of Fire Suppression Agents on Shielded Fires	N Gravestock
98/4	Predicting Ignition Time Under Transient Heat Flux Using Results from Constant Flux Experiments	A Henderson
98/5	Comparison Studies of Zone and CFD Fire Simulations	A Lovatt
98/6	Bench Scale Testing of Light Timber Frame Walls	P Olsson
98/7	Exploratory Salt Water Experiments of Balcony Spill Plume Using Laser Induced Fluorescence Technique	E Y Yii
99/1	Fire Safety and Security in Schools	R A Carter

99/2	A Review of the Building Separation Requirements of the New Zealand Building Code Acceptable Solutions	J M Clarke
99/3	Effect of Safety Factors in Timed Human Egress Simulations	K M Crawford
99/4	Fire Response of HVAC Systems in Multistorey Buildings: An Examination of the NZBC Acceptable Solutions	M Dixon
99/5	The Effectiveness of the Domestic Smoke Alarm Signal	C Duncan
99/6	Post-flashover Design Fires	R Feasey
99/7	An Analysis of Furniture Heat Release Rates by the Nordtest	J Firestone
99/8	Design for Escape from Fire	I J Garrett
99/9	Class A Foam Water Sprinkler Systems	D B Hipkins
99/10	Review of the New Zealand Standard for Concrete Structures (NZS 3101) for High Strength and Lightweight Concrete Exposed to Fire	M J Inwood
99/12	An Analytical Model for Vertical Flame Spread on Solids: An Initial Investigation	G A North
99/13	Should Bedroom Doors be Open or Closed While People are Sleeping? - A Probabilistic Risk Assessment	D L Palmer
99/14	Peoples Awareness of Fire	S J Rusbridge
99/15	Smoke Explosions	B J Sutherland
99/16	Reliability of Structural Fire Design	JKS Wong
99/17	Heat Release from New Zealand Upholstered Furniture	T Enright
00/1	Fire Spread on Exterior Walls	FNP Bong
00/2	Fire Resistance of Lightweight Framed Construction	PCR Collier
00/3	Fire Fighting Water: A Review of Fire Fighting Water Requirements (A New Zealand Perspective)	S Davis
00/4	The Combustion Behaviour of Upholstered Furniture Materials in New Zealand	H Denize
00/5	Full-Scale Compartment Fire Experiments on Upholstered Furniture	N Girgis
00/6	Fire Rated Seismic Joints	M James
00/7	Fire Design of Steel Members	K R Lewis
00/8	Stability of Precast Concrete Tilt Panels in Fire	L Lim
00/9	Heat Transfer Program for the Design of Structures Exposed to Fire	J Mason
00/10	An Analysis of Pre-Flashover Fire Experiments with Field Modelling Comparisons	C Nielsen
00/11	Fire Engineering Design Problems at Building Consent Stage	P Teo
00/12	A Comparison of Data Reduction Techniques for Zone Model Validation	S Weaver
00/13	Effect of Surface Area and Thickness on Fire Loads	H W Yii
00/14	Home Fire Safety Strategies	P Byrne
00/15	Accounting for Sprinkler Effectiveness in Performance Based Design of Steel Buildings in Fire	M Feeney

00/16	**A Guideline for the Fire Design of Shopping Centres**	**J M McMillan**
01/1	**Flammability of Upholstered Furniture Using the Cone Calorimeter**	**A Coles**
01/2	**Radiant Ignition of New Zealand Upholstered Furniture Composites**	**F Chen**
01/3	**Statistical Analysis of Hospitality Industry Fire Experience**	**T Y A Chen**
01/4	**Performance of Gypsum Plasterboard Assemblies Exposed to Real Building Fires**	**B H Jones**
01/5	**Ignition Properties of New Zealand Timber**	**C K Ngu**
01/6	**Effect of Support Conditions on Steel Beams Exposed of Fire**	**J Seputro**
01/7	**Validation of an Evacuation Model Currently Under Development**	**A Teo**
01/8	**2-D Analysis of Composite Steel - Concrete Beams in Fire**	**R Welsh**
01/9	**Contribution of Upholstered Furniture to Residential Fire Fatalities in New Zealand**	**C R Wong**
01/10	**The Fire Safety Design of Apartment Buildings**	**S Wu**

School of Engineering
University of Canterbury
Private Bag 4800, Christchurch, New Zealand

Phone 643 364-2250
Fax 643 364-2758